
Energy-Efficiency Media Access Control in Wireless Ad Hoc Networks

Yuefeng Zhou



A thesis submitted for the degree of Doctor of Philosophy.
The University of Edinburgh.
March 2006



Abstract

Various information and communication appliances, such as cellular phones, laptops, personal digital assistants (PDAs), digital cameras, pocket video games, pagers and others devices, adorn our body and form a Wireless Local Area Network (WLAN) or Personal Area Network (PAN). In the next generation of wireless communication systems, there will be a need for the rapid deployment of these mobile devices to provide more flexibility and convenience than traditional infrastructure networks. One possible solution is the Mobile Ad Hoc Networks (MANETs), which is an autonomous collection of mobile users that communicate over relatively bandwidth constrained wireless links.

Since many portable devices are battery operated, energy exhaustion is one of the critical factors, concerning not only the quality of service but also topology stability. Energy efficient Media Access Control (MAC) strategies have been widely confirmed to be one of the essential solution for power-saving in MANETs. The aim of the work in this thesis is to examine the existing energy efficient MAC protocols for wireless ad hoc networks, and to develop enhanced energy efficient MAC strategies for MANETs.

Taking a typical example of the WLAN ad hoc network power saving mode, a statistical model is proposed for the analysis of the power-saving MAC performance in the presence of Rayleigh fading. The analysis and simulation results show that the power-saving MAC mechanisms will degrade networking performance, such as end-to-end delay, and throughput, on the other hand, the impact of power-saving MAC methods on routing protocols is studied based on the proposed analytical model. Consequently, new power saving MAC mechanisms are proposed to balance the power saving and throughput under dynamic traffic load and improve the routing discovery performance. Power-saving MAC protocols are also strongly linked to the network topology management. Based on the comparison and discussion of various wireless network topologies, a novel hierarchical clustering algorithm is proposed in this thesis to prolong the lifetime of the whole network, improve the network throughput and simplify topology management in a large scale network. In MANETs, because of mobility, the dynamic radio environment, and the distributed networking operations, power control is different from those in other type of networks. Focusing on the solutions of power control in the MAC layer, this thesis also presents a novel power control and interference mitigation method for Wireless Personal Area Networks (WPANs). The method proposed is based on the Piconet Coordinator (PNC) selection mechanism in IEEE802.15-based WPANs, since the PNC is important as it centrally controls all networking operations. A practical implementation of the proposed power control method is also introduced in this thesis. The experiments, supported by Fujitsu Laboratories of Europe Limited, demonstrate that the proposed method can dramatically improve the energy efficiency and network robustness.

Acknowledgements

I would like to thank my family, for their love, support and patience.

I would also like to thank Dr. Dave Laurenson and Prof. Stephen McLaughlin, my supervisors for their guidance and revising this thesis.

The work reported in this thesis has formed part of the Personal Distributed Environment (PDE) area of the Core 3 Research Programme of the Virtual Centre of Excellence in Mobile Personal Communications, Mobile VCE, whose funding support, including that of EPSRC, is gratefully acknowledged.

This work is also supported by the Overseas Research Students Awards Scheme (ORS) of Universities UK, which is greatly appreciated.

I also wish to acknowledge Fujitsu Laboratories of Europe Ltd., for support my wireless PAN research.

Contents

Declaration of originality	iii
Acknowledgements	iv
Contents	v
List of figures	vii
List of tables	x
Acronyms and abbreviations	xi
1 Introduction	1
1.1 Wireless Ad Hoc Networks	1
1.1.1 Heterogeneous Mobile Conductivities	1
1.1.2 Energy Efficiency	2
1.1.3 Media Access Control	3
1.1.4 Routing	3
1.2 Contributions of the Work	3
1.3 Organization of this Thesis	4
2 Media Access Control in Wireless Ad Hoc Networks	5
2.1 MAC Functions	5
2.2 MAC Protocols for WLANs and WPANs	7
2.2.1 IEEE802.11	7
2.2.2 HIPERLAN	8
2.2.3 Bluetooth	11
2.2.4 IEEE802.15	12
2.3 Low Power Consumption MAC Protocols	15
2.3.1 Energy Conservation MAC Design	15
2.3.2 IEEE802.11 Ad Hoc Network Power Saving MAC	16
2.3.3 IEEE802.15.3 Power Saving MAC	17
2.4 Summary	19
3 Analytical Model for Power-Saving MAC in Ad Hoc Network	21
3.1 Analytical Model for Power-saving MAC in Ad Hoc Networks	21
3.1.1 Propagation Model	22
3.1.2 Power Capture Model in Rayleigh Fading Channel	22
3.1.3 Successful Packet Transmission Rate	24
3.1.4 Throughput	31
3.1.5 Delay Analysis	31
3.1.6 Numerical Results	33
3.2 Synchronization and Multi-hop Issues	39
3.2.1 Analysis of Beacon Transmission	41
3.2.2 Analysis of Asynchronism	43
3.2.3 An Effective Power-saving scheme for Multi-hop Networks	46
3.3 Summary and Conclusions	52

4	Interaction between Routing and MAC	55
4.1	Impact of Power-Saving MAC on Ad Hoc Network Routing Protocols	55
4.1.1	Route Discovery Timeout under Power-Saving MAC	55
4.1.2	Numerical Analysis	57
4.1.3	Simulation	59
4.2	Improved Route Discovery with Power-Saving MAC	64
4.3	Summary and Conclusions	66
5	Topology Management in Wireless Ad Hoc Networks	67
5.1	Topologies in Wireless Ad Hoc Networks	67
5.1.1	Peer-to-Peer Topology	67
5.1.2	Star Topology	68
5.1.3	Cluster Topology	69
5.2	Application of Cluster-Tree Topology in Wireless Ad Hoc Sensor Networks . .	70
5.2.1	Wireless Ad Hoc Sensor Network	70
5.2.2	Cluster-Tree Topology in IEEE802.15.4-Based LR-WPAN	71
5.2.3	An Energy-Efficient Distributed Clustering Approach for IEEE802.15.4- Based LR-WPAN	74
5.3	Summary and Conclusions	83
6	Power Control in Wireless Ad Hoc Networks	87
6.1	Power Control Methods for Ad Hoc Networks	87
6.1.1	RTS/CTS-Based Power Control	87
6.1.2	Multiple Channel Access Power Control	89
6.1.3	Power Control Based on Packet Size	90
6.1.4	Power Control and Interference Mitigation	90
6.2	A Novel Power Control and Interference Mitigation Method in WPANs	91
6.2.1	Coordinator Selection and Power Control	91
6.2.2	Simulation Results	94
6.3	Validation of the Method in a Real Network	97
6.3.1	System Architecture	97
6.3.2	Embedded Software	98
6.3.3	Host Software	101
6.4	Summary and Conclusions	102
7	Conclusions	107
7.1	Summary and Achievements of the Work	107
7.2	Limitations of the Work and Scope for Further Research	109
	References	110
A	Original Publications	117

List of figures

1.1	Mobile Ad Hoc Network	2
2.1	A universal radio interface protocol architecture	5
2.2	Basic CSMA scheme for packet transmission	8
2.3	CSMA with four-way handshaking scheme	9
2.4	“Hidden terminal” problem when A and C communicate with B simultaneously	9
2.5	Channel access cycle in HIPERLAN	10
2.6	An example of scatternet, which comprises of two Piconets.	11
2.7	A DEV needs scan the channels to start a Piconet	13
2.8	The channel time and the superframe	15
2.9	IEEE802.11 ad hoc network power saving operations	17
3.1	T_{ATIM} in basic access and four-way handshake access	25
3.2	ATIM packet transmission	26
3.3	The state model to compute $p_{as}(W_A, k)$	28
3.4	The analytical results for $p_a(W_A)$, Basic CSMA/CA	29
3.5	The analytical results for $p_a(W_A)$, CSMA/CA with RTS/CTS	30
3.6	The end-to-end delay in the PS MAC mode	32
3.7	Successful data transmission rate vs. number of stations based on the assumption that the ATIM packet transmission probability is 1. Packet Size: 2048bits, basic CSMA/CA	34
3.8	Successful data transmission rate vs. number of stations based on the assumption that the ATIM packet transmission probability is 1. Packet Size: 2048bits, CSMA/CA with RTS/CTS	34
3.9	Successful data transmission rate vs. number of stations based on the assumption that the ATIM packet transmission probability is 1. Packet Size: 4096bits, basic CSMA/CA	35
3.10	Successful data transmission rate vs. number of stations based on the assumption that the ATIM packet transmission probability is 1. Packet Size: 4096bits, CSMA/CA with RTS/CTS	35
3.11	Successful data transmission rate vs. number of stations. Packet Size: 2048bits, basic CSMA/CA	36
3.12	Successful data transmission rate vs. number of stations. Packet Size: 2048bits, CSMA/CA with RTS/CTS	36
3.13	Total throughput vs. number of stations. $z_0 = 0dB$	37
3.14	Total throughput vs. number of stations. $z_0 = 6dB$	38
3.15	Simulation results of throughput, $W_{ATIM} = 20\%BI$	38
3.16	Average end-to-end delay vs. number of stations. Basic CSMA/CA	39
3.17	Average end-to-end delay vs. number of stations. CSMA/CA with RTS/CTS	40
3.18	Simulation results of average end-to-end delay, $W_{ATIM} = 5\%BI$	40
3.19	Explanation for $p'(n, W, k)$	42

3.20	$p'(n, W)$ with $b=11$, and $W=30$	42
3.21	Analytical results for asynchronism. The fastest node asynchronism time. . . .	45
3.22	Analytical results for asynchronism. The fastest node asynchronism time ratio. .	45
3.23	The enhanced beacon interval structure	47
3.24	An example of the enhanced scheme for IEEE 802.11-based multi-hop MANETs	49
3.25	Simulation results: successful ATIM frame transmission rate	50
3.26	Simulation results: average successful data frame transmission rate	51
3.27	Simulation results: average number of sleep slots per station	51
3.28	Simulation results: average end-to-end delay	52
4.1	The procedure of the route discovery in DSR	56
4.2	Average end-to-end delay of RRP, Basic CSMA/CA	60
4.3	Average end-to-end delay of RRP, CSMA/CA with RTS/CTS	60
4.4	Average route discovery time, Basic CSMA/CA	62
4.5	Average route discovery time, CSMA/CA with RTS/CTS	62
4.6	Average end-to-end delay of RRP, Basic CSMA/CA	63
4.7	Average end-to-end delay of RRP, CSMA/CA with RTS/CTS	63
4.8	Average successful route discovery rate in different PS MAC approaches Basic CSMA/CA, ATIM=5%BI	66
5.1	Peer-to-Peer topology	68
5.2	Star topologies	69
5.3	Cluster topology	70
5.4	Architecture of sensor network and sensor node	71
5.5	General superframe structure with active and inactive periods	72
5.6	An example of hierarchical cluster-tree topology	73
5.7	The dendriform structure of the network	74
5.8	Emission coverage when different stations are selected as the clusterhead. . . .	75
5.9	The structure of a CRPP	78
5.10	The structure of a CHAP	79
5.11	The structure of a CMAP	80
5.12	Comparing the PDSC values, devices decide to associate to clusterheads. a: After comparing the PDSC values, devices send CMAPs to their clusterheads; b: Three clusters are constructed.	80
5.13	The structure of a PSPP	81
5.14	The structure of a PCP	81
5.15	Comparing PDSC values, clusterheads choose a clusterhead as the PNC. a: After comparing PDSC values, clusterheads send PSPPs to the clusterhead with the maximum PDSC value; b: Two-layer cluster-tree topology, where the PNC is selected.	82
5.16	Cluster-tree topology in the example.	83
5.17	An example of a three-layer cluster-tree topology.a: After comparing PDSC values, devices send CMAPs to their clusterheads; b: Cluster members are associated to the clusterheads; c: The clusterheads, which did not send CMAPs, will compare their PDSC values. The clusterheads with smaller PDSC value send PCP to nominate a PNC. d: a three-layer cluster-tree topology is created. .	85

5.18	System lifetime using direct transmission, LEACH, and the proposed clustering method.	86
5.19	System throughput using direct transmission, LEACH, and the proposed clustering method.	86
6.1	The procedure of RTS/CTS power control	88
6.2	A failure of small packet's transmission also results in excessive energy waste. .	89
6.3	More stations will sense the channel is busy, if station <i>A</i> uses a higher transmission power level.	90
6.4	Interference area introduced by different PNC selections	92
6.5	PNC selection procedure	95
6.6	The message sequence chart of the LDV-PNC selection procedure	96
6.7	The interference area introduced by PNC communication in normal PNC selection.	98
6.8	The interference area introduced by PNC communication in LDS PNC selection. .	99
6.9	Average residual energy in each device.	100
6.10	PNC survival probability.	101
6.11	Percentage of the energy consumed by PNC selection mechanism vs. different PNC selection period.	102
6.12	The MICAz MPR2400CA mote	103
6.13	The implemented system	103
6.14	System architecture	104
6.15	The wired interfaces in module, GenericComm	104
6.16	The wired interfaces in component, TrafficModel	105
6.17	The host software	105

LDS-PNC	Least Distance Square PNC
LEACH	Low Energy Adaptive Clustering Hierarchy
LLC	Link Level Control
LOS	Line of Sight
LR	Lower Rate
MAC	Media Access Control Layer
MANETs	Mobile Ad Hoc Networks
MFR	MAC Footer
MHR	MAC Header
NAV	Network Allocation Vector
NBI	Next Wake Beacon Interval
NTL	Network Traffic Load
PCF	Point Coordination Function
PCP	PNC Confirming Packet
PDF	Probability Density Function
PDSC	Potential of a Device to Serve as a Cluster
PHY	Physical Layer
PNC	Piconet Coordinator
Piconet	Coordinator
PS	Power Saving
PSC	PNC Selection Counter
PSPP	PNC Searching Probe Packet
PSPS	Piconet Synchronization Power Saving
PSR	PNC Selection Request
QoS	Quality of Service
RACKP	Route ACK Packet
RDB	Route Discovery Beacon
RDE	Route Discovery End
RFD	Reduced Functional Device
RRC	Radio Resource Control
RRP	Route Request Packet
RSS	Received Signal Strength
RTS	Request to Send
rt-VBR	Real Time Variable Bit Rate
SCT	Size Control Time
SIFS	Short Interframe space
TDMA	Time Division Multiple Access
TLA	Three letter acronym
TSF	Time Synchronization Function
VLSI	Very Large Scale Integration
WBI	Wake Beacon Interval
WiFi	Wireless Fidelity
WLAN	Wireless Local Area Network
WPAN	Wireless Personal Area Network
UWB	Ultra Wide Band

Chapter 1

Introduction

1.1 Wireless Ad Hoc Networks

The earliest packet radio was developed by the Defense Advanced Research Project Agency (DARPA), and the ALOHA [1] project in the 1970s. With the development of packet radio technology, VLSI (Very Large Scale Integration) technology, and the rapidly increasing drive for wireless-capability of portable devices, wireless networks are rapidly becoming common place. Currently, laptops have built-in WiFi (Wireless Fidelity) cards; hotspots are being installed in airports, hotels and coffee shops; and offices are converting their existing cable local area networks to wireless to allow people take advantage of mobility.

Many existing networks use dedicated central nodes to coordinate the communication between participants. This kind of network architecture can simplify the design of protocol stacks. For example, maintaining routing tables in central nodes makes the routing easy. However, a more powerful machine is needed for the central node. The term “powerful” refers to the capability of energy and computation. This network architecture will become more and more infeasible as the number of participants and the network scale increases, and devices will more likely exchange information in an ad hoc fashion.

In the next generation of wireless communication systems, there will be a need for the rapid deployment of independent mobile users to provide more flexibility and convenience than traditional infrastructure networks. One example is the distributed wireless networks for emergency situations like natural or human-induced disasters, military conflicts, emergency medical situations etc. Such network scenarios cannot rely on centralized and organized connectivity, and can be conceived as applications of Mobile Ad Hoc Networks (MANETs). A MANET is an autonomous collection of mobile users that communicate over relatively bandwidth constrained wireless links. Because of the mobility, dynamically changing radio channel, and energy exhaustion, the network topology may change rapidly and unpredictably over time. Protocols that support communication in ad hoc networks have to take into account the mobility of the participants and the variation in the connectivity between associated parties. The network is decentralized, where all network activity, such as routing functionality and delivering messages, must be executed by the nodes themselves. Figure 1.1 shows an example of a MANET in the battle field.

1.1.1 Heterogeneous Mobile Conductivities

In MANETs, various communication devices with different features comprise the wireless network with no fixed infrastructure and unpredictable connectivity. The computation, storage, and communication capabilities, such as data rate, and lifetime of networking, in devices will be different.

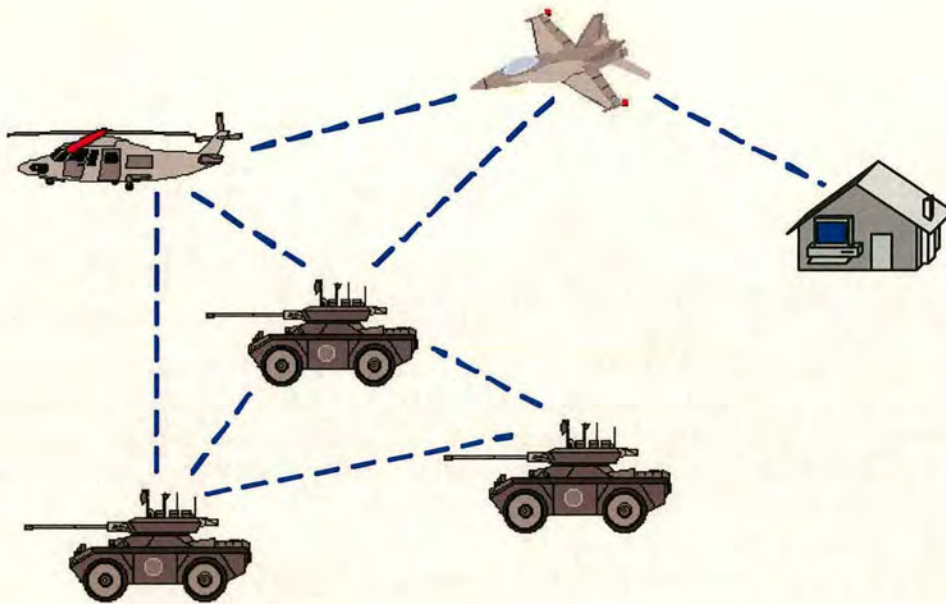


Figure 1.1: *Mobile Ad Hoc Network*

When a new device joins an existing ad hoc network, it has to discover the characteristics of neighbours. Here, the term, ‘characteristics’, might refer to following features:

- Physical layer parameters, such as data rate, modulation schemes, encoding methods, etc. A device must change its physical layer parameters to fit the demands of the presence of connections.
- Parameters relating to the energy consumption, such as residual energy, transmission power, transmission distance etc. These parameters could be seen as important metrics for energy-aware routing protocols.
- Security configurations. For example, a neighbour may not permit relaying of data for the newly entering device. Or, a neighbour may need authorization to be accessed by other devices.

1.1.2 Energy Efficiency

Since many portable devices are battery operated, energy exhaustion is one of the critical factors, concerning not only the quality of service but also topology stability. Energy efficient routing and MAC protocols have been widely discussed in the literature. In most energy efficient routing protocols, based on various energy-aware metrics, the routing selection always results in minimal transmission energy usage, for example, selecting the path with minimal transmission distance, or averaging the energy usage over whole network to avoid network partitioning. The normal method of power-saving in MAC protocols is to switch the mobile devices’ radio circuits to sleep and minimize the time in transmission, reception and idle states. However,

minimizing the transmission time will degrade the throughput. Therefore, the tradeoff between the throughput and power saving should always be considered.

1.1.3 Media Access Control

Without centralized control, the traditional TDMA, and FDMA access methods cannot be directly implemented in ad hoc networks. For example, the TDMA scheme needs strict timing synchronization. Due to the mobility and the distributed manner of wireless ad hoc networks, it is not easy for systems to obtain timing synchronization. The MAC protocols of wireless ad hoc networks must consider the mobility, hidden terminals, exposed nodes, and energy efficiency issues to access to the radio channels and avoid possible collision.

1.1.4 Routing

In wireless ad hoc networks, it is possible that there are many possible paths between source and destination. Therefore, one of the important issues in MANETs is to find and maintain the optimal path. Since the topology is dynamically changing because of the mobility, battery exhaustion, and other factors, a new routing discovery routine is probably needed for each transmission, which means the routing information has to be updated frequently.

There are two classes of MANET routing. One is on-table routing, the other is on-demand routing [2]. Using on-table routing, each node periodically exchanges route information, and maintains routing tables, which cover the topology of the whole MANET. Each node can use an existing route immediately, which is extracted from the routing table, to send data packets, thus minimising latency. However, on-table routing does not scale well to the highly dynamic topology, as periodic route maintenance becomes expensive. On-demand routing does not need to maintain the whole topology information in each node. It tries to discover the routes when this node needs to transmit data packets. This route, which is sufficient for sending its data, is just one part of the whole topology. Thus any intermediate nodes do not need to maintain complete topology information, spanning the entire network. On-demand routing saves resources used in periodic routing table maintenance, and can adapt to sudden topology changes [3].

1.2 Contributions of the Work

The thesis examines energy efficient MAC protocols for wireless ad hoc networks. The objective is to analyse the existing power-saving MAC protocols, and to develop enhanced energy efficient MAC strategies for MANETs. In this thesis, most of the proposed power-saving MAC methods are based on practical examples in IEEE802.11-based WLANs and IEEE802.15-based WPANs, since both of them are very popular MAC standards for potential ad hoc network applications.

Initially, this thesis analyzes the performance of power-saving MAC protocols in the presence of Rayleigh fading. Taking a typical example of the IEEE802.11 ad hoc network power saving mode, a statistical model is proposed for the analysis of the power-saving MAC performance. The analysis and simulation results show that the power-saving MAC mechanisms will degrade

other networking performance, such as end-to-end delay, and throughput, on the other hand, the impact of power-saving MAC methods on routing protocols is studied based on the proposed analytical model. Consequently, new power saving MAC mechanisms are proposed to balance the power saving and throughput under dynamic traffic load and improve the routing discovery performance. Power-saving MAC protocols are also strongly linked to the network topology management. The requirements of topology management in ad hoc networks are described in detail. A novel hierarchical clustering topology management method is designed to meet the aim of energy efficiency in large scale networks. Power control is an essential part of MAC protocols for energy efficiency and interference mitigation. Without a central controller in MANETs, power control needs to be operated in a distributed fashion. A distributed energy efficient power control method is presented in this thesis.

1.3 Organization of this Thesis

Chapter 2 introduces the MAC mechanisms and their performance. The existing power-saving MAC mechanisms in MANETs are also briefly described.

Chapter 3 presents an analytical model of a power-saving MAC mechanism with power capture in Rayleigh fading channels. Synchronization and multi-hop issues are also discussed in detail. A novel power-power saving MAC mechanism for multi-hop ad hoc networks is also presented and examined in this chapter.

Chapter 4 discusses the interaction of the routing protocol and the MAC mechanism, which is a cross-layer issue. Based on the analysis of the impact of a power-saving MAC on routing protocols, improved route discovery methods with the power-saving MAC are presented and validated as well.

To deal with the topology management in large scale networks, a novel energy efficient hierarchical clustering method for wireless ad hoc networks is presented in chapter 5.

Chapter 6 describes the power control issues in an ad hoc network. A distributed power control method is introduced and demonstrated by simulation.

Finally, in chapter 7 overall conclusions are drawn and suggestions for future work made.

Chapter 2

Media Access Control in Wireless Ad Hoc Networks

The protocol architecture of an ad hoc network radio interface can be logically divided into the physical (PHY), media access control (MAC), and data link layer (DLL). Figure 2.1 shows a universal radio interface protocol architecture, which is divided into 3 layers. The media access control (MAC) layer interfaces the physical layer and the DLL. Recently, many papers focus on the network performance of the energy consumption, throughput, and end-to-end delay [4] [5] [6] [7] [8] from the MAC layer's point of view. From these papers, it can be recognized that the MAC protocols can significantly influence the performance of the PHY and the higher layers.

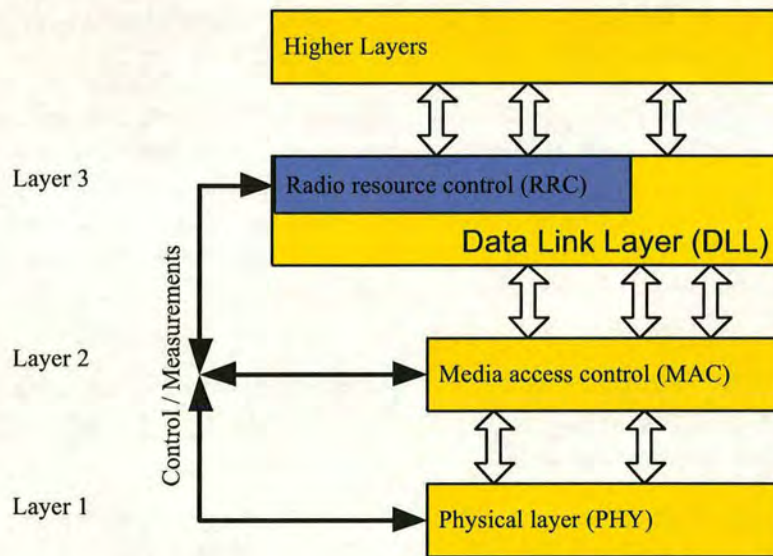


Figure 2.1: *A universal radio interface protocol architecture*

2.1 MAC Functions

As shown in figure 2.1, the MAC layer can be seen as the interface between the PHY and higher layers. Since the data processed in the DLL and PHY have different formats and styles, the MAC should translate the data formats between these two layers in terms of different configuration parameters. Moreover, the MAC will collect and calculate some important measurements, such as traffic volume, quality indications, and predicted energy consumption, and

report them to higher layers for radio resource control (RRC) and QoS control. The MAC also performs, on request of the RRC, execution of radio resource reallocation and changes of MAC parameters.

The functions of the MAC can be described in more detail as follows:

- Mapping the data format between DLL and PHY to fit the requirements of the LLC & PHY layers. These two layers have different functions and objectives, and thus have different formats. A MAC layer should afford functions to transfer these different formats and styles. For instance, in IEEE802.11-based WLAN systems [9], the data from higher layers will be re-fragmented or re-combined to fit the length of the physical service data unit (PSDU) of the PHY. A WLAN MAC also uses the information from higher layers to select between different modulation and encoding schemes in PHY layer.
- Given the transport format combination set assigned by the radio resource control (RRC) and quality of service (QoS) requirements, the MAC selects the appropriate transport format within an assigned transport format set for the data from higher layers. The control of transport formats ensures efficient use of radio channels and QoS. For instance, in WCDMA, the MAC selects the most appropriate frame format with a specified spreading factor (SF). In IEEE802.11-based WLAN, the MAC selects the control set with specified data rate, modulation method, and channel allocation.
- Calculating and reporting the features to higher layers. To operate the routing and service deliver effectively, the MAC has to collect and calculate the parameters, which contribute to the network topology and QoS-guaranteed communication, such as the traffic volume, energy consumption, data rate, end-to-end delay, connection stability, and other features, and report these characteristics to higher layers for QoS management and optimal RRC. Based on the reported information, the RRC performs transport format switching or control set change decisions.
- Identification of radio devices. The identification functionality is naturally placed in the MAC, since it handles access, and multiplexing. Commonly, the identification is based on the MAC address mechanism.
- Priority handling between radio devices by means of dynamic scheduling. In order to utilise the spectrum resources efficiently for bursty transfer, a dynamic scheduling function may be applied in the MAC layer.
- Media State Detection. For example, physical and virtual carrier-sense functions are used to determine the state of the medium (busy or idle) in CSMA/CA-based MAC protocols, such as IEEE802.11. The physical carrier-sense mechanism is provided by the PHY, which also conveys the media state to the MAC. The virtual carrier-sense mechanism is provided by the MAC. This mechanism is also referred to as the network allocation vector (NAV) in the MAC. The NAV maintains a prediction of future traffic on the medium based on duration information that is announced in RTS/CTS frames prior to the actual exchange of data. The carrier-sense mechanism combines the NAV state and the STA's transmitter status with physical carrier sense to determine the busy/idle state of the medium.

- MAC-level acknowledgments. If the received frame is correct, the receiving devices will respond with an acknowledgment, generally an ACK frame. This technique is known as positive acknowledgment in many MAC protocols. For instance, in the IEEE802.11 MAC, there are two ACK mechanisms, the two-way mechanism and the four-way mechanism.
- Controlling the operation state of radio circuits for power control or power saving. Various operating states of radio circuits, such as transmission, reception, idle, and sleeping, have different energy consumption rates. Traditional power-saving MAC protocols always try to put devices to sleep to save energy. Power control is another main function of the MAC, which is used for interference mitigation and power saving.

2.2 MAC Protocols for WLANs and WPANs

Recently, relevant commercial radio technologies have begun to appear, such as the ETSI HIPERLAN Wireless LAN standard, the IEEE 802.11 WLAN standard, the Bluetooth consortium, and IEEE802.15 WPAN standard. Most papers relating to ad hoc network MACs are discussed within these systems. Therefore, it is necessary to review the basic features of these MAC protocols before detailed study.

2.2.1 IEEE802.11

The media access method of the IEEE802.11 MAC protocol is based on the mechanism of carrier sense multiple access with collision avoidance (CSMA/CA). This mechanism can be simply called a “listen before talk” scheme. Before transmitting a packet, a station must sense the medium to determine whether other stations are transmitting or not, to ensure the medium is idle for the duration of a distributed coordination function interframe space (DIFS). If a station, which has a packet to transmit, initially senses the channel is busy, this station will wait for a DIFS period until the channel become idle, and then choose a random “back-off counter”, which determines the time that the station must wait until it is allowed to transmit its packet. During the period in which the channel is clear, the station, which prepares for transmission, decreases its back-off counter. When the channel is busy, it does not decrease its back-off counter. It can decrease its back-off counter again only after the channel is clear for DIFS. This process will be repeated until the back-off counter reaches zero and the station is allowed to transmit.

The idle period following a DIFS period is referred to as the contention window (CW), which is applied to avoid collision. The width of the CW is essential to the performance of the IEEE802.11 MAC [4] [5] [6] [10], affecting the throughput and the MAC delay [7] [8]. The value of CW is initially set to aCW_{min} , which is defined as the minimum contention window. CW is doubled each time the station encounters a collision until CW reaches aCW_{max} (Maximum contention window). When CW is increased to aCW_{max} , it remains the same even if there are more collisions. After every successful transmission, CW is reset to the initial value, aCW_{min} . There are two techniques for CSMA/CA in IEEE802.11. One is basic CSMA/CA, the other is CSMA/CA with request-to-send (RTS) and clear-to-send (CTS). The Basic scheme is a two-way handshaking technique as shown in figure 2.2. In this scheme, if a station has a

packet to transmit, it waits for a DIFS duration before transmitting its packet. When the packet is received successfully, the receiving station sends a positive acknowledgement (ACK) to the source station after a short interframe space (SIFS).

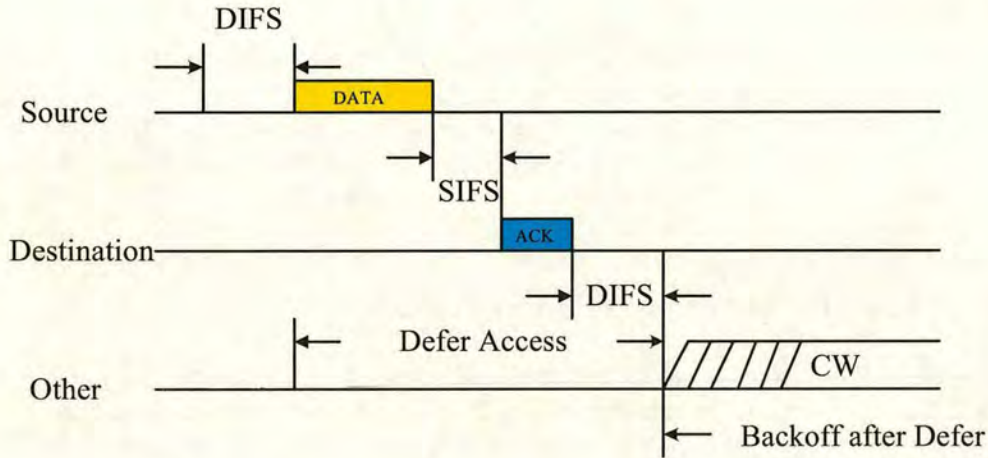


Figure 2.2: Basic CSMA scheme for packet transmission

The second scheme is four-way handshaking with RTS/CTS, which is used to avoid the “hidden terminal” problem [11].

In this scheme, whenever a packet is to be transmitted, the transmitting station firstly sends out a short request-to-send (RTS) packet containing information on the length of the packet, which is used to calculate the time that the transmission needs. If the receiving station hears the RTS, it responds with a short clear-to-send (CTS) packet to allow the transmitting station to send its packet. When the packet is received successfully, the receiving station transmits an ACK packet. Figure 2.3 illustrates the whole procedure of this scheme. In figure 2.4, where the so-called “Hidden Terminal Problem” is illustrated, station A will communicate with station B, but it cannot communicate with station C. Station A may sense that the channel is clear, when station C may be transmitting to station B. The four-way handshaking scheme described above can alert station A that station B is busy, and hence station A must wait before transmitting its packet.

2.2.2 HIPERLAN

The HIPERLAN channel access mechanism (CAM) is based on channel sensing and a contention resolution scheme called elimination yield-nonpreemptive priority multiple access (EY-NPMA) [12] [13] [14]. In the HIPERLAN CAM, the channel status is sensed by the device, which has a data frame to transmit. If the channel is sensed idle for at least 1700 bit periods, then the channel is considered free, and the node is allowed to immediately start transmission of the data frame. Each data frame transmission must be explicitly acknowledged by an ACK transmission from the destination node. Whenever a frame transmission is desired and the channel is considered not free, then, according to HIPERLAN terminology, a channel ac-

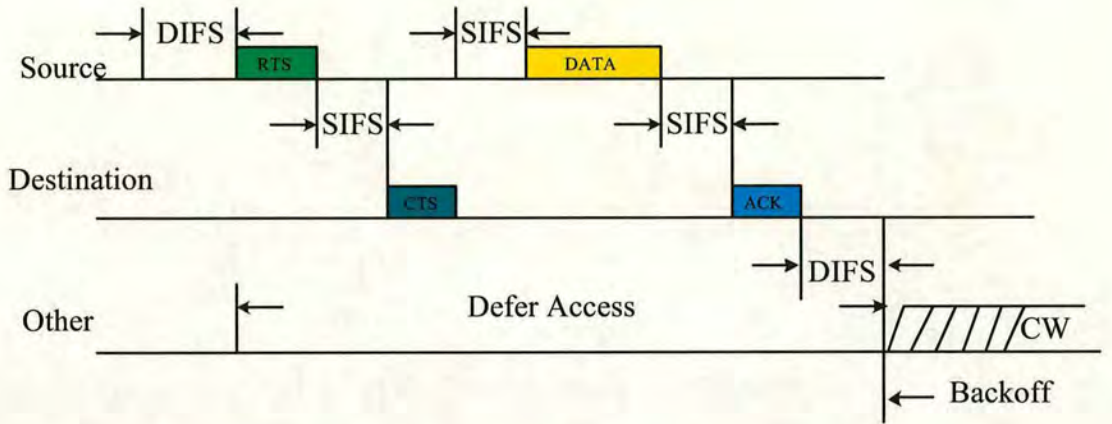


Figure 2.3: CSMA with four-way handshaking scheme

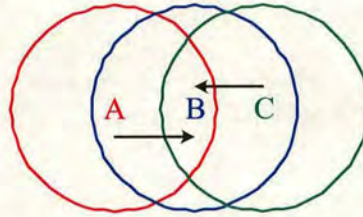


Figure 2.4: "Hidden terminal" problem when A and C communicate with B simultaneously

cess with synchronization takes place. Synchronization is performed at the end of the current transmission interval, and, at that point in time, a channel access cycle begins according to the EY-NPMA scheme. The channel access cycle consists of three phases: the prioritization phase, the contention phase, and the transmission phase. These phases are preceded by a channel access cycle synchronization interval, which is 256 bit periods long. In figure 2.5, an instance of a channel access cycle with synchronization is represented.

The aim of the prioritization phase is to allow the nodes with the highest (CAM) priority frame, among the contending ones, to participate in the next phase. In HIPERLAN, CAM priority levels are numbered from 0 to $H - 1$, where '0' denotes the highest priority level. The CAM priority of a frame starts from an initial level and decreases dynamically as a function of the user priority and the residual lifetime. The user priority is assigned to each packet according to the type of traffic. The residual packet lifetime is the time interval within which the transmission of the packet must occur before the packet has to be discarded. Since multi-hop routing is supported by the HIPERLAN system, the residual packet lifetime NMRL (normalized MPDU residual lifetime) is normalized to the number of hops, which the packet has to traverse to reach the final destination. The prioritization phase consists of at most H prioritization slots, each 256 bit periods long. Each node that has a frame with priority level h senses the channel for the first h prioritization slots (priority detection). If the channel is idle during this interval, then the node transmits a burst in the $(h + 1)^{th}$ slot (priority assertion) and it is admitted to the contention phase, otherwise it stops contending and waits for the next access cycle.

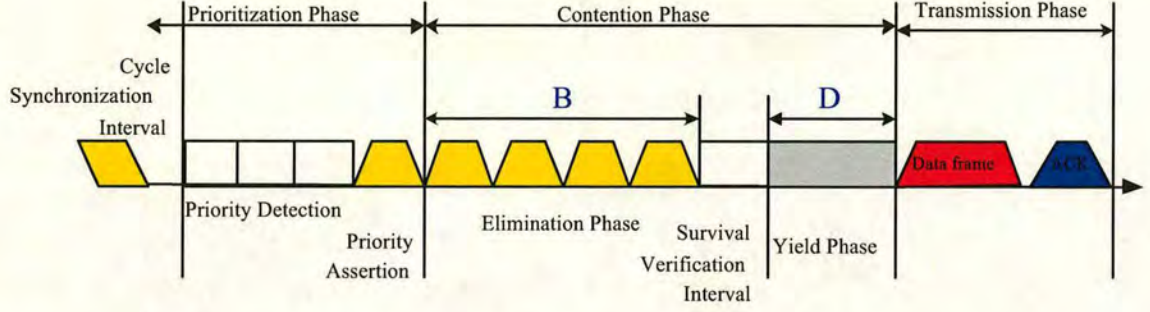


Figure 2.5: Channel access cycle in HIPERLAN

The contention phase starts immediately after the transmission of the prioritization burst, and it further consists of two phases: the elimination phase and the yield phase. The elimination phase consists of at most n elimination slots, each 256 bit periods long, followed by an elimination survival verification slot 256 bit periods long. Starting from the first elimination slot, each node transmits a burst for B , $0 \leq B \leq n$, subsequent elimination slots, according to the following truncated geometric probability distribution function:

$$Pr\{B = b\} = \begin{cases} (1-q)q^b & 0 \leq b < n \\ q^n & b = n \end{cases} \quad (2.1)$$

After the end of the burst transmission, each node senses the channel for the duration of the elimination survival verification slot. If the channel is sensed idle, the node is admitted to the yield phase, otherwise it drops itself from contention and waits for the next channel access cycle. The yield phase starts immediately after the end of the elimination survival verification interval, which is 64 bit-periods long. Each node listens to the channel for D , $0 \leq D \leq m$, yield slots before beginning transmission. D is taken from a truncated geometric distribution:

$$Pr\{D = d\} = \begin{cases} (1-q)q^d & 0 \leq d < m \\ q^m & d = m \end{cases} \quad (2.2)$$

If the channel is sensed idle during the yield listening interval, the node is allowed to enter the transmission phase, otherwise the node loses contention and has to wait for the next channel access cycle. The operating parameters in HIPERLAN, are listed in Table 2.1.

Parameter	Value
Channel Bit Rate (Mbit/s)	23.5294
Channel Access Mechanism Priority Levels (H)	5
Maximum number of subsequent elimination bursts (n)	12
Probability of bursting in an elimination slot (q)	0.5
Maximum number of subsequent Yield Listening (m)	14
Probability of listening in a Yield slot (p)	0.9

Table 2.1: The operation parameters in HIPERLAN

2.2.3 Bluetooth

Bluetooth [15] [16] is one of the wireless technologies available today that can enable devices to wirelessly communicate in the 2.5 GHz ISM (license free) frequency band. Bluetooth focuses on low cost, low size, and low power, which distinguishes it from the IEEE802.11 WLAN technology. It supports both point-point wireless connections without a cable, and point-to-multi-point connections to enable ad hoc wireless networks [17] [18].

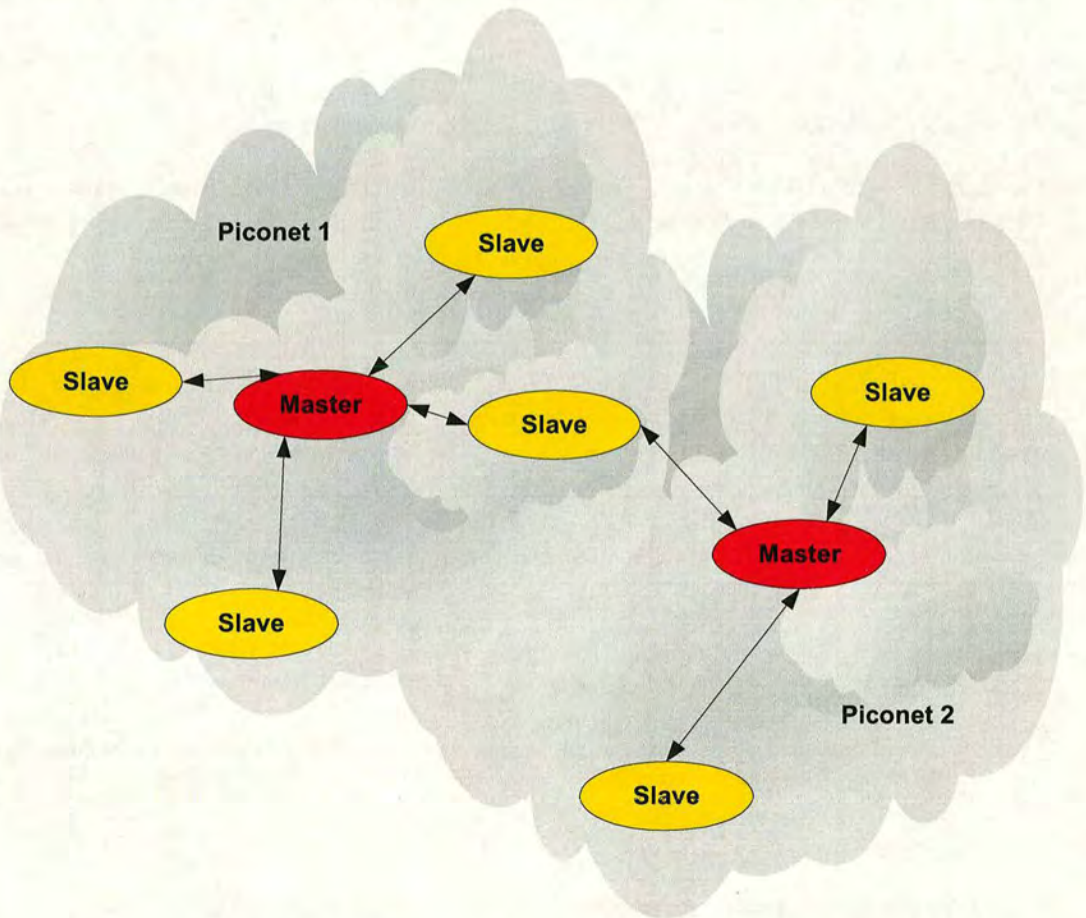


Figure 2.6: *An example of scatternet, which comprises of two Piconets.*

2.2.3.1 Connectivity

A basic Bluetooth network is called a Piconet, which is defined as the set of at most seven active devices, called slave devices, operating under the control of a single device, which is called a master device. A set of Bluetooth networks is called a scatternet.

To be a master device, a device should initially request a connection with another device. If the paged device accepts the link, the calling device becomes a master for that link and the responding device becomes a slave. As can be inferred from the simple manner in which a

device can become a master or a slave, the network for Bluetooth is dynamic. Figure 2.6 shows an example of a scatter network, which comprises two Piconets.

Bluetooth devices have to support two types of traffic, voice and data, whose QoS demands are different. Voice can tolerate a certain number of errors in a link, however, it is susceptible to jitter. Therefore, Bluetooth needs to support a synchronous data stream on the order of tens of kbits per second without the strict error-free requirement. On the other hand, data services generally don't need strict timing requirements compared to voice service, but require lower bit error rates.

2.2.4 IEEE802.15

Compared to other similar wireless networks, such as WLAN, and wireless cellular networks, the wireless personal area network (WPAN) is operated within a smaller personal space, whose diameter is less than 10m, and support higher data rates, of more than 20Mbit/s. Moreover, a WPAN will have less infrastructure than WLANs, so it should be operate in an ad hoc network style.

There are two branches in IEEE802.15 MACs. One is IEEE 802.15.3 [19], issued in September 2003, which is suitable for low power consumption and high data rate wireless WPANs. This protocol has the QoS capability through selecting the high priority packet. Because of the reasonable power saving, power control management, QoS, and security mechanisms in IEEE 802.15.3, it is also the potential MAC protocol for ultra wide band (UWB) communication. The other is IEEE802.15.4 [20], which could be used for a sensor network with low data rate and energy efficiency.

2.2.4.1 Piconet

In IEEE 802.15.3/4, the network is divided into piconets, which have the following characteristics:

- Ad Hoc data communication system;
- Operated within a small area around person or object (Diameter < 10m);
- The communication devices may be stationary or in motion;
- Devices within a Piconet are most likely to be battery operated.

As in a Bluetooth network, in a Piconet, a dynamic "master" device, manages other network members. This device is called the Piconet Coordinator (PNC). Other devices are called DEV. The PNC uses the beacon frame to manage the QoS requirements, power saving modes, and the media access control to the piconet. The PNC also classifies the various packet transmissions, which are requested by the DEVs. Different packets have different priority levels for transmission. For instance, control packets have priority to access the media. If the PNC finds other devices are more capable than itself, it hands over control of this piconet to the more appropriate DEV. That means the piconet in IEEE 802.15.3/4 has a dynamic membership, thus adapting to the dynamically changing environment and topology.

2.2.4.2 Starting, Maintaining, and Stopping Piconets

An unconnected device should scan all the radio channels and collect the statistics of each channel, thus detecting any active Piconets. If none are found then the device may initiate a new piconet. To start a piconet, the device management entity (DME), which is a layer-independent entity with the function of gathering the layer-dependent status and parameters from the various layer management entities, sends a channel-scan request to the MAC. Then the DEV enters receive mode and traverses through all the indexed channels. The DEV will listen to each channel for a while to look for a beacon from the PNC. If the DEV cannot find the beacon from any PNCs in a scanned channel, then this channel is a possible channel to start a new piconet. Finishing the scan of all the channels, the DEV returns the results to the MAC layer. Figure 2.7 shows the scan operation between the DME and the MAC/MLME (MAC Layer Management Entity). After scanning all the possible channels, a DEV will choose an appropriate channel to start the piconet. This channel should have the least amount of interference. Once a PNC has built a piconet, it will periodically scan the channel. If there is another piconet in the same channel, the PNC will move to a different channel or reduce the piconet's transmission power to improve coexistence with other piconets. If the PNC finds that it cannot have the capability for a PNC any longer, or the PNC prepares to leave the piconet, it will start the handover procedure, which will transfer its PNC functionality to another capable DEV. The PNC will stop the piconet operation under the following instances:

- It receives a shut down request from higher layer;
- No DEV is capable of taking over as PNC in the Piconet;
- There is insufficient time for a handover operation.

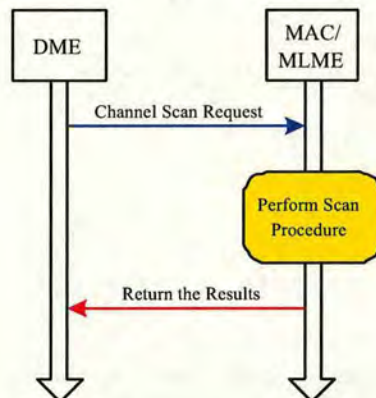


Figure 2.7: *A DEV needs scan the channels to start a Piconet*

2.2.4.3 Association, and Disassociation with a Piconets

A device entering a piconet should initially send an association request to the PNC. Then the PNC will send a response to this DEV to indicate that the DEV has been accepted or rejected.

The PNC will send the reason for the rejection to the DEV as well. The rejection reasons are listed below:

- Already serving a maximum number of DEVs;
- Lack of available channel time to serve the DEV;
- Channel too severe to serve the DEV;
- PNC turning off with no PNC capable DEV in the piconet;
- Not allowed by neighbouring Piconets ;
- Channel change in progress;
- PNC handover is in progress

After accepting a new DEV, the PNC will broadcast the piconet information to all the DEVs in the piconet again.

If the DEV wants to leave the piconet, or the PNC wants to remove the DEV from the piconet, a disassociation request command with the disassociation reason is required. To indicate their existence, all the DEVs should send frames to the PNC often enough. If the PNC does not receive any information from a DEV within the association timeout period (ATP), the PNC will disassociate that DEV. (When a DEV does not have any traffic needed to send to the PNC, it will send a so-called Probe Request command to make the PNC reset the ATP time counter.) This is important for the PNC to keep the valid information about the piconet. The association or disassociation procedure should co-operate with higher layer protocols. For example, the network layer might need the set of valid nodes for the routing protocol.

2.2.4.4 Channel Access

In IEEE 802.11, the media access is based on CSMA/CA, in which each station has equal right to access the channel. In IEEE 802.15.3/4, the PNC globally controls the channel access of each DEV in a Piconet. The channel time is divided into superframes. As illustrated in figure 2.8, a superframe has three parts, the Beacon, the Contention Access Period (CAP), and the Channel Time Allocation Period (CTAP).

The CAP and the CTAP are optional periods. The allocation information about the CAP and the CTAP is indicated in the beacon. In a CAP, DEVs access the channel based on CSMA/CA. The CAP is used for commands or non-stream data, which ensures a light traffic load. In order to minimize the collision, a DEV should wait for a random period at first, and then begin to transmit. Before transmission, a DEV should check the remaining time in the CAP. If there is insufficient time for the whole frame transmission, the DEV will suspend the transmission in the current superframe. In IEEE 802.15.3, being outside of a CAP period or if there is not enough time remaining in a CAP will also cause the backoff counter to be suspended. When a DEV cannot receive an ACK after sending a packet, it will retransmit the packet, but no more than 3 times. In a CTAP, the channel access is based on TDMA. The CTAP is divided into many

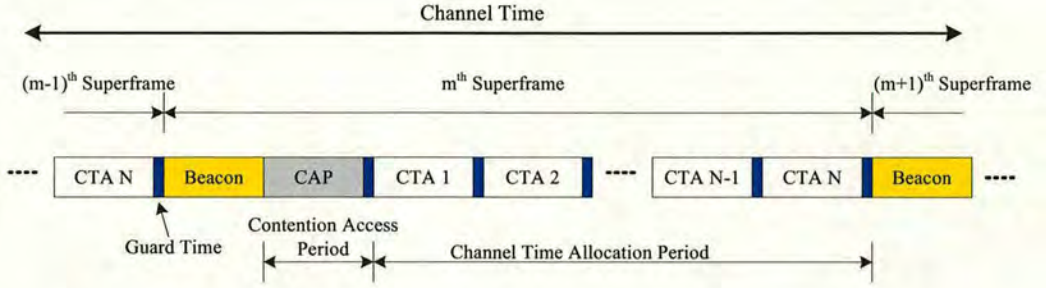


Figure 2.8: *The channel time and the superframe*

Channel Time Allocations (CTAs) with fixed duration and start time. Each CTA is assigned to an individual DEV or a group DEVs. The location of each CTA and the duration is specified in the beacon. The CTAP is suitable for all kinds of data. A DEV requests that the PNC to allocate a CTA for its data exchange. Normally, the CTA can support bulk data (such as multi-Megabyte sized image files), and isochronous data (such as a video stream) equally well. The IEEE 802.15.3/4 standard does not specify how to allocate the CTAs to DEVs.

2.3 Low Power Consumption MAC Protocols

Many mobile devices are battery operated. Energy exhaustion is an important issue relating to topology stability and quality of service (QoS). This issue should be considered through all layers [21] [22] [23].

Considering MAC related activities, the main contribution of energy consumption in wireless communication devices is introduced by the transmitter and the receiver. The radio operation can be divided to four modes: sleep, standby, receive, and transmit. In general, the radio operations consume more energy in the transmit mode than in the receive mode, and consume least power in the sleep mode. One of the main objectives of a power-saving MAC protocol design is to minimize the duration of transmission and receiving, or to try to put the radio unit to sleep for a longer time.

2.3.1 Energy Conservation MAC Design

Roughly speaking, the MAC layer is responsible for data framing, efficient sharing of the channel, and possibly some error control. There are several options for an energy efficient MAC protocol design. In general, simple protocols need relatively less power than complex protocols. For example, a large number of necessary control messages negatively influences energy efficiency. In the following, some options are outlined for power-saving MAC design.

Packet Structure

Due to excessively long headers or trailers, the energy-per-data-bit performance may be degraded. One solution to this problem is header compression. Moreover, higher power con-

sumption is generally required for higher bit rates. One reason is the frequently required higher equalization complexity needed to deal with the inter-symbol interference at higher bit rates. Therefore, another idea regarding the packet structure, is to split the packet into different parts with different data rates. For example, a low-bit-rate part for control information, and a high-bit-rate part for data assigned by higher layers.

Awake and Sleep Mode

To save energy the network interface card/unit may be switched off when there are no transmissions. Following this idea, using the sleep mode has the potential to achieve power saving gains. Unfortunately, this may disrupt the capability to communicate in both directions, since a station in this kind of power saving mode would not know of any data arriving. Nevertheless, it is possible to switch off the communication unit if some methods are developed to ensure stations' communication capabilities. For instance, time synchronization functions could guarantee each station to be awake to exchange traffic information. Besides the power saving impacts on the MAC design, there are impact on other protocol layers, such as routing protocols in the network layer.

MAC-Level Error Control

The channel quality is often improved by forward error correction (FEC) on the PHY layer. If the offered channel quality is still not satisfactory, MAC-level retransmissions may be used. Since the radio channel quality may be persistent in a state for a while (good or impaired), retransmission of MAC packets in the impaired radio channel states is ineffective and therefore expensive. Short low-power probe packets may be useful, improving the efficiency of communication. When one probe packet has been successfully transmitted indicating an appropriate channel quality, retransmission of the data packet is scheduled. In other words, retransmission of data at a relatively high power level is only scheduled if the channel quality is sufficient. As a result, no energy is wasted on retransmission during channel impairments.

2.3.2 IEEE802.11 Ad Hoc Network Power Saving MAC

In the IEEE 802.11 standard, there are two power saving (PS) modes, infrastructure network PS (INPS), and ad hoc network PS (AHNPS). The main difference between these two modes is the synchronization method. In INPS, the access point (AP) centrally controls synchronization by sending periodic beacon frames. In AHNPS, all stations have the chance to send synchronization beacons in a distributed manner. Following the beacon frame, there is an ATIM window, during which each station keeps awake to listen to packet exchange information.

In AHNPS, it is assumed that the power-saving stations can be fully connected and synchronized so that they can periodically wake up at the same time for a short ATIM window. The first thing that the stations do when their ATIM window starts is to contend to send a beacon frame. To avoid the collision, a station selects a backoff window, of up to $2 \times aCW_{min}$ slots, for the backoff algorithm to attempt to send a beacon frame. Here, aCW_{min} is the minimum contention window size defined in the standard. The successfully sent beacon is the synchronization clock signal for all stations. This beacon stops other stations trying to send a beacon frame in the current ATIM window. Stations adjust their clock only if the timestamp in the received beacon frame is beyond their own timestamp. The stations with buffered unicast packets

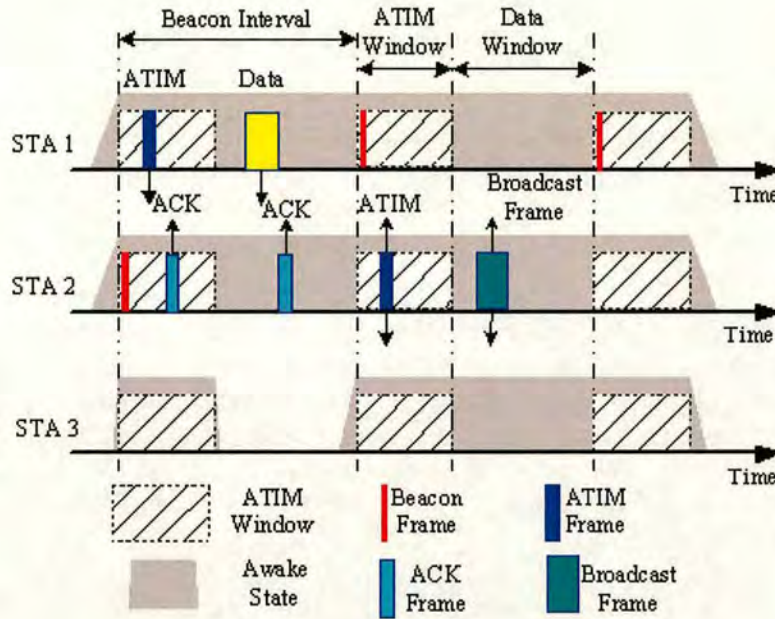


Figure 2.9: IEEE802.11 ad hoc network power saving operations

contend to send ATIM frames to each of their intended receivers in PS mode. After transmitting an ATIM frame, the station waits for an ACK from the corresponding station. If the sender does not receive an ACK, it will re-send the ATIM frame in the next ATIM window. After the ATIM window, stations with buffered packets should keep awake during the remaining time of the beacon period, which includes the data window, to fulfill packet exchange tasks, other stations go into sleep mode. The buffered unicast packets are sent within the data window. If a station has buffered broadcast packets, it sends an ATIM frame and transmits the broadcast packets without waiting for ACK frames. Figure 2.9 illustrates the AHNPS operations. Station 1 wants to transmit a data frame to station 2. Firstly, Station 1 transmits an ATIM frame during the ATIM window. Station 2 will send an ACK to station 1 after receiving the ATIM frame. If station 1 receives the ACK frame, it transmits the buffered data frame to station 2 after the ATIM window. When station 2 has a broadcast frame, it transmits the ATIM frame within the ATIM window, and then send that broadcast frame after the ATIM window. No ACK frames are needed in this case. When a station receives a beacon, it sets its time synchronization function (TSF) timer to the timestamp, enclosed in the beacon, if the value of its own timestamp is less than the timestamp in the beacon, which means the clocks only move forward and never backward.

2.3.3 IEEE802.15.3 Power Saving MAC

IEEE802.15.3 Based WPAN and its Superframe

In IEEE 802.15.3, the PNC globally controls channel access for each DEV. The channel time is divided into superframes. As illustrated in Figure 2.8, a superframe has three parts, Beacon,

Contention Access Period (CAP), and Channel Time Allocation Period (CTAP). The CAP and the CTAP are optional periods. The allocation information about the CAP and the CTAP is indicated in the beacon.

The CAP is used for commands or non-stream data, which ensures a light traffic load. In a CAP, DEVs access the channel based on CSMA/CA. In order to minimize collisions, a DEV should wait for a random length of time at first, and then begin to transmit. When a DEV cannot receive an ACK after its sending a packet, it retransmits the packet, for up to 3 times [19].

The channel access in a CTAP is based on TDMA. The CTAP is divided into many Channel Time Allocations (CTAs) with fixed duration and start time. Each CTA is assigned to an individual DEV or a group of DEVs. The location of each CTA and its duration is specified in the beacon by the PNC. The CTAP is designed for all kinds of data. A DEV makes a request of the PNC for a CTA in which to exchange data. Because the full duration of the CTA can be utilized by a DEV or a group of DEVs, successful transmission will result. The CTA can support bulk data (such as multi-Megabyte sized image files), and isochronous data (such as a video stream) effectively.

Superframe portion	APS	PSPS or DSPS
Beacon	Awake	Awake
CAP	May sleep	Awake
CTA	May sleep	May sleep

Table 2.2: *Power management rules for superframe*

IEEE802.15.3 Power-saving Mode

There are three power saving modes in IEEE802.15.3, which are Piconet synchronized power save (PSPS) mode, device synchronized power save (DSPS) mode, and asynchronous power save (APS) mode. In any given PS mode, a DEV may be in one of two power states, either awake or sleep states. Table 2.2 shows the possible state a DEV may entry during different portions of a superframe.

Piconet Synchronized Power-saving (PSPS) Mode

In PSPS mode, a DEV should be awake to hear the beacons, announced by the PNC. A DEV also should be awake during CAP to obtain the instructions send from the PNC to control its state during CTA. If a DEV in PSPS mode does not correctly receive the system wake beacon, it remains in the awake state during the expected beacon transmission times to receive the following beacons until a beacon is correctly received. DEVs obtain timestamps from beacon frames to synchronize. Since the PSPS mode is very similar to the ad hoc network power-saving mode in IEEE802.11, the analysis of power-saving mode in IEEE802.11 can be equivalently applied to the PSPS. Therefore, in this thesis, we mainly focus on the PSPS for the power-saving MAC study in WPANs.

Device Synchronized Power-saving (DSPS) Mode

The DSPS mode allows a DEV that is sensitive to power to synchronize its awake state with other DEVs. The DSPS mode is based on grouping DEVs that have similar power save re-

quirements into DSPS sets. These DSPS sets are managed by the PNC, but the parameters of the sets are determined by the DEVs. Each DSPS set has two important associated parameters: the wake beacon interval (WBI) and the next wake beacon (NBI). The WBI is the number of superframes between two successive wake beacons of that DSPS set. This value is set by the DEVs. The NBI is the beacon number corresponding to the next wake beacon of that DSPS set.

Asynchronous Power-saving (APS) Mode

The APS mode allows a DEV to conserve power by remaining in a sleep state for an extended period of time. The only responsibility of a DEV in APS mode is to communicate with the PNC before the end of its ATP in order to preserve its membership in the Piconet. In the APS mode, the DEV is not required to listen to any beacons or other traffic until it changes to either active or a different power saving mode.

2.4 Summary

The MAC layer can be seen as the interface between the PHY and higher layers. The main functions of MAC protocols were presented in this chapter. This chapter also discusses different MAC protocols used for WLAN and WPAN. Functions in the MAC layer can be amended to decrease the energy consumption. However, the cost of energy saving by MAC layer functions might be reducing the networking performance, such as increased MAC delay and lower throughput. Since the power-saving MACs in IEEE802.11 WLANs and IEEE802.15 WPANs will be frequently mentioned as examples in other chapters, these two typical energy-efficiency MACs were discussed in this chapter.

is the basic channel access method in the IEEE802 standard family, has been well studied before. However, the analytical model for the IEEE802.11 power-saving mode has not been fully investigated before. Since other power-saving MACs have similar structure and use the same media access mechanism, CSMA/CA, the same analytical methods can be applied to evaluate their performance. To obtain a generic result, other effects, such as a channel model with Rayleigh fading, and power capture, are considered in the analysis.

3.1.1 Propagation Model

The propagation model can be statistically modelled by three independent multiplicative propagation mechanisms; which are multipath fading, shadowing and path loss in groundwave propagation [30]. The area-mean power w_a , which is determined by the pass loss, at a distance r_i from the transmission station can be denoted by:

$$w_a = r_i^\xi \quad (3.1)$$

where the path-loss exponent, ξ , for indoor channels is typically between 3 and 4 [31].

When shadowing is superimposed on path loss, the local-mean power, ω_L , can be described as a lognormal distribution with logarithmic standard deviation σ_s . Assume the absence of direct path between the transmitter and the receiver in an indoor environment [31], which means the envelop of transmitted signal is characterized by Rayleigh fading. Therefore, the instantaneous received power, ω_s , of a signal from a remote station is exponentially distributed around the local-mean power ω_L .

Including all the above factors, the Probability Density Function (PDF) of the instantaneous power, ω_s , of a received packet can be described as [30] [31]:

$$f_{\omega_s}(\omega_s) = \int_0^\infty \int_0^\infty \frac{1}{\omega_L} \exp\left(-\frac{\omega_s}{\omega_L}\right) \cdot \frac{f(r_i)}{\sqrt{2}\sigma_s\omega_L} \cdot \exp\left(-\frac{(\ln(r_i^\xi\omega_L))^2}{2\sigma_s^2}\right) dr_i d\omega_L \quad (3.2)$$

where $f(r_i)$ is the PDF of the propagation distance. Assume the wireless stations are uniformly distributed in a circle of unit radius, which means a uniform spatial distribution, the PDF is given by a beta distribution [32]:

$$f(r_i) = \frac{1}{2} \frac{1}{B(2, 2.5)} \frac{r_i}{2} \left(1 - \frac{r_i}{2}\right)^{3/2}, \quad r_i \in (0, 2) \quad (3.3)$$

where $B(a,b)$ is the beta function.

3.1.2 Power Capture Model in Rayleigh Fading Channel

In an indoor environment, such as a Wireless LAN, it is unrealistic to assume that all simultaneously sent packets are destroyed because of collision. The received signal strength (RSS) of

the packets from different remote stations is not the same due to the differences of the transmission power and channel fading. As the power capture effect, a packet can be decoded by the receiver when its RSS is greater than the joint power of other simultaneous transmissions by a certain threshold for a period of time. The conditional probability that the k^{th} station's packet is captured in the presence of n interfering sources can be described as:

$$p_{cap}(r_0 \cdot g(S_f)|n) = \Pr \left\{ \omega_k / \sum_{i=1}^n \omega_i > z_0 \cdot g(S_f) | n \right\} \quad (3.4)$$

where ω_k is the detected power of the captured packet, $\sum_{i=1}^n \omega_i$ is the incoherent sum of other mobile powers, z_0 is the capture threshold radio, and $g(S_f)$ is the processing gain of the correlation receiver. Assume that the preamble of a frame is enough for a receiver to obtain a successful frame capture, and the transmission power of this period is assumed to be constant. For instance, in IEEE 802.11b, using Direct Spreading Sequence Spectrum (DSSS) modulation, the preamble is modulated by a fixed 11-chip Barker spreading sequence, where the spreading factor S_f is 11. Using the results in [33], $g(S_f)$ can be specified by the equation below when rectangular-shaped chips are applied.

$$g(S_f) = \frac{2}{3 \cdot S_f} \quad (3.5)$$

If we assume the power control is not applied by any stations and all the detected power of stations are mutually independent, then the capture probability that the k^{th} station's packet is captured in the presence of n interfering sources can be written as in [32]:

$$p_{cap}(z_0 \cdot g(S_f)|n) = \int_0^\infty f_{w_1}(w_1)dw_1 \cdots \int_0^\infty f_{w_n}(w_n)dw_n \int_{z_0 \cdot g(S_f) \sum_{i=1}^n w_i}^\infty f_{w_k}(w_k)dw_k \quad (3.6)$$

where $\int_0^\infty f_{w_i}(w_i)dw_i$, ($i = 1, 2, \dots, n; i \neq k$), is the probability that the i^{th} station has a local mean power, w_i , and $\int_{z_0 \cdot g(S_f) \sum_{i=1}^n w_i}^\infty f_{w_k}(w_k)dw_k$ is the probability that the k^{th} station's local mean power, w_k , is bigger than the capture threshold.

As discussed in [33], the probability, τ , that a station transmits a packet in an observed slot when using the CSMA/CD MAC mechanism is dependent on the number of contending stations, N , and other parameters in IEEE 802.11 DCF. The probability, $p_r(i)$, that i stations simultaneously send packets in a slot is:

$$p_r(i) = \binom{N}{i} \tau^i (1 - \tau)^{N-i} \quad (3.7)$$

where N is the total number of stations. Then the unconditional capture probability can be estimated as:

$$p_{cap}(N) = \sum_{i=2}^N p_i(i) \cdot p_{cap}(z_0 \cdot g(S_f)|i) \quad (3.8)$$

3.1.3 Successful Packet Transmission Rate

To simplify the performance study under AHNPS mode, it is assumed that the transmission queue of each PS station is always nonempty. As discussed in [33], the probability, $p_{tr}(N)$, of at least one transmission in the observed time slot under the N -station condition is expressed as:

$$p_{tr}(N) = 1 - (1 - \tau(N))^N \quad (3.9)$$

Obviously, if just one station sends a packet in a slot, collision is avoided and this station successfully transmits the packet. On the other hand, if some stations send packets simultaneously, due to the capture effect, one station may still successfully transmit a packet. So the probability, p_s , of exactly one of the N stations successfully transmitting a packet, which is conditioned on at least one station transmitting, is the probability that just one station transmits a packet in a slot without any collision plus the probability that the signal strength of a packet meets the power capture condition. So p_s can be written as:

$$p_s(N) = [N \cdot \tau(N) \cdot (1 - \tau)^{N-1} + p_{cap}(N)] / p_{tr}(N) \quad (3.10)$$

Define $p_a(W_A)$ as the probability that a station successfully transmits an ATIM packet in the ATIM window, W_A , under the N -station condition. Firstly, we investigate the probability $p_{as}(W_A, k)$, which denotes that a station successfully transmits an ATIM packet, and this is the k^{th} ATIM packet transmission within the ATIM window. At the beginning of the ATIM window, N stations start to contend to transmit an ATIM packet. Assume the 1^{st} successful transmission occurs in the slot m_1 , which means there are no successful transmissions before m_1 (Figure 3.2), and all other stations are scheduled to send packets within the window $[m_1+1, W_A]$. Then the probability $p_{as}(W_A, 1)$ can be written as:

$$p_{as}(W_A, 1) = \sum_{m_1=0}^{W_A-T_{ATIM}+1} \sum_{x=1}^N \binom{N}{x} \left(\frac{W_A-m_1}{W_A} \tau(N) \right)^{N-x} \left(\frac{1}{W_A} \tau(N) \right)^x \times p_{cap}(z_0 \cdot g(S_f)|x) \quad (3.11)$$

where $\binom{N}{x} \left(\frac{W_A-m_1}{W_A} \tau(N) \right)^{N-x} \left(\frac{1}{W_A} \tau(N) \right)^x = (W_A - m_1)^{N-x}$ is the probability that x stations transmit in slot m_1 , and all other stations transmit in the window $[m_1+1, W_A]$.

For simplicity, define:

$$\psi_s(N, W_A, m_1) = \sum_{x=1}^N \binom{N}{x} (W_A - m_1)^{N-x} \cdot p_{cap}(z_0 \cdot g(S_f)|x) \quad (3.12)$$

Then $p_{as}(W_A, 1)$ can be written as:

$$p_{as}(W_A, 1) = \sum_{m_1=0}^{W_A - T_{ATIM} + 1} \psi_s(N, W_A, m_1) \quad (3.13)$$

The values of T_{ATIM} (Figure 3.1) in the basic access mechanism and in the RTS/CTS access mechanism are specified by (3.14).

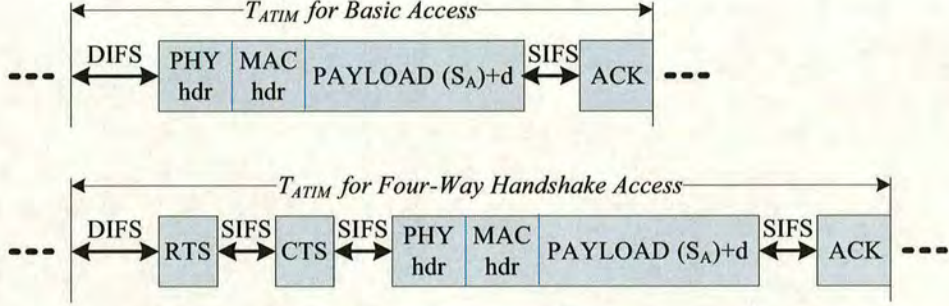


Figure 3.1: T_{ATIM} in basic access and four-way handshake access

$$\begin{aligned} T_{ATIM, Basic} &= H + S_A + SIFS + ACK + DIFS + \delta \\ T_{ATIM, RTS} &= RTS + SIFS + CTS + SIFS + H + S_A + SIFS + ACK + DIFS + \delta \end{aligned} \quad (3.14)$$

In (3.14), S_A is the size of the ATIM packet, H is the size of the packet header, including PHY_{hdr} and MAC_{hdr} , and δ is a slot time. It is clear that the four-way handshake CSMA/CA, which uses RTS and CTS, will prolong the transmission time, though this mechanism can save bandwidth resource when collisions occur.

Equation (3.13) depicts the probability that the first successful ATIM packet transmission occurred in slot m_1 with capture. Conversely, when the received signal strength of those x stations, who transmit simultaneously in slot m_1 , do not meet the power capture condition, a collision will occur. This collision will affect the subsequent transmission in a size-limited window. Let $p_{ac}(W_A, 1)$ be the collision probability, which can be defined as:

$$p_{ac}(W_A, 1) = \sum_{m_1=0}^{W_A - T_{ATIM} + 1} \sum_{x=1}^N \binom{N}{x} (W_A - m_1)^{N-x} (1 - p_{cap}(z_0 \cdot g(S_f)|x)) \quad (3.15)$$

For simplicity, define:

$$\psi_c(N, W_A, m_1) = \sum_{x=1}^N \binom{N}{x} (W_A - m_1)^{N-x} \cdot (1 - p_{cap}(z_0 \cdot g(S_f)|x)) \quad (3.16)$$

Then $p_{ac}(W_A, 1)$ can be written as:

$$p_{ac}(W_A, 1) = \sum_{m_1=0}^{W_A - T_{ATIM} + 1} \psi_c(N, W_A, m_1) \quad (3.17)$$

The RTS/CTS mechanism can dramatically reduce the average time the channel is busy during a collision. The average busy time of the channel for the two different access mechanisms is given in (3.18). The collision duration in the four-way handshake access mechanism is shorter than that in the basic access scheme, which means the former saves bandwidth under severe channel access competition.

$$\begin{aligned} T_{c,Basic} &= H + S_A + DIFS + \delta \\ T_{c,RTS} &= RTS + DIFS + \delta \end{aligned} \quad (3.18)$$

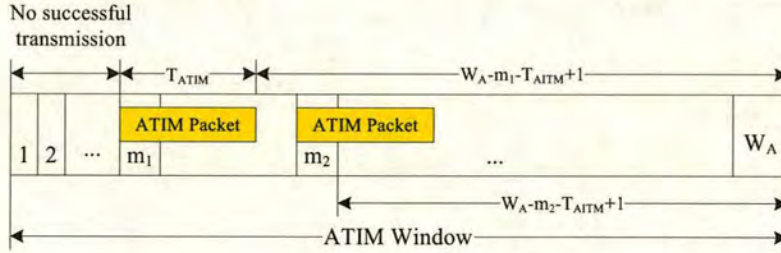


Figure 3.2: *ATIM packet transmission*

After the 1st successful ATIM packet transmission, the remaining $(N-1)$ stations continue to try to send their ATIM packets within a narrower ATIM window, whose size is $W_{A.S}^{(1)} = W_A - m_1 - T_{ATIM} + 1$ (Figure 3.2). When a collision occurs in slot m_1 , the N stations will try again to send ATIM packets within a narrower ATIM window, whose size becomes $W_{A.C}^{(1)} = W_A - m_1 - T_C + 1$. The probability, $p_{as}(W_A^{(1)}, 2)$, that the second ATIM transmission is successful in slot m_2 is given as:

$$\begin{aligned} p_{ac}(W_A^{(1)}, 2) &= \Pr\{\text{A successful transmission in slot } m_2 | p_{as}(W_A, 1)\} \\ &+ \Pr\{\text{A successful transmission in slot } m_2 | p_{ac}(W_A, 1)\} \end{aligned} \quad (3.19)$$

The first part of equation (3.19) can be written as:

$$p_{s2s}(1) = p_{as}(W_A, 1) \sum_{m_2=m_1+T_{ATIM}-1}^{m_2=W_A-T_{ATIM}+1} \psi_s(N-1, W_{A.S}^{(1)}, m_2); \quad W_{A.S}^{(1)} = W_A - m_1 - T_{ATIM} + 1 \quad (3.20)$$

The second part of equation (3.19) is:

$$p_{c2s}(1) = p_{ac}(W_A, 1) \sum_{m_2=m_1+T_C-1}^{m_2=W_A-T_{ATIM}+1} \psi_s(N, W_{A.C}^{(1)}, m_2); W_{A.C}^{(1)} = W_A - m_1 - T_C + 1 \quad (3.21)$$

Similarly, the probability, $p_{ac}(W_A^{(1)}, 2)$, that a collision occurs in slot m_2 is composed of two parts, given by:

$$p_{ac}(W_A^{(1)}, 2) = \Pr\{\text{A collision in slot } m_2 | p_{as}(W_A, 1)\} + \Pr\{\text{A collision in slot } m_2 | p_{ac}(W_A, 1)\} \quad (3.22)$$

The first part of the equation (3.22) may be written as:

$$p_{s2c}(1) = p_{as}(W_A, 1) \sum_{m_2=m_1+T_{ATIM}-1}^{m_2=W_A-T_{ATIM}+1} \psi_c(N-1, W_{A.S}^{(1)}, m_2); W_{A.S}^{(1)} = W_A - m_1 - T_{ATIM} + 1 \quad (3.23)$$

The second part of (3.22) is given by:

$$p_{c2c}(1) = p_{ac}(W_A, 1) \sum_{m_2=m_1+T_C-1}^{m_2=W_A-T_{ATIM}+1} \psi_c(N, W_{A.C}^{(1)}, m_2); W_{A.C}^{(1)} = W_A - m_1 - T_C + 1 \quad (3.24)$$

The probability $p_{as}(W_A^{(k-1)}, k)$, which is the probability that k^{th} ATIM transmission is successful, can be written as:

$$\begin{aligned} p_{as}(W_A^{(k-1)}, k) &= p_{s2s}(k-1) + p_{c2s}(k-1) \\ &= p_{as}(W_A^{(k-2)}, k-1) \sum_{m_k=m_{k-1}+T_{ATIM}-1}^{m_k=W_A-T_{ATIM}+1} \psi_s(N_s^{(k-1)} - 1, W_{A.S}^{(k-1)}, m_k) \\ &\quad + p_{ac}(W_A^{(k-2)}, k-1) \sum_{m_k=m_{k-1}+T_C-1}^{m_k=W_A-T_{ATIM}+1} \psi_s(N_c^{(k-1)}, W_{A.C}^{(k-1)}, m_k) \end{aligned} \quad (3.25)$$

where $W_{A.S}^{(k-1)} = W_A - m_{k-1} - T_{ATIM} + 1$, $W_{A.C}^{(k-1)} = W_A - m_{k-1} - T_C + 1$, $N_s^{(k-1)}$ is the number of stations in the $(k-1)^{th}$ successful transmission, and $N_c^{(k-1)}$ is the number of stations in the $(k-1)^{th}$ collision transmission.

The probability $p_{ac}(W_A^{(k-1)}, k)$, which is the probability that the k^{th} ATIM transmission is in collision, can be written as:

$$\begin{aligned}
p_{ac}(W_A^{(k-1)}, k) &= p_{s2c}(k-1) + p_{c2c}(k-1) \\
&= p_{as}(W_A^{(k-2)}, k-1) \sum_{m_k=W_A-T_{ATIM}+1}^{m_k=W_A-T_{ATIM}+1} \psi_c(N_s^{(k-1)} - 1, W_{A.S}^{(k-1)}, m_k) \\
&\quad + p_{ac}(W_A^{(k-2)}, k-1) \sum_{m_k=m_{k-1}+T_C-1}^{m_k=W_A-T_{ATIM}+1} \psi_c(N_c^{(k-1)}, W_{A.C}^{(k-1)}, m_k)
\end{aligned} \tag{3.26}$$

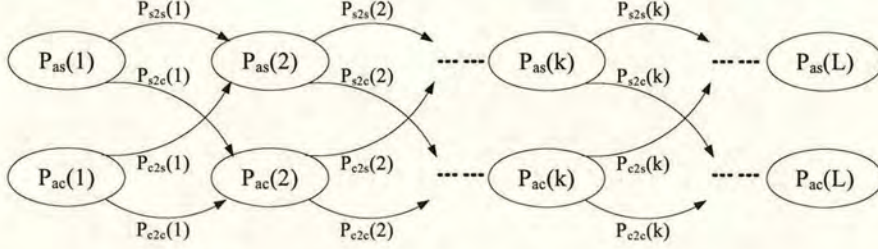


Figure 3.3: The state model to compute $p_{as}(W_A, k)$

A state model to calculate $p_{as}(W_A, k)$ is given in Figure 3.3, where p_{s2s} , p_{s2c} , p_{c2s} , and p_{c2c} are the transfer probabilities between consecutive ATIM packet transmissions. The generic definition of these transfer probabilities is given by (3.25), and (3.26). The value of L , which is the maximum number of ATIM transmissions, is determined by the size of remaining ATIM window. Before computing $p_{as}(W_A, k)$ and other transfer probabilities, the value of the remaining ATIM window, $W_{A.S}^{(k-1)}$, is checked. If the residual ATIM window is less than T_{ATIM} , the calculation will be terminated. L satisfies the following condition:

$$2T_{ATIM} \geq W_{A.S}^{(L-1)} \geq T_{ATIM} \tag{3.27}$$

Finally, the probability, $p_a(W_A)$, is the aggregation of all the possible successful transmissions in the ATIM window. Therefore, $p_a(W_A)$ is:

$$p_a(W_A) = \sum_k p_{as}(W_A^{(k-1)}, k), \quad 1 \leq k \leq N \tag{3.28}$$

The analytical results for $p_a(W_A)$ are illustrated in Figure 3.4 and 3.5. The successful transmission rate of the ATIM packet is very sensitive to the number of stations, the width of the ATIM window and the capture rate. When the number of stations is large, increasing the percentage of the ATIM window size will significantly improve transmission performance. However, large ATIM windows degrade bandwidth utility, since no data packets can be exchanged in the ATIM window. The impact of the capture effect is stronger when the number of stations is large, so the capture effect should be considered in the performance evaluation. The ATIM packet transmission rate with the basic mechanism is higher than that with RTS/CTS, because the time required to send an ATIM packet with the RTS/CTS mechanism is longer. Though the

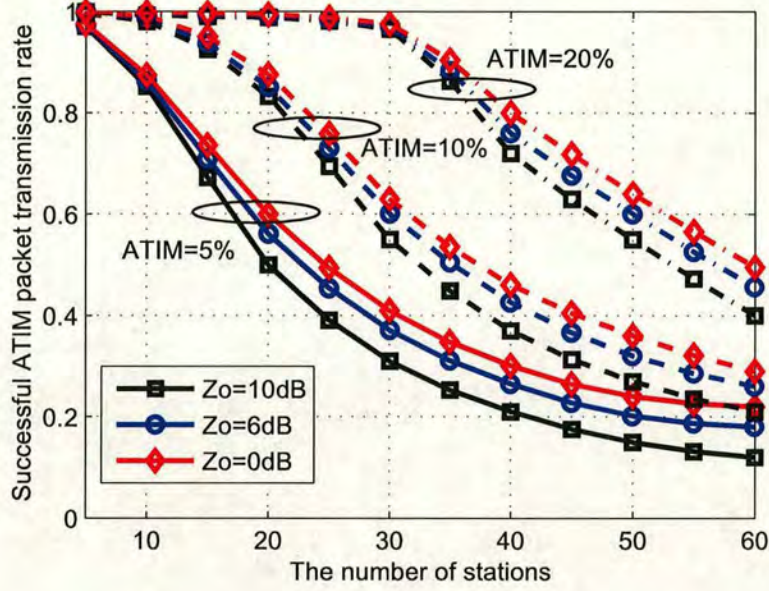


Figure 3.4: The analytical results for $p_a(W_A)$, Basic CSMA/CA

RTS/CTS access mechanism can decrease the time that the channel is busy during collision, the difference of these durations both in the basic mechanism and in the RTS/CTS mechanism are barely discernible, since the ATIM packet is small.

In the AHNPS mode, a station only has the right to send a data packet after successful transmission of its ATIM packet. We can define $p_d(W_D)$ as the probability that a station successfully transmits a data packet based on the condition that the ATIM packet has been successfully transmitted, and $p_{ds}(W_D, k)$ as the probability that the k^{th} data packet transmission is successful within the data window, W_D . In the same manner the analysis of $p_a(W_A)$, assumes the 1^{st} successful data packet transmission occurs in the slot l_1 , and all other stations are scheduled to send data packets within the window $[l_1, W_D]$. Then the probability $p_{ds}(W_D, 1)$ can be written as:

$$p_{ds}(W_D, 1) = p_a(W_A) \cdot \sum_{l_1=0}^{l_1=W_D-T_{DATA}+1} \psi_s(N, W_D, l_1) \quad (3.29)$$

where T_{DATA} is the time that the channel is sensed busy because of a successful data frame transmission. The values of T_{DATA} with different access mechanisms are specified in (3.30). If the packet is a broadcast packet, there is no item, "SIFS+ACK", in (3.30). S_D is the size of the data packet. From (3.29), which is multiplied by $p_a(W_A)$, it is clear that the data packet transmission performance is strongly linked to the transmission rate of ATIM packets.

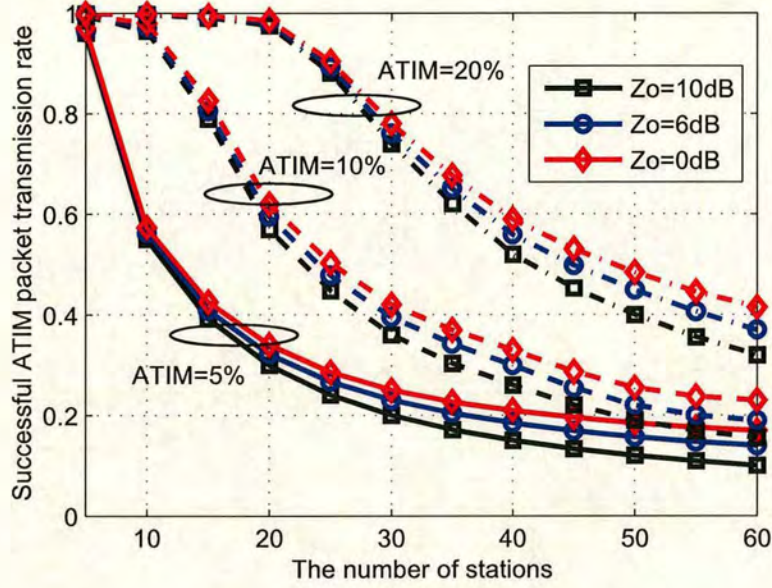


Figure 3.5: The analytical results for $p_a(W_A)$, CSMA/CA with RTS/CTS

$$\begin{aligned}
 T_{DATA,Basic} &= H + S_D + SIFS + ACK + DIFS + \delta \\
 T_{DATA,RTS} &= RTS + SIFS + CTS + SIFS + H + S_D + SIFS + ACK + DIFS + \delta
 \end{aligned} \tag{3.30}$$

Let $p_{dc}(W_D, 1)$ denote the probability that a collision occurs in the slot l_1 as follows:

$$p_{dc}(W_D, 1) = r(W_A) \cdot \sum_{l_1=0}^{l_1=W_D-T_{DATA}+1} \psi_c(N, W_D, l_1) \tag{3.31}$$

Like the analysis for the ATIM packet transmission rate, the probability $p_{ds}(W_D^{(k-1)}, k)$, which is the probability that the k^{th} data transmission is successful, can be written as:

$$\begin{aligned}
 p_{ds}(W_D^{(k-1)}, k) &= p_a(W_A) \cdot [p_{ds}(W_D^{(k-2)}, k-1) \sum_{l_k=l_{k-1}+T_{DATA}-1}^{l_k=W_D-T_{DATA}+1} \psi_s(N_s^{(k-1)} - 1, W_{D-S}^{(k-1)}, l_k) \\
 &\quad + p_{dc}(W_D^{(k-2)}, k-1) \sum_{l_k=l_{k-1}+T'_c-1}^{l_k=W_D-T_{DATA}+1} \psi_s(N_c^{(k-1)}, W_{D-C}^{(k-1)}, l_k)]
 \end{aligned} \tag{3.32}$$

where $W_{D-S}^{(k-1)} = W_D - l_{k-1} - T_{DATA} + 1$ is the width of the remaind data window for k^{th} successful transmission, $W_{D-C}^{(k-1)} = W_D - l_{k-1} - T_C + 1$ is the width of the remaind data window

for k^{th} collision transmission, $N_s^{(k-1)}$ is the number of stations in the $(k-1)^{th}$ successful transmission, and $N_c^{(k-1)}$ is the number of stations in the $(k-1)^{th}$ collision transmission. The average channel busy time, T'_c , in the data window is different in the two different access mechanisms, and given by:

$$\begin{aligned} T'_{c,Basic} &= H + S_D + DIFS + \delta \\ T'_{c,RTS} &= RTS + DIFS + \delta \end{aligned} \quad (3.33)$$

Similarly, the probability $p_{dc}(W_D^{(k-1)}, k)$, which is the probability that the k^{th} data transmission is in collision, can be written as:

$$\begin{aligned} p_{dc}(W_D^{(k-1)}, k) &= p_a(W_A) \cdot [p_{ds}(W_D^{(k-2)}, k-1) \sum_{l_k=W_D-T_{DATA}+1}^{l_k=W_D-T_{DATA}+1} \psi_c(N_s^{(k-1)}-1, W_{D-S}^{(k-1)}, l_k) \\ &+ p_{dc}(W_D^{(k-2)}, k-1) \sum_{l_k=l_{k-1}+T'_c-1}^{l_k=W_D-T_{DATA}+1} \psi_c(N_c^{(k-1)}, W_{D-C}^{(k-1)}, l_k)] \end{aligned} \quad (3.34)$$

The probability, $p_d(W_D)$, is the aggregation of all possible successful transmissions in the data window, and given by:

$$p_d(W_D) = \sum_k p_{ds}(W_D^{(k-1)}, k), \quad 1 \leq k \leq N \quad (3.35)$$

3.1.4 Throughput

In the Ad Hoc Network PS mode, data packets can only be transmitted in the data window, so the throughput in the data window, ϕ_d , can be expressed as:

$$\phi_d = N \cdot p_d(W_D) \cdot T_{DATA}/W_D \quad (3.36)$$

The total throughput, ϕ , can be written as:

$$\phi = \phi_d \cdot W_D / (W_D + W_A) \quad (3.37)$$

Clearly, the throughput in the PS mode is lower than that in the active mode, because the station cannot transmit any data in the ATIM window, and the data packet transmission rate is strongly affected by the ATIM packet transmission in the narrow ATIM window.

3.1.5 Delay Analysis

In this section, the packet transmission delay due to media access is investigated. For simplicity, the impact of the higher layer on packet transmission delay, such as the higher layer process-

ing delay, is ignored in the analysis. Because packets can only be transmitted after obtaining synchronization, and receiving packet-exchange information in AHNPS mode, the end-to-end delay, τ , may be much bigger than that in the normal operating mode.

If a station is unable to transmit an ATIM frame or a buffered data packet, for example due to severe contention, the station retains the buffered data packets and announces this data packet again by transmitting an ATIM in the next ATIM window. Assume that the data packet is successfully sent in the γ^{th} BI. This means that in $\gamma - 1$ BIs the packet was not successfully transmitted. The probability of γ can be specified as:

$$\Pr\{\gamma = k\} = (1 - p_d(W_D))^{k-1} \cdot p_d(W_D), \quad 0 < k < M \quad (3.38)$$

where M is the maximum retransmission time.

The average delay, $E[\mu]$, within the last beacon interval, in which the packet is successfully transmitted, can be evaluated as:

$$E[\mu] = W_A + \sum_{u=1}^{W_D} \mu \cdot p_{ds}(W_D, \mu) \quad (3.39)$$

Moreover, a new data packet, arriving from a higher layer, cannot be transmitted immediately, it will be held in the buffer until the beginning of the next new beacon interval. The probability of this delay, β , is a normalized distribution with maximum value BI and minimum value 0 . This average delay is $BI/2$.

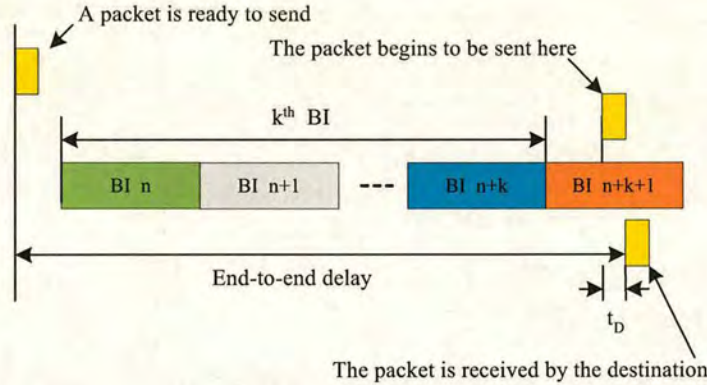


Figure 3.6: The end-to-end delay in the PS MAC mode

Finally, the average end-to-end delay $E[\tau]$ is composed of four parts (Figure 3.6), the average delay in the buffer before the first ATIM window announcing this packet, the sum of beacon intervals where transmission failed, the average delay within the last beacon interval, in which the packet is successfully transmitted, and the transmission delay τ_T . Thus $E[\tau]$ is given by:

$$E[\tau] = \frac{BI}{2} + BI \cdot \left(\sum_{k=0}^{M-1} k \cdot Pr\{\gamma = k\} - 1 \right) + (W_A + E[\mu]) + \tau_T \quad (3.40)$$

The transmission delay, τ_T , is different in the basic access and four-way handshake access. τ_T can be written as:

$$\begin{aligned} \tau_{T,Basic} &= DIFS + \delta \\ \tau_{T,RTS} &= RTS + SIFS + CTS + SIFS + DIFS + \delta \end{aligned} \quad (3.41)$$

From (3.40), it is obvious that the structure of BI will also affect the packet delay. This is different from the situation in the active mode, where the packet delay is mainly determined by competition.

3.1.6 Numerical Results

The analytical model and the simulation in NS2 [34] use the parameters for the Direct Spread Sequence Spectrum (DSSS) physical layer of IEEE 802.11b. Table 3.2 lists some key parameters.

Parameters	Value
MAC header (Include FCS)	272bits
PHY header	192bits
ACK	112bits + PHY header
RTS	160bits + PHY header
CTS	112bits + PHY header
ATIM Frame (Include FCS)	224bits + PHY header
Beacon Interval	100ms
SIFS	10s
DIFS	50s
Slot Time	20s
aCWmin	31
aCWmax	1023
Maximal retransmission time, M	16
Packet size	2048bits

Table 3.2: Parameters in Analytical Model

Successful Data Packet Transmission Rate

In order to illustrate the impact of the data window size and packet size on the transmission rate, we assume the ATIM packets are always successfully exchanged (Figure 3.7, 3.8, 3.9, 3.10). If the number of stations is large, the contention is severe and the data transmission rate with the RTS/CTS mechanism is higher than that with the basic mechanism. The reason is that the RTS/CTS mechanism dramatically reduces the average time the channel is busy during a collision. Decreasing the capture ratio z_0 results in higher transmission rate.

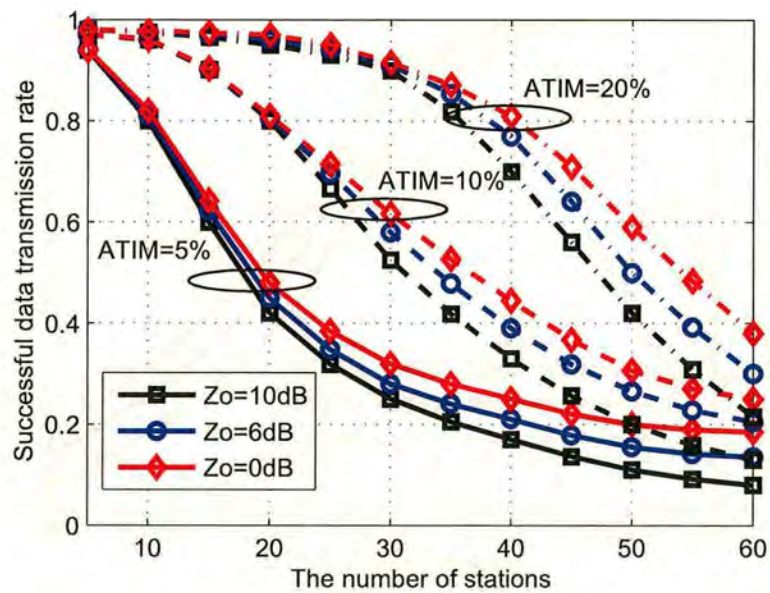


Figure 3.11: Successful data transmission rate vs. number of stations. Packet Size: 2048bits, basic CSMA/CA

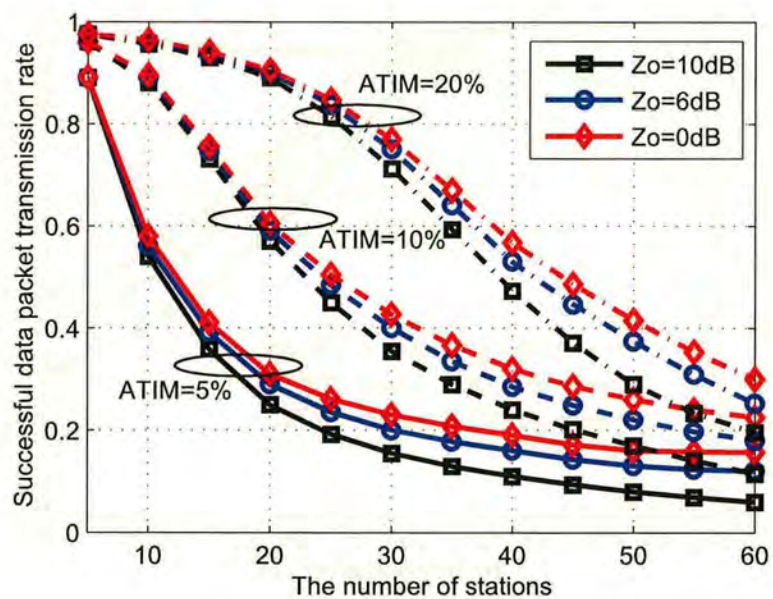


Figure 3.12: Successful data transmission rate vs. number of stations. Packet Size: 2048bits, CSMA/CA with RTS/CTS

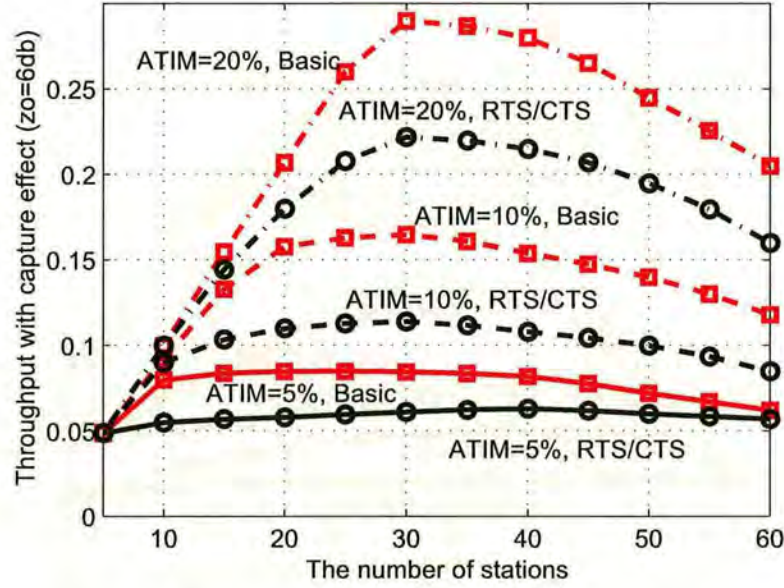


Figure 3.13: Total throughput vs. number of stations. $z_0 = 0dB$

Given the actual ATIM packet transmission probability, the data packet transmission rate is shown in Figure 3.11 and 3.12. Comparing Figures 3.7, 3.8, 3.9, and 3.10, with Figure 3.11, and 3.12, it can be seen that the data packet transmission rate is strongly linked to that of the ATIM packet transmission rate. This means the ATIM packet transmission rate has a strong influence on the data packet transmission rate (This is also clearly shown in equation (3.32), which is multiplied by $r(W_A, N)$). To improve throughput and bandwidth utility, it is necessary to improve the successful ATIM packet transmission rate.

Throughput

From Figures 3.13 and 3.14, it is clear that throughput is strongly related to the ATIM packet transmission probability, which is in turn determined by the ATIM window size. The total throughput reaches a maximum, when the number of stations is about 30, then increasing the number of stations, the total throughput decreases rapidly as the channel access contention is very severe, and more data packets are discarded. Use of the RTS/CTS mechanism results in an increase in the time that the channel is busy due to frame transmission time, T_{Data} , and a corresponding decrease in the time that the channel experiences a collision. When the number of stations increases to 40 or more, the RTS/CTS mechanism results in a slower throughput decrease than the basic contention mode as the signalling overhead is outweighed by the benefits of reduced data transmission collisions. Note that the capture effect results in a throughput improvement as z_0 decreases. For example, if the basic access scheme is utilized, given $z_0 = 6dB$ and $W_A = 20\%$, the peak throughput is estimated to be 22%, as opposed to 20% in the absence of capture ($z_0 = 0dB$). We found the throughput in the IEEE 802.11 AHNPS mode is very low. For example, it is less than 20% in most cases. This means that energy saving is achieved at the cost of bandwidth. The simulation results are shown in figure 3.15. The difference between the

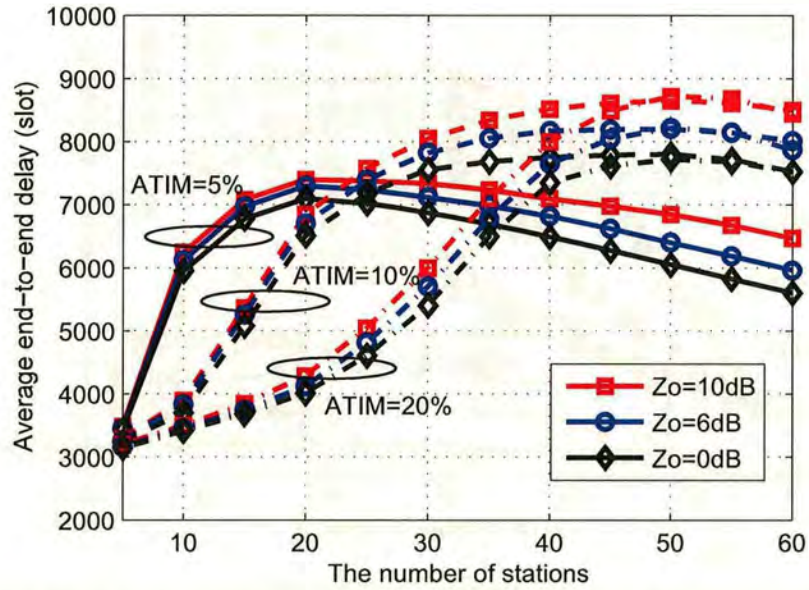


Figure 3.17: Average end-to-end delay vs. number of stations. CSMA/CA with RTS/CTS

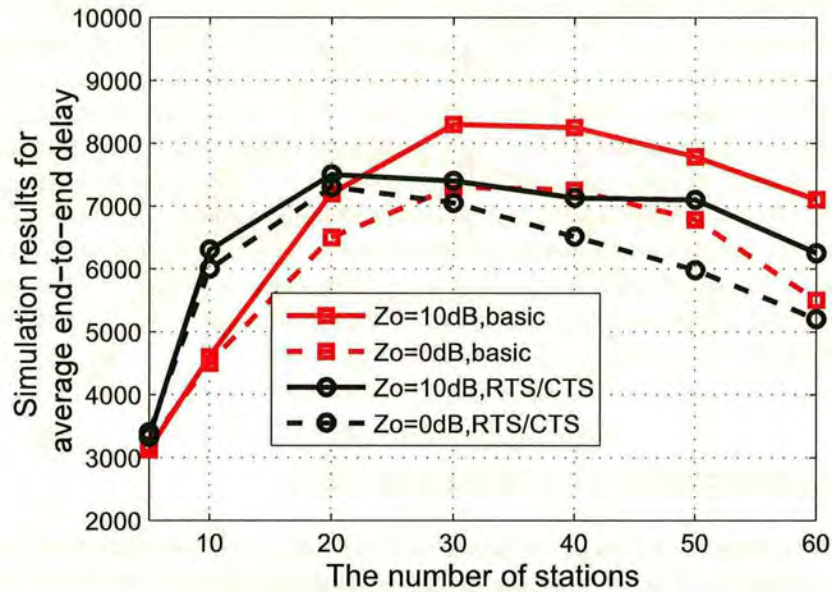


Figure 3.18: Simulation results of average end-to-end delay, $W_{ATIM} = 5\%BI$

transmitted beacon frames by every station. A station adopts the timing in a received beacon if the received time is later than the station's own TSF timer. Due to beacon contentions, mobility, communication delays, and transmission range limitations, stations may be out of synchronization with others, thus degrading power management. In this section, the synchronization problems produced by the beacon transmission are analyzed and simulated. Then, the multi-hop problems in existing standards and their improvements are introduced. Finally, an effective power-saving scheme for multi-hop networks is proposed.

3.2.1 Analysis of Beacon Transmission

In some networks, such as an IEEE802.15.3-based WPAN, a central controller or network coordinator broadcasts a beacon to manage the power-saving operations. However, situations are more complicated in ad hoc network IEEE802.11-based power-saving mode, since each station has the right to transmit beacons. As mentioned in the preceding sections, at the beginning of the beacon interval, all stations contend with each other to send beacon frames. The number of stations has a strong influence on the performance of beacon transmissions, thus affecting synchronization.

Let the probability that at least one of the n stations succeeds in beacon transmission during a beacon interval be $p(n, W)$. Here the beacon generation window is $[0, W]$. Three disjoint sub-events can be found when a successful beacon transmission occurs in window $[0, W]$:

E1: There is no beacon transmission in slot 0, but there is a successful transmission in window $[1, W]$;

E2: A beacon is successfully transmitted in slot 0;

E3: A collision occurs in slot 0, but at least one successful beacon transmission occurs during $[1, W]$.

$p(n, W)$ can be written as:

$$\begin{aligned} p(n, W) &= \Pr(E_1) + \Pr(E_2) + \Pr(E_3) \\ &= \left(\frac{W}{W+1}\right)^n p(n, W-1) + n \left(\frac{1}{W+1}\right) \left(\frac{W}{W+1}\right)^{n-1} + \Pr(E_3) \end{aligned} \quad (3.42)$$

Let $q(n, W) = \Pr(E_3)$. Assume the length of the beacon frame is b slots. If a beacon transmission collides at slot 0, the collision will occupy all the slots from 0 to $b-1$. Thus, for $W > b$ and $n > 1$, $q(n, W)$ has following formula:

$$q(n, W) = \sum_{i=2}^n \sum_{j=0}^{n-i} \left\{ C_i^n C_j^{n-i} \left(\frac{1}{W+1}\right)^i \left(\frac{b-1}{W+1}\right)^j \left(\frac{W-b+1}{W+1}\right)^{n-i-j} p(n-i-j, W-b) \right\} \quad (3.43)$$

The boundary condition is:

$$q(n, W) = 0, W \leq b \text{ or } n \leq 2 \quad (3.44)$$

Let $p'(n, W)$ be the probability that a particular station, say A, successfully sends a beacon in a given beacon interval. Let $p'(n, W, k)$ denote the conditional probability that station A successfully transmits a beacon given that it is scheduled to transmit in slot k . Then we have the following equation:

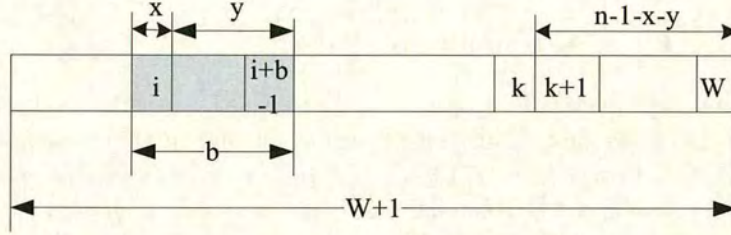


Figure 3.19: Explanation for $p'(n, W, k)$

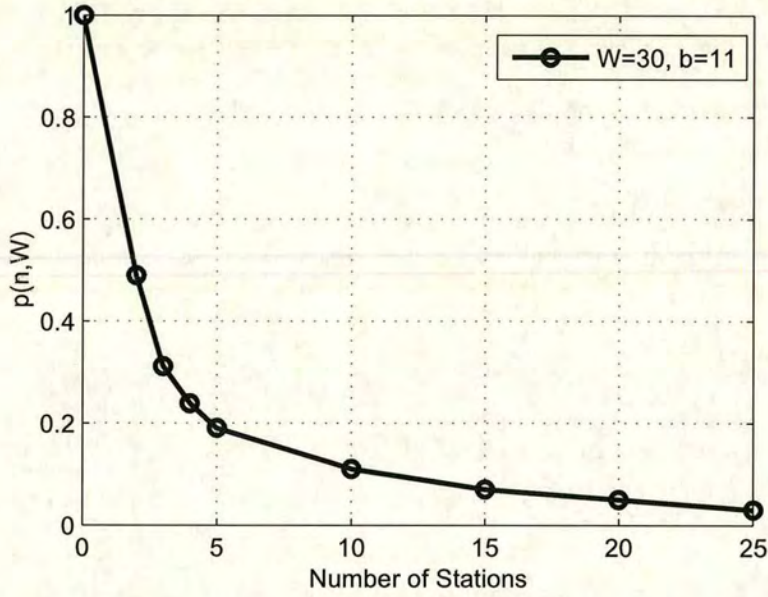


Figure 3.20: $p'(n, W)$ with $b=11$, and $W=30$

$$p'(n, W) = \frac{1}{W+1} \sum_{k=0}^W p'(n, W, k) \quad (3.45)$$

where $\frac{1}{W+1}$ is the probability that A is scheduled to transmit in slot k . To compute $p'(n, W, k)$, five events are defined as follows (Figure 3.19):

- a. All other stations are scheduled to transmit after slot k ;
- b. No station transmits before slot i , $0 \leq i \leq k - b$;
- c. Exactly x ($2 \leq x \leq n - 1$) stations are scheduled to transmit in slot i ;
- d. Exactly y ($0 \leq y \leq n - 1 - x$) stations are scheduled to transmit in slots $i + 1$ through $i + b - 1$;
- e. $N - x - y$ stations are scheduled to transmit within window $[i + b, W]$, the station in question successfully transmits in slot k .

Then $p'(n, W, k)$ can be described as:

$$p'(n, W, k) = \Pr(a) + \Pr(b \cap c \cap d) \cdot \Pr(e|b \cap c \cap d) \quad (3.46)$$

$$\Pr(b \cap c \cap d) = C_x^{n-1} C_y^{n-1-x} \left(\frac{1}{W+1} \right)^x \left(\frac{b-1}{W+1} \right)^y \left(\frac{W-i-b+1}{W+1} \right)^{n-1-x-y} \quad (3.47)$$

Then, $p'(n, W, k)$ satisfies the following recurrence:

$$p'(n, W, k) = \left(\frac{W-k}{W+1} \right)^{n-1} + \sum_{i=0}^{k-b} \sum_{x=2}^{n-1} \sum_{y=0}^{n-1-x} \left\{ C_x^{n-1} C_y^{n-1-x} \left(\frac{1}{W+1} \right)^x \left(\frac{b-1}{W+1} \right)^y \cdot \left(\frac{W-i-b+1}{W+1} \right)^{n-1-x-y} \cdot p'(n-x-y, W-i-b, k-i-b) \right\} \quad (3.48)$$

The boundary condition for equation (3.48) is $p'(0, W, k) = p'(n, 0, k) = 0$. Using (3.45) and (3.48) the value for $p'(n, W)$ can be computed, is shown in Figure 3.20.

3.2.2 Analysis of Asynchronism

When the clocks of two stations are out of synchronization, the power management of these stations cannot work properly. Let Δ be the maximum clock difference tolerable by power management. If the clocks of two stations are different by more than Δ , then they are out of synchronization. In this section, we analyze the fastest-station asynchronism, which refers to a situation where the clock of the fastest station is ahead of the clocks of all other stations by more than Δ . For instance, in IEEE 802.11-based ad hoc network power-saving mode, the time synchronization function specifies that the stations set their timers forward, but never backwards, which means slower clocks synchronize with faster clocks, but faster clocks do not synchronize themselves with slower clocks. Therefore, if the fastest station fails to transmit beacons for too many beacon intervals, its clock will be ahead of all other clocks by more than Δ . The purpose of this analysis is to calculate the probability of the asynchronism occurring and its average duration.

Let T be the length of a beacon interval, and let d denote the difference of clock accuracy between the fastest station and the second fastest station. Once the stations have been synchronized, if the fastest node fails to transmit a beacon in each of $\lceil \frac{\Delta}{d \cdot T} \rceil$ continual beacon intervals, then the fastest node will be out of synchronization with all other stations by at least Δ . Let $E(H)$ be the expected duration of a fastest-node asynchronism, and $E(L)$ be the expected length of time between two consecutive incidents of fastest-node asynchronism. Once an incident of fastest-node asynchronism occurs, it lasts at least for one beacon interval. After one beacon interval, with probability $(1 - p'(n, W))^k$, the asynchronism will continue for at least k additional beacon intervals. Thus the expected duration of a fastest-node asynchronism is:

$$E(H) = 1 + (1 - p'(n, W)) + (1 - p'(n, W))^2 + \dots = 1/p'(n, W) \quad (3.49)$$

Let S_i denote the event that the next synchronization occurs in the i^{th} beacon interval. Then,

$$E(L) = \sum_{i=1}^{\infty} \{\Pr(S_i) \cdot E(L|S_i)\} \quad (3.50)$$

where $\Pr(S_i) = p'(n, W)(1 - p'(n, W))^{i-1}$, and the expected length of L given event S_i , $E(L)$ is:

$$E(L) = \begin{cases} E(L) + i & 1 \leq i \leq \frac{\Delta}{d \cdot T} \\ \tau = (\frac{\Delta}{d \cdot T}) & i > \frac{\Delta}{d \cdot T} \end{cases} \quad (3.51)$$

Therefore,

$$\begin{aligned} E(L) &= \sum_{i=1}^{\tau} p'(n, W) (1 - p'(n, W))^{i-1} (E(L) + i) + \tau \\ &= (p'(n, W))^{-1} \left((1 - p'(n, W))^{-\tau} - 1 \right) \end{aligned} \quad (3.52)$$

Then, the fastest-node asynchronism time ratio can be evaluated as:

$$E(R) = E(H) / (E(H) + E(L)) = (1 - p'(n, W))^{\tau} \quad (3.53)$$

The numerical results of the asynchronism time, and the ratio are shown in Figures 3.21 and 3.22 respectively. They clearly show that when the contention is severe, asynchronism is more likely to occur. From figure 3.22, we can observe that the fastest station is out of synchronization with all other stations for 10% of the time, when there are 30 stations. Obviously, in an ad hoc network power saving MAC, when the number of station increases, more stations are likely to be out of synchronization.

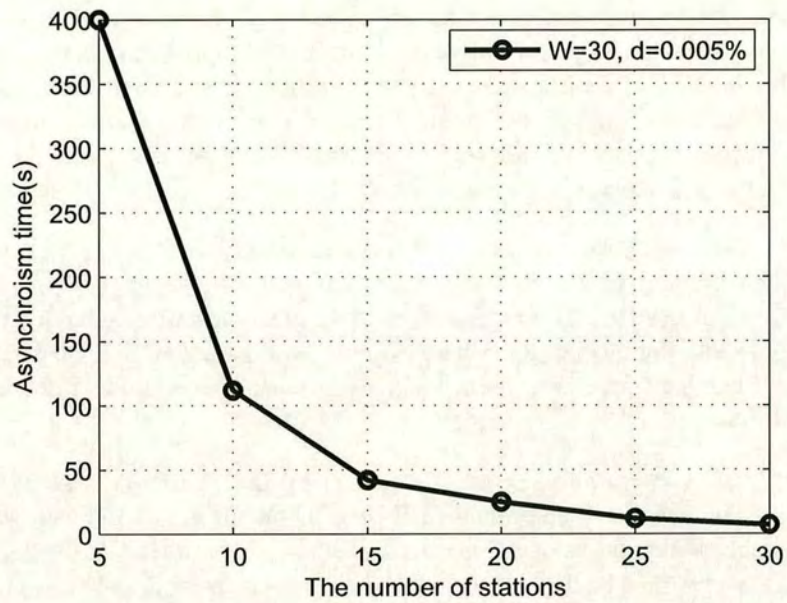


Figure 3.21: Analytical results for asynchronism. The fastest node asynchronism time.

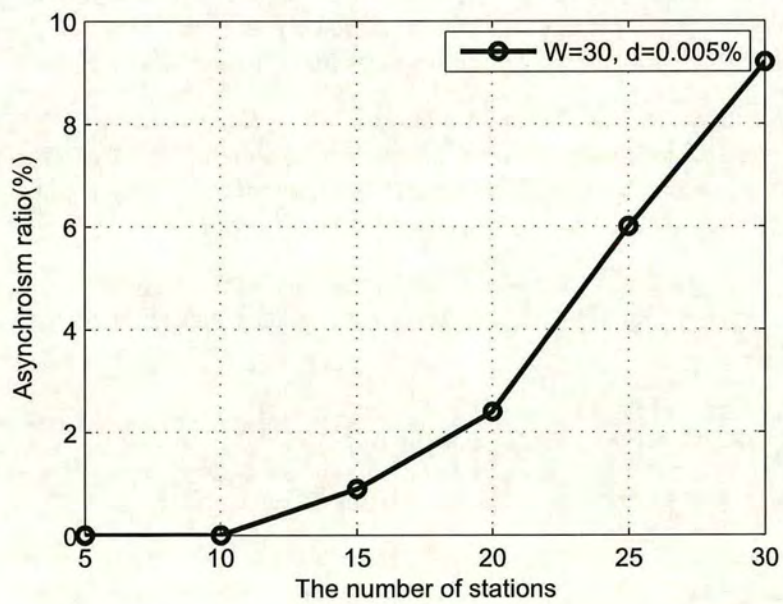


Figure 3.22: Analytical results for asynchronism. The fastest node asynchronism time ratio.

3.2.3 An Effective Power-saving scheme for Multi-hop Networks

In a single-hop ad hoc network, all power-saving stations are fully connected so that they gain synchronization through hearing one beacon. In a multi-hop MANET, some stations may be out of the transmission range of the beacon sending station. In addition, mobility and communication delays will make synchronization difficult. The fixed-size window means some stations are unable to transmit data frames in time under heavy traffic load, thus increasing the end-to-end delay and degrading the network performance.

In multi-hop MANETs, it is clear that each station's transmission range may not cover all the stations. Different parts of the MANET may have their own independent beacons. The whole network may be partitioned into several groups and lose synchronization through different beacon timing. In [35], the authors let all the stations continue to send their beacons after receiving a beacon, thus keeping all stations in contact with each other. However, these flooded beacons will increase the congestion, and overhead.

Moreover, under a heavy traffic load, many stations will have buffered packets waiting for transmission. In this case, for instance, in the IEEE802.11 ad hoc network power saving mode, a short ATIM window may not allow all the stations to successfully send ATIM frames. Some buffered packets would then be delayed by at least one beacon interval. A long ATIM window allows for more successful ATIM frames. However, this will increase the contention in the data window so that some stations will lose the opportunity to send data packets and are required to keep awake during the data window, thus wasting more energy.

In this section, based on the original IEEE 802.11 power saving mode in multi-hop MANETs, an enhanced PS scheme, using an adaptive window size, is proposed through minor modification of the standard. This scheme makes the power saving mode adapt to different traffic loads, improves the performance of synchronization, decreases the amount of retransmission, and balances the bandwidth utility. The purposes of this enhanced scheme are:

- 1) *To achieve reliable synchronization:* A robust timing synchronization is essential to guarantee efficient data exchange in the power saving mode. In a multi-hop MANET, some stations may not hear the beacon. A reliable time synchronization function (TSF) should ensure that all the stations in power saving mode hear each beacon and adjust clock errors.
- 2) *To allow the size of the ATIM and data window to be adjustable:* An adaptive size of windows can let the power saving mode adapt to different traffic loads with energy efficiency.

3.2.3.1 Reliable Synchronization in a Multi-Hop MANET

We propose an improvement to the IEEE 802.11-based TSF as follows:

The channel time is divided into beacon intervals (BIs), with each beacon interval beginning with a beacon frame. The beacon interval is composed of three major parts: the beacon, followed by a fixed length guard time (GT), the ATIM window, followed by a fixed length size-control time (SCT), and the data window, as shown in Figure 3.23. The differences between this enhanced scheme and the original IEEE 802.11 PS mode are the addition of GT, SCT, and the adaptive size of the windows.

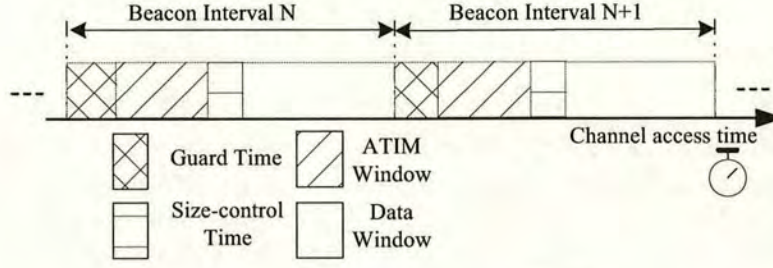


Figure 3.23: *The enhanced beacon interval structure*

A mobile station continues to send beacons even if it has heard other beacons. This will allow others to be aware of its existence and exchange timing information for synchronization. To ease the pressure of access contention in the ATIM window, a size-fixed GT duration is used by stations to send the beacon. This short GT allows most of the beacons to transmit, since the beacon is very small. In a large-scale network, beacon transmissions can extend into the ATIM window. As a result of the ATIM window size being adaptive to the traffic load, those beacons, which extend into the ATIM window, will just slightly affect the transmission of the ATIM frame.

A mobile station, which initially enters the PS mode, should keep awake for 2 normal BIs to hear other station's beacon frames. Once a beacon is heard, this station can get synchronization and then enter PS mode.

If a mobile station has not heard any beacon frames for two BIs, it means this station may have moved out of the PS network. This station should alternate between awake and idle states for a BI. When it hears a beacon, it re-synchronizes, and enters PS mode.

If a PS station does not receive any beacon frames with a timestamp value later than its own for N BIs, it will simply replace its own timestamp value T_{Stamp} with $T_{Stamp} + (T_{Stamp} - T_{LastReceivedStamp})$. $T_{LastReceivedStamp}$ is the last received timestamp value. This can prevent clock drift in a station with a faster clock.

3.2.3.2 Adaptive Window Size

Ideally, the optimised ATIM window size, W_{opATIM} , for a contention-free schedule for ATIM frame transmission should satisfy:

$$R_{ATIM|W_{ATIM} \geq W_{opATIM}} = 1, \quad W_{ATIM} \in [W_{min}, W_{max}] \quad (3.54)$$

$$W_{min} > 0, \quad W_{max} < W_{BI} - W_{GT} - W_{SCT} \quad (3.55)$$

where R_{ATIM} is the successful rate of sending ATIM frames, and W_{ATIM} is the ATIM window

size. Each station monitors its R_{ATIM} in every ATIM window. If $R_{ATIM} < 1$, the station extends its next ATIM window by Δ ($\Delta > 0$) until W_{ATIM} reaches W_{max} . If R_{ATIM} is 1 for two consecutive BIs, the station subtracts its ATIM window size in the next BI by Δ until it reaches W_{min} .

In this enhanced scheme, a PS station uses all the successful ATIM packets during the ATIM window to estimate the appropriate data window size. The transmission time information of the data packets is easily added into the frame body of ATIM, since the ATIM frame in the standard only specifies MAC header, Frame Check Sequence (FCS), and an empty frame body. An estimated total data transmission time, L' , can be expressed as:

$$L' = \sum_{i=1}^N T_i + N \cdot (T_{DIFS} + T_{SIFS} + T_{ACK}) \quad (3.56)$$

where N is the number of received ATIM frames, and T_i is the data transmission duration, which is dependent on the data packet's length, indicated in the ATIM frame. T_{DIFS} and T_{SIFS} are the distributed coordination function interframe space and the short interframe space respectively. T_{ACK} is the ACK frame transmission time. The current data window size, W_{Data} , is the remaining time of the BI.

$$W_{Data} = W_{BI} - W_{GT} - W_{ATIM} - W_{SCT} \quad (3.57)$$

When $W_{Data} < L'$, it means that some data packets will fail to transmit. To alleviate the access contention, the station will extend the current data window by one BI.

A station, which intends to extend its ATIM window or data window, should broadcast this size-control request to its neighbours during the SCT so that they can change window size simultaneously. To avoid collisions, at the beginning of the SCT, the station should wait a random number of slots between 0 and $2 \times CW_{min} - 1$ before sending this short request frame.

Once a station has received this frame, it increases the data window size in the current BI or changes the ATIM window size in the next BI. If a station receives more than one size-control request, it always responds to the request for increasing the window size.

When a station finishes data exchange and the remainder of the data window is bigger than a threshold Th , it switches to sleep mode during the remaining data window. To prevent using extra energy for the switching between modes [36], an appropriate Th is necessary.

Figure 3.24 shows an example for this enhanced scheme. At the beginning of all the BIs, stations send a beacon frame using CSMA/CA with an initial random backoff. Within the N^{th} beacon interval, station 2 hears ATIM frames, indicating that two stations have some buffered data packets for it. Station 2 calculates the transmission time of those data packets. If the transmission time is larger than its residual time in the current BI, station 2 broadcasts a SCT frame to command to widen the current data window by a normal BI length. Stations remain awake during the GT, ATIM, and SCT windows. If a station does not receive ATIM frames, it goes to sleep during the data window, otherwise, it remains awake. When stations finish data

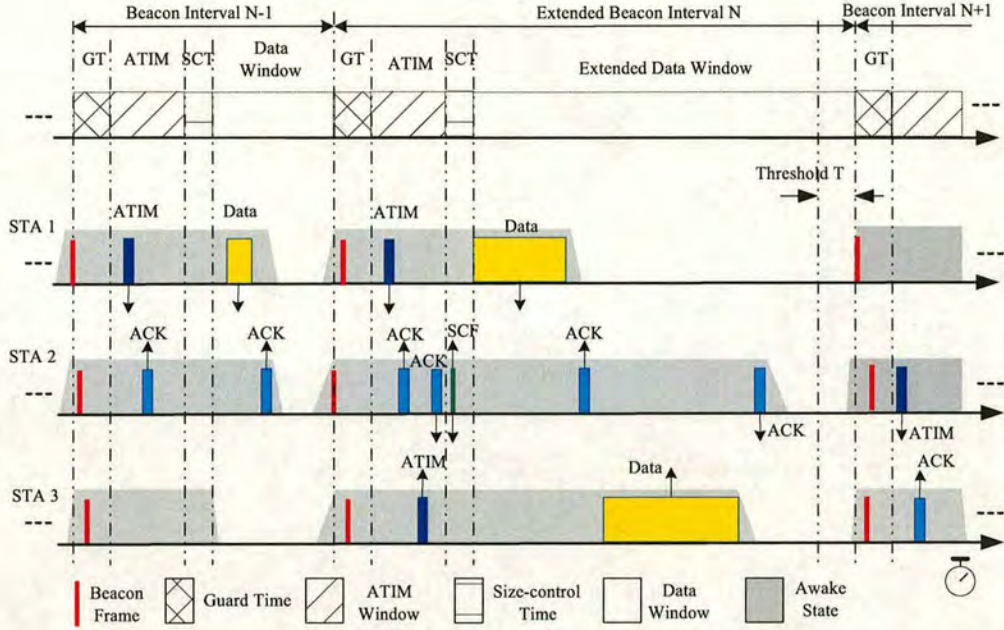


Figure 3.24: An example of the enhanced scheme for IEEE 802.11-based multi-hop MANETs

exchange, and the remaining time of the data window is larger than a threshold Th , they go to sleep for the remaining data window time.

3.2.3.3 Simulation and Validation

In the simulation, the BI is set to the standard value of 100ms (the extended beacon interval is 200ms). In IEEE 802.11 for DSSS, the slot length is $20\mu s$. We select 50 slots for the minimum ATIM window length. The size of the GT and SCT is 250 slots.

Three aspects of the enhanced scheme are compared with the original IEEE 802.11 ad hoc network PS mode, packet-sending success rate, power efficiency, and end-to-end delay. The maximum ATIM window size and the network traffic loads were adjusted in the simulation.

The network traffic load (NTL) is defined as:

$$NTL = (N \times S) / R \quad (3.58)$$

In this equation, N is the number of source stations, S is the traffic source's bit rate, and R is the channel bit rate. For example, if 10 stations periodically send packets, whose size is 512 bits, with a fixed interval of 0.1s, and the channel bit rate is 1 Mbps, then the network traffic load (NTL) is $10 \times 512 / 0.1 / (1024 \times 1024) = 4.8\%$.

In the simulation, the channel bit rate is 2Mbps, the data packet size is 1k bits, and the packet-

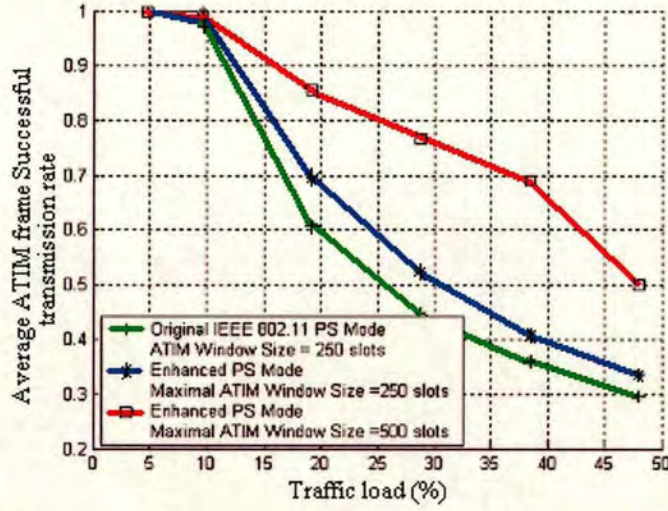


Figure 3.25: Simulation results: successful ATIM frame transmission rate

sending interval is 0.1s. The stations are randomly located in a $600m \times 600m$ area with a speed selected from a uniform probability distribution function with a maximum speed of $10m.s^{-1}$.

Figures 3.25, and 3.26 are the simulation results for the successful ATIM frame transmission rate and the successful data frame transmission rate respectively. The successful ATIM frame transmission rate in the enhanced scheme with the maximum ATIM window size of 250 slots is a little better than that in the original IEEE 802.11 standard. This demonstrates that the synchronization problem in multi-hop MANETs may affect ATIM frame transmission. The successful data frame transmission rate of the enhanced algorithm is higher than that of the original IEEE 802.11, since the data window size can double the normal size under heavy traffic load.

Figure 3.27 shows that the PS station with the enhanced scheme spends more time in sleep, which means that energy is saved. The reasons are that the enhanced scheme allows stations to sleep immediately after finishing data exchange, and the size adapting window means PS stations decrease the frequency of re-transmission, especially under heavy traffic loads. The number of the sleep slots per station in the original IEEE 802.11 increases, with an increasing traffic load, because unsuccessful ATIM frame transmission results in some stations not being awake during the data window.

Normally, in PS mode, the end-to-end delay performance is poor, because stations simply exchange packets periodically. The adaptive window size allows stations to adapt to dynamically changing traffic loads, and decrease re-transmissions, so the enhanced algorithm improves the end-to-end delay substantially (Figure 3.28).

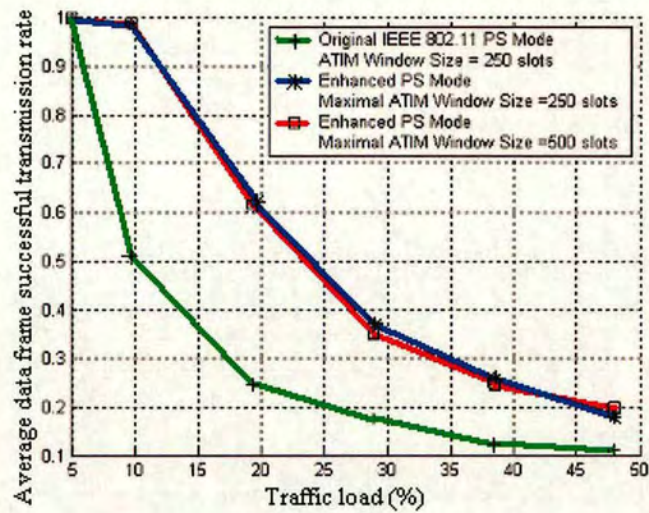


Figure 3.26: Simulation results: average successful data frame transmission rate

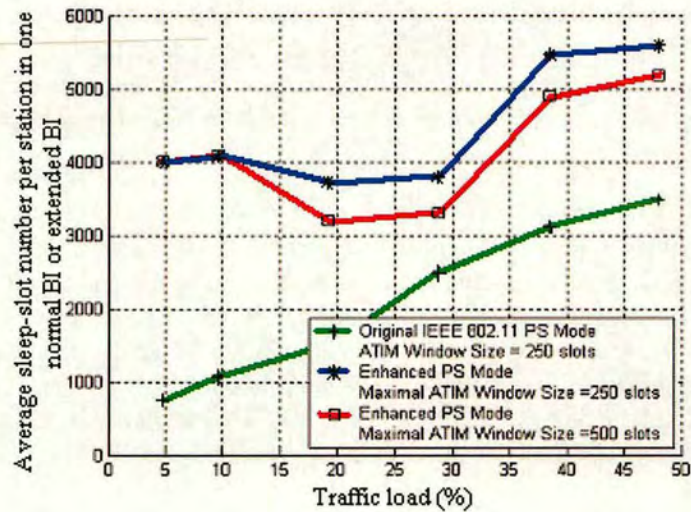


Figure 3.27: Simulation results: average number of sleep slots per station

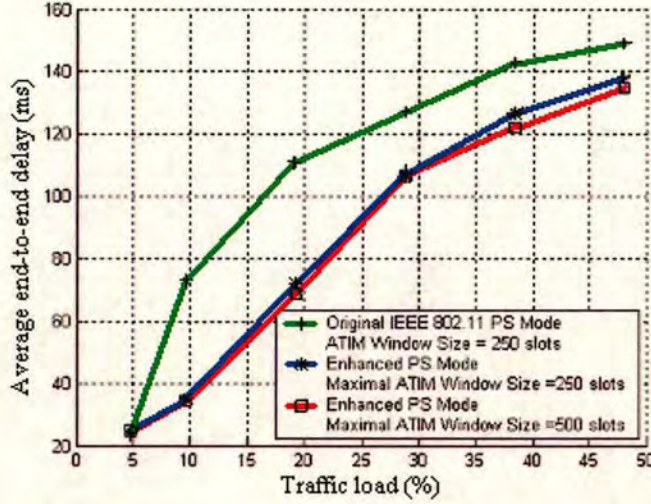


Figure 3.28: Simulation results: average end-to-end delay

3.3 Summary and Conclusions

Many communication devices with the capability of mobile and wireless networking are becoming widely available. Power awareness is an essential component of MANETs, due to the limited energy stored in battery operated mobile equipment. To meet these demands, MAC protocols, such as IEEE 802.11, and IEEE802.15.3, can support a power-saving mode with ad hoc networking. Using the IEEE802.11 ad hoc network power saving MAC with two types of CSMA/CA protocols, including basic and four-way handshake access mechanisms, we have developed an analytical approximation to evaluate the successful packet transmission rate in the ATIM and data windows, the throughput, and the latency in the ad hoc network power saving MAC mode with capture effect, operating on a channel impaired by Rayleigh fading, lognormal shadowing, and the near-far effect.

The performance of the power saving MAC is lower than that in the active mode, and is sensitive to the number of stations, the size of the different portion of the superframe, and the capture effect. In the IEEE802.11 power saving mode, the ATIM packet transmission rate strongly affects the data packet transmission rate, the throughput and the packet delay. Increasing the width of the ATIM window will improve throughput, but may degrade latency performance, especially when the number of stations is large. The capture effect improves the performance of IEEE 802.11 AHNPS mode, since it allows for successful reception even if packets collide. Because the ATIM window is limited in size, increasing the size of data packets will not result in higher throughput.

In multi-hop MANETs, the limited transmission range and mobility make the topology complicated, thus increasing the difficulty of obtaining synchronization. Moreover, the fixed size window in the standard is not flexible in different network traffic conditions. The proposed power saving MAC scheme modifies the beacon-sending behaviour to improve synchronization and use an adaptive window size. The simulation results show that this enhanced scheme

can improve the transmission efficiency, and save energy in multi-hop MANETs.

Chapter 4

Interaction between Routing and MAC

To manage energy limitation problems in Mobile Ad Hoc Networks (MANETs), current power saving MAC designs mainly concentrate on using various methods to minimize the time in transmission, reception and idle states. This may degrade the latency performance and impacts on the route discovery procedure of MANET routing protocols. However, an analytical model of the impact of power-saving MAC scheme on routing has not been presented before. In this chapter, an analytical framework that addresses a gap in the theoretical performance, which includes the latency of the power-saving MAC and route discovery, is proposed. The investigation verifies that the power saving MAC scheme leads to serious latency and will significantly degrade the route discovery performance of an on-demand routing protocol. Section 4.1 presents the analytical model along with numerical and simulation results. Two possible enhanced schemes are proposed and validated by simulation in section 4.2.

4.1 Impact of Power-Saving MAC on Ad Hoc Network Routing Protocols

Assume that the ad hoc network power-saving mode can be used for multi-hop MANETs. Packets can only be transmitted after obtaining synchronization and receiving packet-exchange information in power-saving MAC mode, thus increasing the end-to-end delay. When using on-demand MANET routing methods, such as dynamic source routing (DSR) [37], a source station sends a route request packet (RRP) to search for a path to the destination station. The severe latency characteristic in the PS mode can cause this route discovery operation to timeout, especially when the route has multiple hops.

The IEEE 802.11 AHNPS mode, which is a typical and widely researched PS scheme, is selected as an example to analyse the causes of the low success rate of route discovery within the PS MAC in detail. The analytical and simulation results, for both four-way handshake with RTS/CTS and basic media access mechanisms of the PS mode, simultaneously with on-demand routing, are illustrated and compared. To improve the performance of the PS mode in MANET routing, some possible enhanced schemes are proposed and verified.

4.1.1 Route Discovery Timeout under Power-Saving MAC

There are two classes of ad hoc network routing, on-table routing and on-demand routing. Using on-table routing, each station periodically exchanges route information, and maintains routing tables, which cover the whole network. However, on-table routing does not scale well, as periodic route maintenance becomes expensive. On-demand routing does not need to maintain complete topology information in each station. It tries to discover the routes when this

$$\begin{aligned}
p_{ac}(W_A, 1) &= \sum_{m_1=0}^{W_A-T_{ATIM}+1} \sum_{x=2}^N \binom{N}{x} \left(\frac{W_A-m_1}{W_A} \tau(N) \right)^{N-x} \left(\frac{1}{W_A} \tau(N) \right)^x \\
&= \sum_{m_1=0}^{W_A-T_{ATIM}+1} \varphi_c(N, W_A, m_1)
\end{aligned} \tag{4.6}$$

$$\text{where } \varphi_c(N, W_A, m_1) = \sum_{x=2}^N \binom{N}{x} \left(\frac{W_A-m_1}{W_A} \tau(N) \right)^{N-x} \left(\frac{1}{W_A} \tau(N) \right)^x.$$

The probability $p_{as}(W_A^{(k-1)}, k)$, which is the probability that k^{th} ATIM transmission is successful, can be written as:

$$\begin{aligned}
p_{as}(W_A^{(k-1)}, k) &= p_{as}(W_A^{(k-2)}, k-1) \sum_{m_k=W_A-T_{ATIM}+1}^{m_k=W_A-T_{ATIM}+1} \varphi_s(N_s^{(k-1)} - 1, W_{A-S}^{(k-1)}, m_k) \\
&\quad + p_{ac}(W_A^{(k-2)}, k-1) \sum_{m_k=m_{k-1}+T_C-1}^{m_k=W_A-T_{ATIM}+1} \varphi_s(N_c^{(k-1)}, W_{A-C}^{(k-1)}, m_k)
\end{aligned} \tag{4.7}$$

The probability $p_{ac}(W_A^{(k-1)}, k)$, which is the probability that the k^{th} ATIM transmission is in collision, can be written as:

$$\begin{aligned}
p_{ac}(W_A^{(k-1)}, k) &= p_{as}(W_A^{(k-2)}, k-1) \sum_{m_k=m_{k-1}+T_{ATIM}-1}^{m_k=W_A-T_{ATIM}+1} \varphi_c(N_s^{(k-1)} - 1, W_{A-S}^{(k-1)}, m_k) \\
&\quad + p_{ac}(W_A^{(k-2)}, k-1) \sum_{m_k=m_{k-1}+T_C-1}^{m_k=W_A-T_{ATIM}+1} \varphi_c(N_c^{(k-1)}, W_{A-C}^{(k-1)}, m_k)
\end{aligned} \tag{4.8}$$

Finally, the probability, $p_a(W_A)$, is the aggregation of all the possible successful transmissions in the ATIM window. Therefore, $p_a(W_A)$ is:

$$p_a(W_A) = \sum_{k=1}^L p_{as}(W_A^{(k-1)}, k), \quad 1 \leq k \leq N \tag{4.9}$$

Like the analysis for the ATIM packet transmission rate, the probability $p_{ds}(W_D^{(k-1)}, k)$, which is the probability that the k^{th} data transmission is successful, can be written as:

$$\begin{aligned}
p_{ds}(W_D^{(k-1)}, k) &= p_a(W_A) \cdot [p_{ds}(W_D^{(k-2)}, k-1) \sum_{l_k=l_{k-1}+T_{DATA}-1}^{l_k=W_D-T_{DATA}+1} \psi_s(N_s^{(k-1)} - 1, W_{D-S}^{(k-1)}, l_k) \\
&\quad + p_{dc}(W_D^{(k-2)}, k-1) \sum_{l_k=l_{k-1}+T'_c-1}^{l_k=W_D-T_{DATA}+1} \psi_s(N_c^{(k-1)}, W_{D-C}^{(k-1)}, l_k)]
\end{aligned} \tag{4.10}$$

The probability, $p_d(W_D)$, is the aggregation of all possible successful transmissions in the data window, and given by:

$$p_d(W_D) = \sum_k p_{ds}(W_D^{(k-1)}, k), \quad 1 \leq k \leq N \quad (4.11)$$

Finally, the average end-to-end delay $E[\tau]$ is given by:

$$E[\tau] = \frac{BI}{2} + BI \cdot \left(\sum_{k=0}^{M-1} k \cdot Pr\{\gamma = k\} - 1 \right) + (W_A + E[\mu]) + \tau_T \quad (4.12)$$

The stochastic variable for the route discovery time, D , can be expressed as:

$$D = \bar{h} \cdot (\beta + BI \cdot (k' - 1) + u' + W_A + \tau_T) + \bar{h} \cdot (\beta + BI \cdot (k'' - 1) + u'' + W_A + \tau_T) \quad (4.13)$$

where $'$ and $''$ denote response to the RRP and RACKP respectively. Normally, the size of the RRP and RACKP are the same, so (4.13) can be simplified to:

$$D = 2\bar{h} \cdot (\beta + BI \cdot (k' - 1) + u' + W_A + \tau_T) \quad (4.14)$$

If the maximal route request period is Φ , then the successful route discovery rate, v , is:

$$v = Pr \left[2 \left[\beta + BI \cdot (k' - 1) + u' + W_A + \tau_T \right] > \Phi / \bar{h} \right] \quad (4.15)$$

From (4.11), and (4.14), it is clear that D is strongly depend on p_{ds} . In PS mode, only after successful ATIM packet transmission can the station begin to transmit the data packet, so the ATIM packet transmission rate will affect the transmission of RRP and RACKP.

4.1.3 Simulation

In this section, several examples illustrate the impact of the PS mode of the MANET routing protocol. DSR is selected as the routing protocol in the simulation. The nodes are randomly located in a 600m \times 600m area. The station's mobility follows a "Random Waypoint" model [22] with a speed selected from a uniform probability distribution function (PDF) with a maximum speed of 10ms⁻¹. This model, whilst describing an unrealistic node behaviour, is typically used by many researchers, and hence useful for comparison purposes. The transmission range of each station is configured as 150m. Other key parameters are shown in Table 4.1.

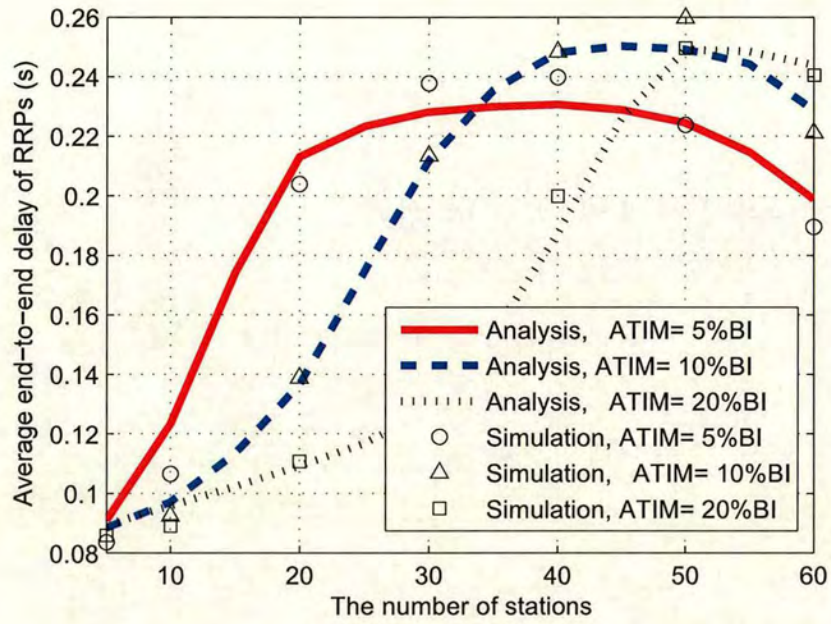


Figure 4.2: Average end-to-end delay of RRP, Basic CSMA/CA

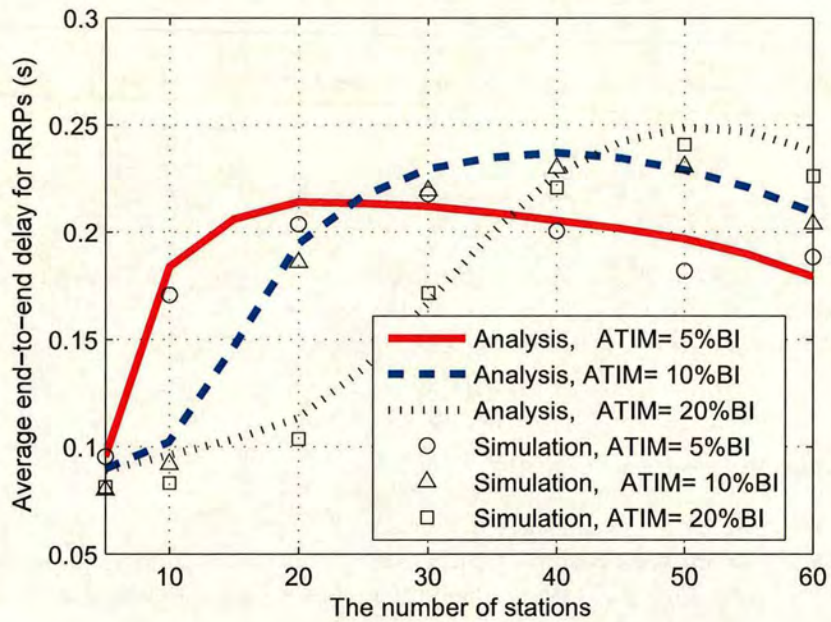


Figure 4.3: Average end-to-end delay of RRP, CSMA/CA with RTS/CTS

Parameter	Value
MAC header (Include FCS)	272bits
PHY header	192bits
Beacon interval	100ms
SIFS	10s
DIFS	50s
Slot time	20s
Maximum route request period	500ms
Channel bit rate	2Mbit/s
Maximal retransmission time, M	16

Table 4.1: *Simulation parameters*

4.1.3.1 Average End-to-end Delay of Route Request Packet

Figures 4.2, and 4.3 show the numerical and simulation results of the average end-to-end delay of each successful RRP transmission. With the PS MAC, the latency is poor, being greater than 0.07s. As the number of stations in the network increases, the end-to-end delay increases up to a maximum value. After reaching the maximum value, the delay begins to decrease, as more packets are discarded due to severe channel access contention, which also means more stations begin to be blocked. When the number of stations is high, the RTS/CTS mechanism can improve the performance of the end-to-end delay, since it decreases the collision duration. The difference between the simulation and analytical results is negligible.

4.1.3.2 Average Route Discovery Time and Rate

Figures 4.4, 4.5, 4.6, and 4.7 show the average successful route discovery time and successful discovery rate respectively. The trend of the route discovery time is the same as the end-to-end delay. In the simulation where most paths take about 2 to 3 hops, in terms of equation (4.1), the route discovery time is dramatically higher than in the active mode. As shown in Figures 4.4, and 4.5, when the number of stations is small, e.g. 5, the successful route discovery rate is low in the simulation, because the network is so sparse that a station can be out of transmission range. This is different from the analytical results, because the analytical model does not consider the density of nodes. When the number of stations increases, the analytical results get close to those in simulations. In DSR, when a RACKP is not received within 0.5s, another RRP is broadcast again. The high latency in AHNPS mode will easily cause the route discovery time to exceed 0.5s. In this case, we can see the average successful route discovery rate is much lower than the active mode. As the size of the ATIM window increases, the rate improves. Another observation is that the rate is slightly higher for CSMA/CA with RTS/CTS compared to that without RTS/CTS due to severe collisions. This example shows that the AHNPS mode significantly degrades the performance of a MANET routing protocol. To improve network operation, one solution is to increase the timeout parameters of the routing protocol appropriately. However, this will result in network inefficiency. Another possible idea to obtain fast route discovery is improve the transmission of control packets for route discovery.

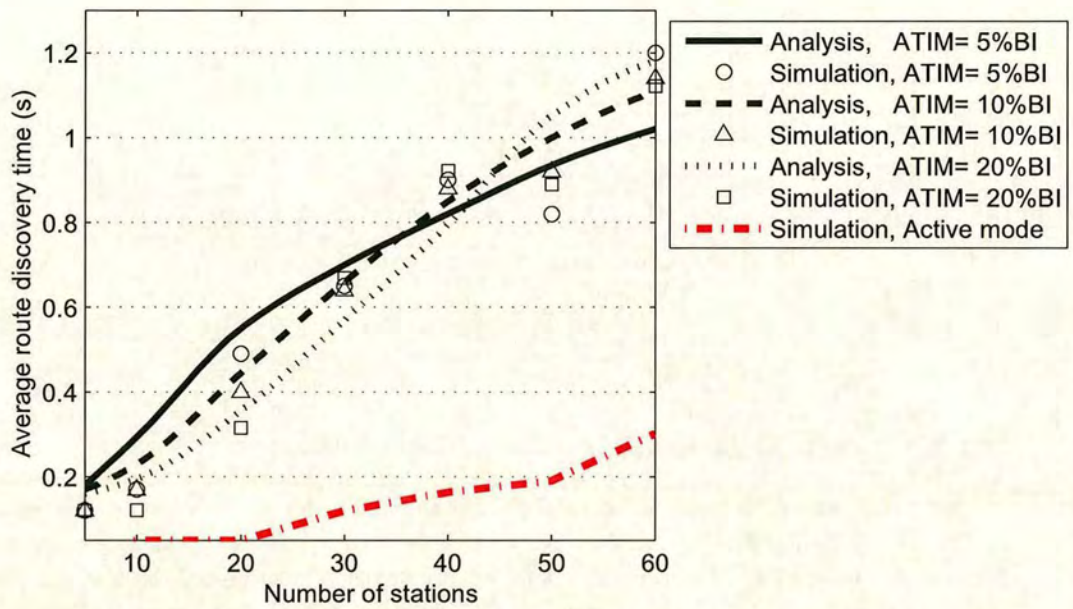


Figure 4.4: Average route discovery time, Basic CSMA/CA

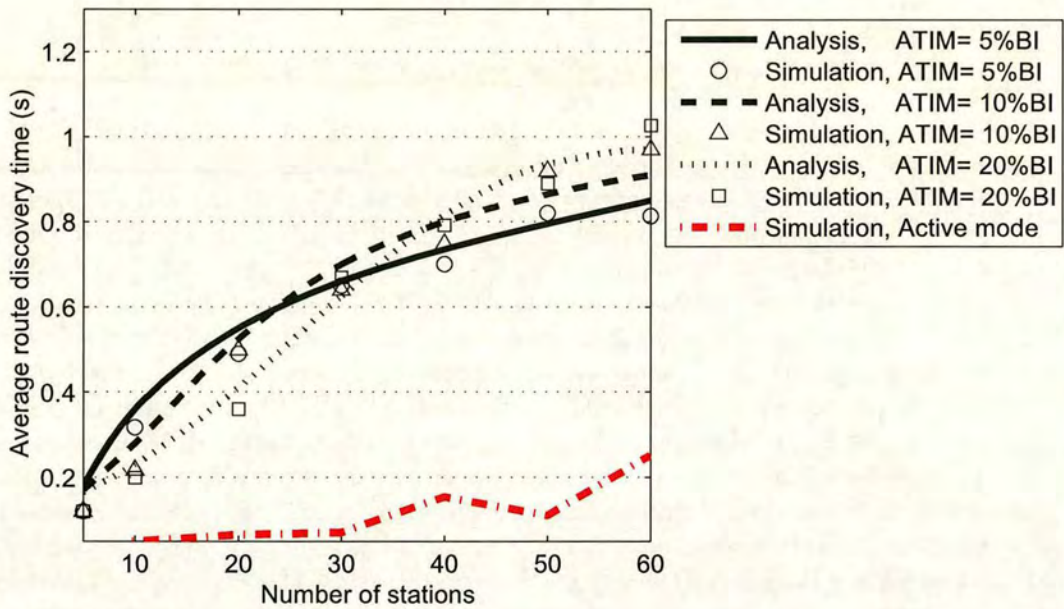


Figure 4.5: Average route discovery time, CSMA/CA with RTS/CTS

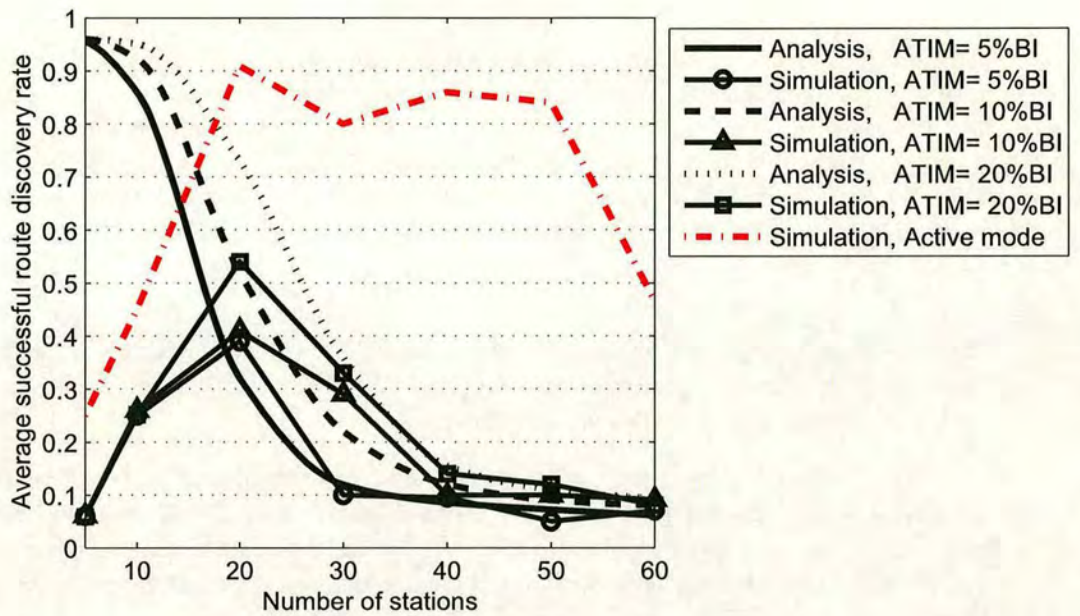


Figure 4.6: Average end-to-end delay of RRP, Basic CSMA/CA

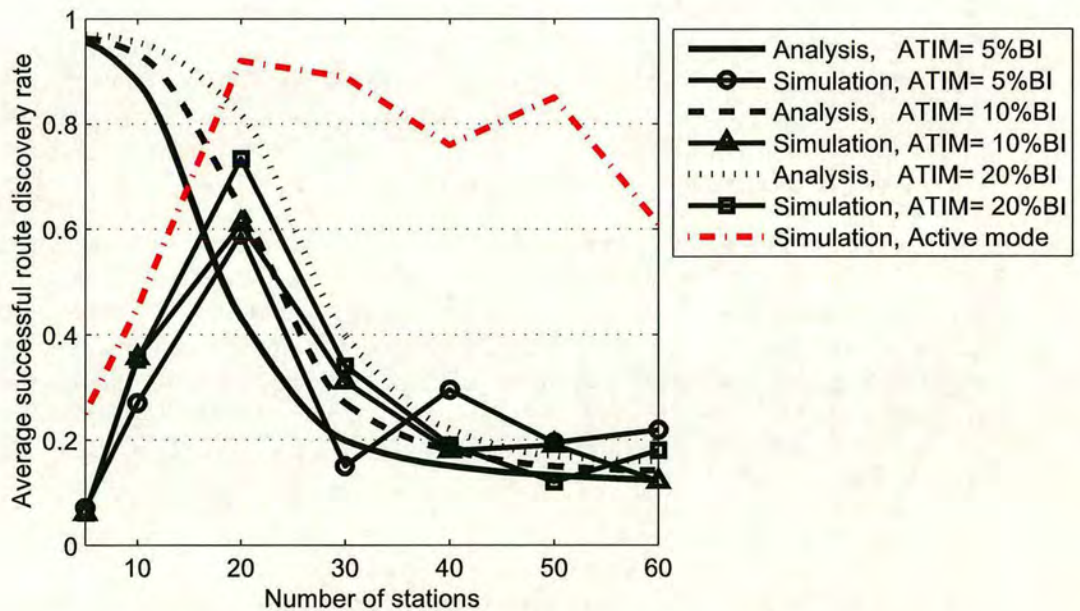


Figure 4.7: Average end-to-end delay of RRP, CSMA/CA with RTS/CTS

4.2 Improved Route Discovery with Power-Saving MAC

To achieve the power saving objective, a station can transmit packets only after getting synchronization and exchanging ATIM packets, resulting in high latency. Comparing the simulation results in PS mode against those in active mode, shown in Figures 4.4, and 4.5, it is clear that the packet delay increase caused by the IEEE 802.11 PS mode affects the collection of topology information in on-demand MANET routing. To ensure successful routing operation in PS WLANs, the transmission mechanism for routing control packets should be altered, while maintaining compatibility to the original standard and low energy consumption.

Approach A

In this solution, to improve the latency characteristic and achieve a fast route discovery, routing control packets related to route discovery, such as RRP and RACKP, can be exchanged during the whole BI. This approach is described below:

If a station wants to initiate a route discovery, it should send a route-discovery beacon (RDB), which is a normal beacon tagged with route-discovery mark, to other stations at the beginning of the ATIM window. Any PS stations, which receives an RDB, should relay this beacon to its neighbours, thus informing all the stations of the route-discovery operation in advance.

The source station and other PS stations, which receive an RDB should stay awake for a period of $m \cdot BI$. The value of m should satisfy the condition: $(m - 1) \cdot BI \leq \Phi \leq m \cdot BI$, Φ is the maximum route request period.

After sending the RDB, the source node sends an RRP to start the route-discovery routine, during the ATIM window or the data window. Other stations also can relay the RRP/RACKP during the ATIM window. Because all the neighbours are awake, the time penalty in route discovery decreases. When the source node receives the RACKP from the destination node, at the beginning of the next BI, it will broadcast a beacon tagged with a route-discovery-end (RDE) mark. Any PS station, which receives an RDE beacon, will relay this beacon to its neighbours, and enter the normal PS mode. If the source node cannot receive the RACKP within $m \cdot BI$, the same route-discovery process will be repeated.

Since routing control packets can be exchanged, as in the active mode, this method can decrease the end-to-end delay for routing control packets. However, it will result in higher energy consumption, since all the stations remain awake during route discovery. The tradeoff, between the energy and reliability of routing, of this method depends on the topology stability. In light of the DSR mechanism, the more stable the topology is, the fewer route-discovery operations are needed.

Approach B

In this method, to decrease the delay of route discovery control packets and minimize energy consumption, a higher priority for transmitting is given to the routing control packets and their respective ATIM packets. Since transmission of all kinds of packets uses the surferframe specified in the standard, this approach is more backward compatible than approach A.

In the original IEEE802.11 standard, if a station with an ATIM or data packet to transmit ini-

tially senses the channel is busy, then this station waits until the channel becomes idle for a DIFS period, and then chooses a random “back-off counter”, which determines the amount of time the station must wait until it is allowed to transmit its packet. During the period in which the channel is clear, the transmitting station decreases its back-off counter. This process is repeated until the back-off counter reaches zero and the station is allowed to transmit. The idle period after a DIFS period is referred to as the contention window (CW), whose size is randomly selected from $[0, W]$. W is initially set to aCW_{min} . W is doubled each time the station experiences a collision until W reaches aCW_{max} (Maximum Contention Window), which is equal to $2^m \cdot aCW_{min}$. When W reaches aCW_{max} , it remains the same even if there are more collisions. After every successful transmission, W is reset to the initial value aCW_{min} . The normal value of aCW_{min} in the standard is 31, and m is 5. With CSMA/CD, the probability, $\tau(N)$, that a station transmits a packet in a slot is [33]:

$$\tau(N) = \frac{2}{1 + aCW_{min} + p \cdot aCW_{min} \cdot \sum_{i=0}^{m-1} (2p)^i} \quad (4.16)$$

where p is the probability that a transmitted packet encounters a collision. It is clear that a smaller aCW_{min} will result in a higher probability for transmission. In our approach, if a station transmits routing control packets and their relative ATIM packets, it sets the aCW_{min} to 7, which is less than the normal value defined in the standard. In this case, the route control packets obtain a higher priority for transmission than other packets, which can improve the transmission rate for RRP, RACKP, and their ATIM packets. As depicted in the analysis and simulation, increasing the transmission rate is equivalent to decreasing the packet delay, thus improving the route discovery rate.

Compared to approach A, this method makes only slight modifications to the standard, so it is more compatible. Since the routing control packets have higher priority in transmission, when the contention is severe, this method will achieve better performance than that under normal contention conditions. On the other hand, since approach B reserves the PS surperframe, it will not degrade power-saving performance. However, because the transmission of routing control packets in approach B is still affected by the ATIM exchange, the performance of route discovery rate in approach A will be better than approach B.

Simulation

Figure 4.8 shows the simulation results to compare the performance of the proposed approaches against the original PS and active modes. In the simulation, the size of ATIM window is fixed at 5ms, and no RTS/CTS mechanism is applied. In the approach A, routing control packets can be transmitted during the whole BI, which is very similar to the active mode, so the route discovery rate of the approach A is very close to that in the active mode. Some extra beacon transmissions, such as RDB, are necessary in the route discovery procedure, so, compared to the successful route discovery rate of the active mode, the successful rate of approach A is still a little lower. However, all the stations keep awake during the route discovery procedure, which will result in more energy consumption than other PS modes.

When the number of stations is larger than 20, the successful rate of approach B is higher than that in the original PS mode, because approach B gives a higher priority to routing control packet transmission, thus protecting the routing control packets' transmission when contention

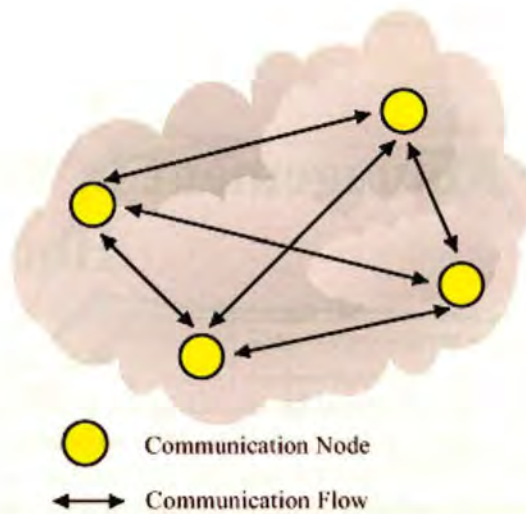


Figure 5.1: *Peer-to-Peer topology*

chapter, without a good network synchronization, power-saving operations in ad hoc networks perform poorly.

5.1.2 Star Topology

With the star topology, a network coordinator can centrally execute operations with relation to the global quality metrics, thus improving the network efficiency. These networking operations include adjusting the traffic load of each communication flow, and distributing the media access period in a TDD MAC or the spreading codes in CDMA etc. Since the capacity of a device may be dynamically changing, for example, losing battery power, it is not sensible for a device to permanently act as a coordinator in a wireless ad hoc network. Normally, the most capable device is dynamically selected as the network coordinator in terms of the capacity function. For instance, in power-aware networks, the residual battery energy of devices can be considered as the important criteria for coordinator selection. On the other hand, if all data exchange passes through the coordinator, the traffic load in a coordinator will rise sharply. In wired networks, the coordinator always has sufficient capability to deal with the heavy traffic. However, resource limitation is always a problem in wireless ad hoc networks. Therefore, a better network structure for wireless ad hoc networks may be using a hybrid topology, as shown in Figure 5.3, which combines the star topology with a peer-to-peer topology. A typical application of this hybrid topology is the IEEE802.15.3-based WPAN, where the star topology is used for control information exchange between the coordinator and other devices, while normal data exchange is over the peer-to-peer topology. This means the coordinator need not relay data packets for other devices.

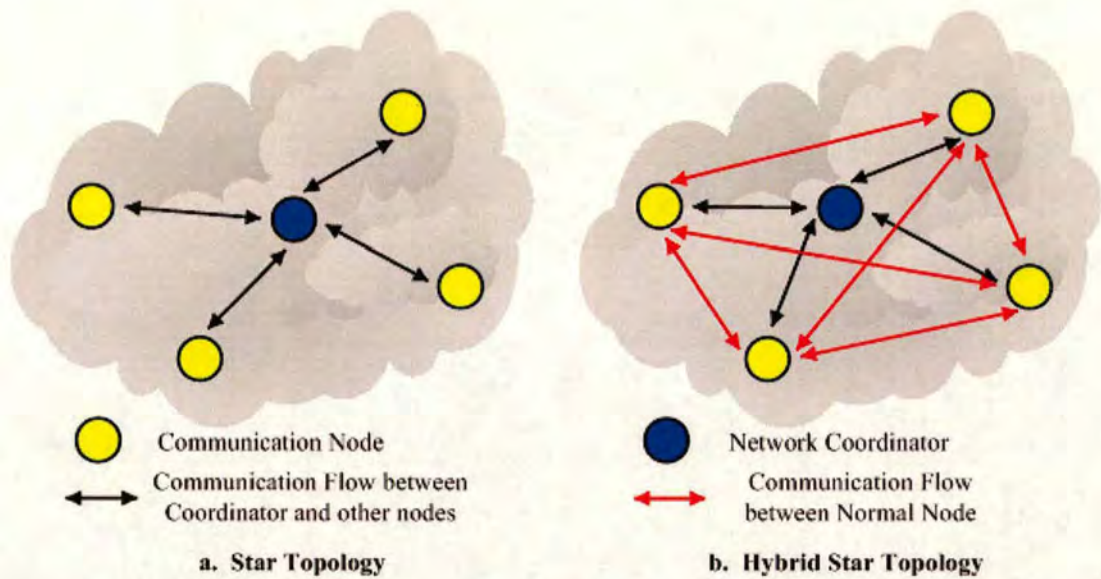


Figure 5.2: *Star topologies*

5.1.3 Cluster Topology

Contention for channel access and the control overhead are linear in the number of nodes of an ad hoc network in the star topology or peer-to-peer topology. Obviously, the cluster topology reduces the number of devices contending for channel access, and minimizes control overhead. Clustering is particularly useful for applications that require scalability to hundreds or thousands of nodes [40]. Here, “scalability” means the need for load balancing, efficient resource utilization, and data aggregation. Figure 5.3 shows a cluster topology, where the entire network is divided into some areas, called clusters. The most capable device in a cluster is selected as the cluster head, and is the overall coordinator for the communication in this cluster. Other devices in a cluster can only communicate with the cluster head. If they want to communicate with devices in other clusters, they have to use the communication flows between the cluster heads. In some specific applications, such as sensor networks, when a device wants to transmit information to a remote observer (e.g., a base station), it firstly sends the data to the cluster head, then the cluster head will relay the information to the remote observer [41]. Routing can only be performed between cluster heads, which has a relatively small diameter. In distributed systems, a device could act as both a common node and cluster head, which motivates the demand for efficient algorithms to select a set of cluster heads. For instance, in power-aware systems, periodic reclustering could select devices with higher residual energy to act as cluster heads to prolong network lifetime.

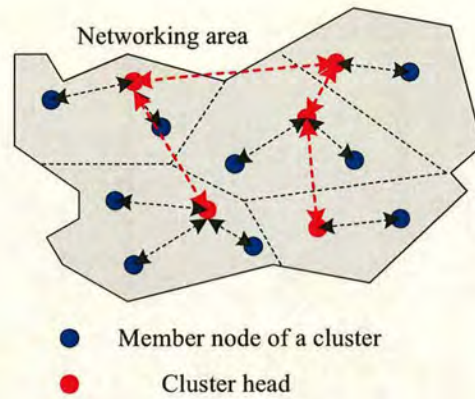


Figure 5.3: *Cluster topology*

5.2 Application of Cluster-Tree Topology in Wireless Ad Hoc Sensor Networks

5.2.1 Wireless Ad Hoc Sensor Network

As the result of advances in sensor technology, micro-electro-mechanism systems (MEMSs), and wireless communication technologies, sensor networks, which were initially driven by military applications [42], have appeared as the important tool for habitat monitoring, remote ecological observation, health monitoring, the smart home/office, and enemy tracking in the battlefield [43] [44] [45]. Figure 5.4 shows the architecture of a sensor network. Generally, in a sensor network, a large number of wireless unattended sensors are scattered randomly in a monitoring area. One sink node is specified to relay the data of this monitoring area to the remote central stations. These sensor nodes are low cost, energy-restrained, and functionally limited. Each node typically consists of four units (figure 5.4), a data acquisition unit, a processing unit, a communication unit and a power supply unit. Wireless communication links are maintained by an energy-efficient, low-transmission-power communication unit. Aided by micro operating systems, such as TinyOS [46], developed in Berkeley, the central processing unit schedules the tasks of data acquisition and communication. Like mobile ad hoc networks (MANETs), a wireless ad hoc sensor network has no fixed infrastructure and unpredictable connectivity. Without centralized configuration, sensor nodes are not only the means to data interchange but also the managers for the routes to data and access to control operations.

Prolonging network lifetime is one of the critical issues in sensor networks, widely discussed in the literature, since the sensor nodes are battery operated and not easily recharged. To improve link survivability and stability of the topology, research has been done in each aspect of sensor network communication, such as routing protocols in the network layer and media access schemes in the MAC layer. Current MAC designs for wireless sensor networks concentrate on using various methods to put the communication unit of a sensor node to sleep and minimizing the time in transmission, reception and idle states [47] [48], or to decrease interference with neighbouring nodes by clustering [40]. Power-aware routing is another means to make the connections more reliable. Generally, there will be many possible communication paths between

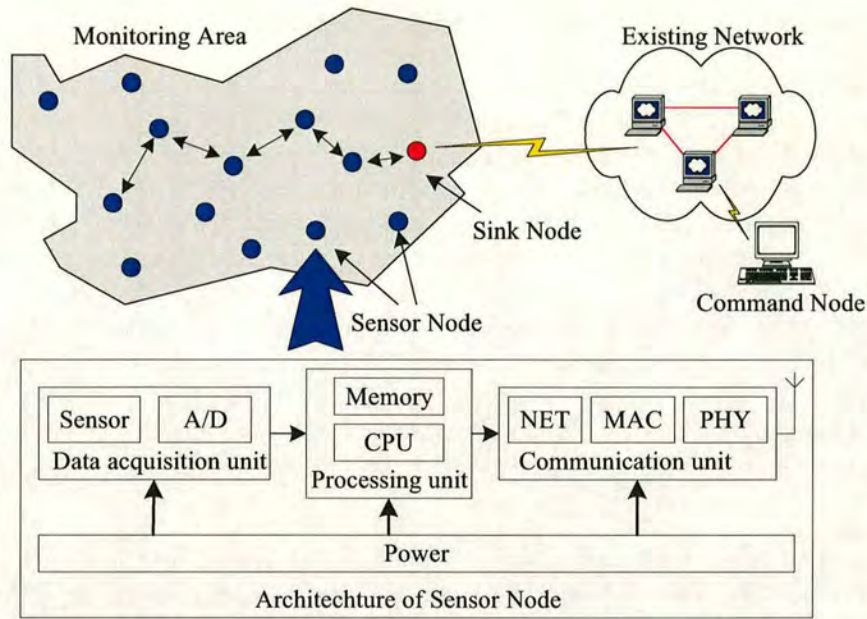


Figure 5.4: *Architecture of sensor network and sensor node*

source and sink nodes in such a dense network. Most of the existing protocols try to find the minimum energy path to improve the energy usage of a node.

5.2.2 Cluster-Tree Topology in IEEE802.15.4-Based LR-WPAN

The IEEE802.15.4 MAC standard [20] is designed for emerging applications with easy installation, reliable data transfer, short-range operation, and reasonable battery life. These objectives can be achieved in low-rate wireless personal networks (LR-WPANs), a simple low-cost communication network, which supports wireless connectivity with limited power and light throughput requirements. The data rate in an IEEE802.15.4-based LR-WPAN is either 250kb/s, 40kb/s, or 20kb/s.

An IEEE802.15.4-based LR-WPAN is composed of two different device types, full-function devices (FFD), and a reduced-function devices (RFD). An FFD could be selected as a PAN coordinator. It can talk to RFDs or other FFDs, while an RFD can talk only to an FFD. An RFD is intended for applications that are extremely simple, such as a light switch or a passive sensor, which do not need to send large amounts of data and may only be associated with a single FFD at a time. Consequently, the IEEE802.15.3-based LR-WPAN can be used for some sensor network applications.

5.2.2.1 Channel Access in IEEE802.15.4-Based LR-WPANs

A low-rate WPAN can be initialized by an FFD, performing an active or passive channel scan at the beginning. The active channel scan consists of transmitting the beacon request command in every channel. In the passive channel scan procedure, an FFD simply listens for beacons in every channel. After completing the scan, the FFD will select a suitable PAN identifier to act as a network coordinator in a channel, in which there are no other coordinators. Device discovery is important in a PAN, as it enables a variety of applications to be supported. To associate with a network, a device should perform a channel scan to find existing networks to join. If more than one network is operating, the device must select a PAN to join in terms of the policies specified by application developers. After selecting a network, the device can initiate association by sending an association request command during the contention access period of an existing PAN. When the coordinator receives the association request, it will decide whether there are enough resources available for the device and if so assign a 16-bit address to the device.

In the LR-WPAN MAC, there are four frame structures: beacon frame, data frame, acknowledgment frame, and MAC command frame. The beacon is transmitted without the use of CSMA. In the beacon, the network coordinator provides information about the permitted packet size, the current network coordinator operational state, and the length of the contention period. These parameters could be dynamically changing, so the coordinator must keep the information contained in the beacon up to date. Depending on whether the network is beacon-enabled or not, the LR-WPAN MAC uses two types of channel access: networks without a beacon using a CSMA/CA channel access mechanism and networks with a beacon use a slotted CSMA/CA channel access protocol. In this slotted CSMA/CA scheme, a station that wants to transmit senses the channel. If the channel is idle it will wait for a random number of slots and begin transmitting on the next available slot boundary. The contention period starts immediately after the beacon, which means the backoff slots are aligned with the start of the beacon. The beacon itself and acknowledgments are sent without CSMA/CA.



Figure 5.5: *General superframe structure with active and inactive periods*

The IEEE802.15.4 LR-WPAN standard allows the optional use of a superframe structure. The superframe format is defined by the network coordinator. A superframe consists of a beacon, contention access period (CAP), and contention-free period (CFP) as shown in Figure 5.5. While this is similar to the superframe used in IEEE802.15.3, the contention-free period is optional. The channel access mechanism during the CAP is slotted CSMA/CA. The CFP is divided into dedicated slots, which are called guaranteed time slots (GTSs), for different devices. Therefore, a TDMA mechanism is operated within the CFP. The beacons sent by the network coordinator are used to synchronize devices and to identify the network. A superframe may have an active and inactive portion, as illustrated in Figure 5.5. During the inactive portion of a superframe, devices can enter low-power mode, thus saving energy.

Because the network is wireless, and may be mobile, it is possible for a device to stop receiving beacons from the coordinator for an extended period of time. Devices that become lost should not transmit to avoid conflicts on the wireless medium. A lost device can do an orphan scan to realign itself. It sends an orphan notification command on each channel. If a coordinator receives the orphan notification command, it will check its device list to determine whether the orphaned device is a member of its PAN. If the device is a member of its PAN, the coordinator will send a coordinator realignment command back to the orphaned device. If the orphan scan is unsuccessful, the device will assume that it has permanently lost the connection, and then it will inform the higher layers for further reaction.

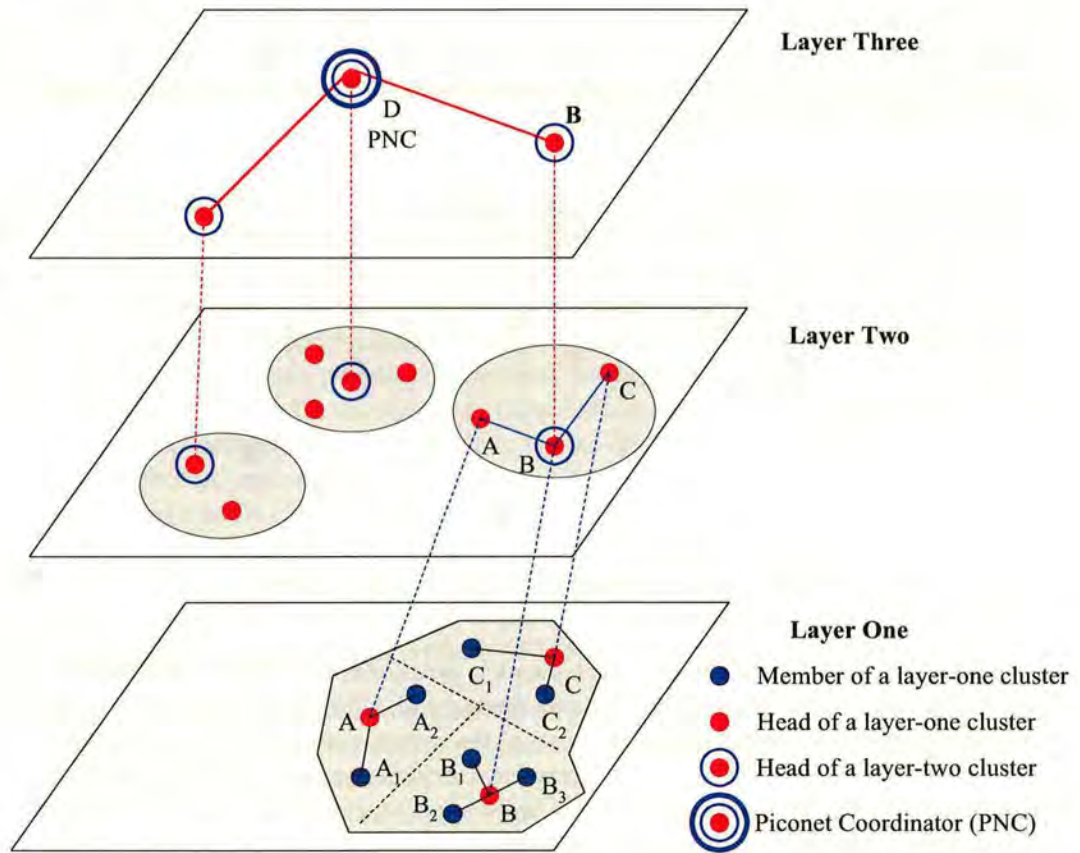


Figure 5.6: An example of hierarchical cluster-tree topology

5.2.2.2 Hierarchical Cluster-Tree Topology

When the networking area is large, or the devices have different capabilities, it is appropriate to organize the devices into different layers of the cluster-tree topology (figure 5.6). On each layer, a set of clusters is created to support scalable routing solutions and efficient resource management.

The cluster-tree network is a special case of a peer-to-peer network, in which FFDs and RFDs

- Each cluster is a one-hop system. The whole network is a hierarchical cluster architecture. These topology characteristics simplify routing operations in a large scale network.

5.2.3.1 The Potential of a Device to Serve as a Clusterhead

In this section, we formulate the potential of an FFD to serve as a clusterhead (PDSC), which relates to the relative position, residual energy, and other properties of an FFD.

As shown in Figure 5.8, the shorter the distance between cluster members and the clusterhead, the smaller the coverage this cluster has. In other words, the distances between the clusterhead and other cluster members should be considered. In many proposed clustering methods, the location and distance can be obtained by using the global positioning system (GPS) [51]. However, applying GPS will increase the prime cost of the implementation of the mobile communication devices and reduce the marketability, especially for cheap low-rate WPANs. To make the clustering algorithm more practicable, the received signal power, which is a measured value from the PHY, is used to roughly estimate the distance in our clustering algorithm. As explained in [52], the desired receiving power level for a correctly decoded packet, P_r , can be derived as:

$$P_r = \frac{P_t \cdot G_t \cdot G_r}{PL(d) \cdot L}; \quad (d \gg 2D^{2/\lambda}) \quad (5.1)$$

where P_t is the transmitted power, G_t and G_r are the transmitter and receiver antenna gains, PL_d is the path loss (PL) with distance d , L is the system loss factor ($L \geq 1$), D is the maximum dimension of transmitting antenna, and λ is the corresponding wavelength of the propagating signal. The measurement unit of P_r is milliwatt (mW). The antenna gain G is equal to $4\pi \cdot A_e / \lambda^2$. A_e is the effective aperture of the antenna. The value of λ can be found by $\lambda = c/f = 3 \times 10^8 / f$, where f is the carrier frequency. P_r can be represented in dBm as:

$$\begin{aligned} Pr(d) &= 10 \log(P_r[mW]) \\ &= P_t + G_t + G_r - PL(d) - L \end{aligned} \quad (5.2)$$

Under free space propagation, there is only one clear line-of-sight (LOS) path between the transmitter and receiver. For a LOS path, the PL can be evaluated as:

$$PL(d) = \left(\frac{4}{\lambda}\right)^m \quad (5.3)$$

where m is the path loss exponent, typically between 2 and 4. We assume $m = 2$, then PL is given by:

$$PL(d) = 92.4 + 20 \log(f) + 20 \log(d) \quad dB \quad (5.4)$$

Combined with equations 5.1 and 5.3, the distance between the transmitter and receiver can be found:

$$d = \lambda \sqrt{\frac{P_t G_t G_r}{P_r L}} / 4\pi \quad (5.5)$$

Consider a group of n devices:

$$X = \{x_1, x_2, \dots, x_n\} \quad (5.6)$$

Then we define a measure of the potential of device i to act as a clusterhead as:

$$P_i = k_i \sum_{j=1}^n e^{-\frac{\Delta E_i}{N \cdot T} \frac{\|d_{i,j}\|^2}{r^2}}; \quad (N = 1, 2, 3, \dots) \quad (5.7)$$

where $d_{i,j}$ is the distance between device i and j , which can be estimated by equation 5.5, r is a positive constant as an effectively normalized radius defining a neighbourhood. Devices outside this radius have little influence on the potential. We can use this value to adjust the size of clusters. It is clear that if more devices are close to device i , its PDSC will become bigger, thus device i will have a higher probability to be chosen as the clusterhead. T is the cluster refreshing period, i.e. the period between clusterhead reselections. ΔE_i is the decreased residual energy in device i during $N \cdot T$. The value of $\Delta E_i / N \cdot T$ depicts how fast the energy is depleted. The objective of using this metric is to avoid selecting devices with a higher load of communication or computation. For example, if an FFD was frequently selected as the clusterhead, energy will be faster used than in other devices. Therefore, the metric, $\Delta E_i / N \cdot T$, can be used to average the probability of being selected as a clusterhead, and the energy consumption among all FFDs, thus postponing the time to network partition, and improving the topology stability. This metric is more appropriate than other metrics, such as the number of times a node is selected as clusterhead, as used in the LEACH (Low Energy Adaptive Clustering Hierarchy) clustering method [53], since a device acting as a clusterhead more frequently does not mean its energy will be exhausted more quickly than other devices.

In equation 5.7, k_i is defined as follows:

$$k_i = \begin{cases} 1, & E_{Residual_i} \geq E_{TH} \\ 0, & otherwise \end{cases} \quad (5.8)$$

where $E_{Residual_i}$ is the residual battery energy in device i , E_{TH} is the threshold of the residual energy to serve as a clusterhead. This metric prevents FFDs with low residual energy from being chosen as the clusterhead. Obviously, at least, the threshold, E_{TH} , should be bigger than the energy used by a clusterhead for all possible operations during the cluster refresh period, T . In some cases, if other characteristics, such as capacity, MC_i , and computation speed, CS_i , are considered in the selection of clusterheads, equation 5.8 can be expanded:

$$k_i = \begin{cases} 1, & E_{Residual_i} \geq E_{TH}, MC_i \geq MC_{TH}, CS_i \geq CS_{TH} \\ 0, & otherwise \end{cases} \quad (5.9)$$

5.2.3.2 The Hierarchical Clustering Algorithm

The proposed clustering algorithm partitions the multihop network into non-overlapping clusters. Within each cluster, devices can communicate with each other in at most one hop. Only FFDs are selected as the clusterhead or PNC. The following assumptions are made in the construction of the algorithm in a radio network.

1. Every device has a unique ID. This can be provided by the physical layer for mutual location and identification of radio devices.
2. Every device has a cluster refresh counter (CRC), which controls the frequency of the clustering operation.
3. A packet sent by a device can be received correctly within a finite time by all of its one-hop neighbours.
4. The network topology does not change or changes very slowly during the clustering algorithm execution.
5. An FFD's maximum transmission power can cover the whole Piconet.

All devices initially set the CRC to the same value T . This initial value could be changed by the PNC. Devices decrease the CRC until it reaches zero, and then the cluster-refreshing routine is triggered. At the beginning of the routine, each FFD or RFD broadcasts a cluster-refreshing probe packet (CRPP), whose frame payload is empty. Referring to the frame format specified in the standard IEEE802.15.4 [20], the structure of CRPP is illustrated in Figure 5.9, where "MHR" and "MFR" means "MAC Header" and "MAC Footer" respectively. Since the CRPP is just used for announcing the beginning of the cluster-refreshing routine, in beacon-enabled LR-WPANs, the beacon packet could replace the CRPP to minimize the bandwidth cost.

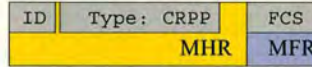


Figure 5.9: The structure of a CRPP

The transmission power of CRPP is fixed at P_{clu} , which is specified by the PNC. All the FFDs will listen to their neighbour's CRPP and calculate the corresponding PDSC. For instance, if a FFD i receives a CRPP from a device j , it can estimate the distance, $d_{i,j}$, between the device i and j in terms of the receiving signal power, P_{rj} :

$$d_{i,j} = \lambda \sqrt{\frac{P_{clu} G_t G_r}{P_{rj} L}} / 4\pi \quad (5.10)$$

Then, the weight of the PDSC introduced by the device j , P_{ij} , can be computed by device i as follows:

$$P_{ij} = e^{-\frac{\Delta E}{N \cdot T} \frac{\|d_{i,j}\|^2}{r^2}} \quad (5.11)$$

If the number of received CRPPs in FFD i is n_i , FFD i can calculate its PDSC, P_i , as follows:

$$P_i = k_i e^{-\frac{\Delta E}{N \cdot T}} \sum_{j=1}^{n_i} P_{ij} \quad (5.12)$$

If $P_i = 0$, FFD i will give up applying to be the clusterhead, otherwise, it will broadcast its PDSC value, using a clusterhead-application packet (CHAP) with a transmission power, P_{clu} . The CHAP format is shown in Figure 5.10.

ID	Type: CHAP	PDSC	Pt _{clu}	Pr _{dsr}	FCS
MHR		MAC Payload			MFR

Pt_{clu}: Transmission power for this CHAP

Pr_{dsr}: Desired receiving power for this clusterhead

Figure 5.10: The structure of a CHAP

The transmission power of this CHAP, P_{clu} , is enclosed in the MAC frame body. An FFD, who has the right to send the CHAP, computes the desired signal receiving power, $P_{r_{dsr}}$, and writes it into the CMAP's (cluster-member-association packet) MAC frame payload as well. If the FFD becomes the clusterhead, its cluster members will determine a desired transmission power, $P_{t_{dsr}}$, for their packet transmissions with the clusterhead. The objective of controlling this cluster member's transmission power is to reduce the coverage, thus decreasing interference to neighbouring clusters and saving energy. $P_{t_{dsr}}$ for a cluster member device, j , can be defined as:

$$P_{t_{dsr_j}} = L \cdot P_{r_{dsr}} \cdot (4\pi d_{j,Head})^2 / (G_t G_r \lambda^2) \quad (5.13)$$

All the devices will listen to the CHAPs, and find the maximum PDSC value among the PDSC set, which consists of the received values of PDSC, and its own PDSC value. Then, a device will send a cluster-member-association packet (CMAP) to the FFD, with the maximum PDSC value. The transmission power of a CMAP is calculated by equation 5.13. The FFD, which receives CMAPs, will become the clusterhead, and record the IDs of the source of the CMAPs. The sender of the CMAP becomes a member of the corresponding cluster. The frame structure of a CMAP is shown in Figure 5.11.

An example of this low-layer clustering operation is shown in Figure 5.12. Based on the CRPP transmission, all FFDs calculate their PDSC values, and broadcast this value to their neighbours. For instance, in Figure 5.12, RFD_1 received two PDSC values from FFD_4 and

ID	Type: CMAP	Destination FFD	FCS
MHR			MFR

Figure 5.11: The structure of a CMAP

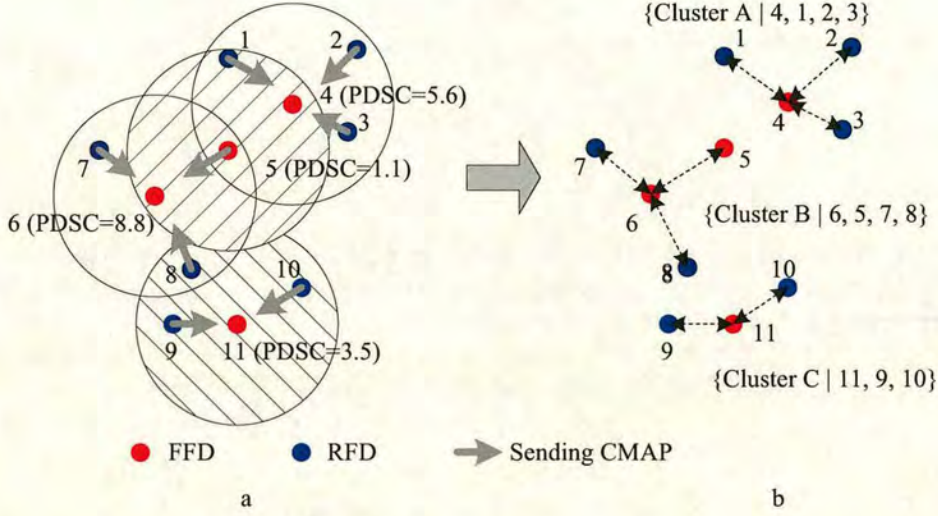


Figure 5.12: Comparing the PDSC values, devices decide to associate to clusterheads. *a*: After comparing the PDSC values, devices send CMAPs to their clusterheads; *b*: Three clusters are constructed.

*FFD*₅. Since the PDSC from *FFD*₄ is bigger, *RFD*₁ sends a CMAP to *FFD*₄, which means *RFD*₁ becomes a cluster member, and can be associated with the clusterhead, *FFD*₄. *FFD*₅ will compose three PDSC values, which come from *FFD*₄, *FFD*₆ and itself. After comparing the PDSC values, *FFD*₅ sends a CMAP to *FFD*₆. Finally, the whole network is partitioned into three clusters, which are:

1. Cluster A; Clusterhead: *FFD*₄; Cluster Members: *RFD*₁, *RFD*₂, *RFD*₃;
2. Cluster B; Clusterhead: *FFD*₆; Cluster Members: *FFD*₅, *RFD*₇, *RFD*₈;
3. Cluster C; Clusterhead: *FFD*₁₁; Cluster Members: *RFD*₉, *RFD*₁₀.

An FFD can control its number of cluster members through adjusting the value of r . For example, if *FFD*₆ wants to decrease the number of cluster members, it can decrease r , when calculating its PDSC through equation 5.12.

After finishing the layer-one clustering, the cluster members should use $P_{t_{dsr}}$ for their packet transmission, and the clusterhead uses the transmission power, P_{clu} , to communicate with their cluster members.

To decide the PNC, the clusterheads, which did not send CMAP, for example, *FFD*₄, *FFD*₆, and *FFD*₁₁, should broadcast PNC-searching probe packets (PSPPs), which enclose their

PDSC values, with a maximum transmission power. The frame structure of a PSPP is shown in Figure 5.13.

ID	Type: PSPP	PDSC	$P_{t_{MAX}}$	$P_{r_{Desr}}$	FCS
MHR		MAC Payload			MFR

$P_{t_{MAX}}$: Transmission power for this PSPP

$P_{r_{Desr}}$: Desired receiving power for this clusterhead

Figure 5.13: The structure of a PSPP

Then, the clusterheads will search for the FFD with the highest PDSC value, and send a PNC-confirming packet (PCP) (figure 5.14) to this FFD. A FFD receiving PCPs will become the PNC for the Piconet. Similarly, the clusterheads will calculate a desired transmission power, $P_{t_{Desr}}$, in terms of $P_{t_{MAX}}$ and $P_{r_{Desr}}$ using equation 5.13. The clusterheads and PNC will use a corresponding $P_{t_{Desr}}$ for packet transmission among clusterheads and PNC. For example, as shown in Figure 5.15, the clusterheads, FFD_4 and FFD_{11} send PSPPs to FFD_6 , because FFD_6 has the highest PDSC value. FFD_4 and FFD_{11} should use transmission power $P_{t_{Desr4}}$ and $P_{t_{Desr11}}$ respectively to communicate with the PNC. The final cluster-tree topology is shown in Figure 5.15.b. The layer two cluster is $\{FFD_6, FFD_4, FFD_{11}\}$. The whole cluster-tree topology is shown in Figure 5.16.

ID	Type: PCP	Destination FFD	FCS
MHR			MFR

Figure 5.14: The structure of a PCP

In the example shown in Figure 5.12, the FFDs, which have been nominated for clusterheads, do not send CMAPs to other clusterheads. However, in some cases, some clusterheads may also send CMAPs to other clusterheads, thus the topology will be more complicated than that in Figure 5.12. As shown in Figure 5.17, when the PDSC values have been broadcast through CHAPs, devices send CMAPs to nominate the clusterheads (fig. 5.17.a). Though RFD_2 and RFD_3 send CMAPs to FFD_4 , which means FFD_4 can become a clusterhead, FFD_4 also needs to send a CMAP to FFD_5 , since its PDSC value is less than FFD_5 's. Similarly, FFD_5 has to send a CMAP to FFD_6 . Then, four clusters, $\{FFD_4, RFD_2, RFD_3\}$, $\{FFD_5, RFD_1, FFD_4\}$, $\{FFD_6, RFD_7, RFD_8, FFD_5\}$, and $\{FFD_{11}, RFD_9, RFD_{10}\}$, are formed (Figure 5.17.b). Since clusterheads, FFD_4 and FFD_5 , are associated with FFD_5 and FFD_6 respectively, they lose the right to be a PNC. The clusterheads, FFD_6 , and FFD_{11} , will broadcast PSPPs to inform the PDSC values to each other. Because FFD_6 has the biggest PDSC value, FFD_{11} sends a PCP to FFD_6 , and FFD_6 becomes the PNC (Figure 5.17.c). Finally, a three-layer cluster-tree topology is obtained (Figure 5.17.d).

5.2.3.3 Simulation Results

A 100-node wireless ad hoc network simulation environment was developed to compare the performance of our proposed algorithm against LEACH and direct communication. The nodes

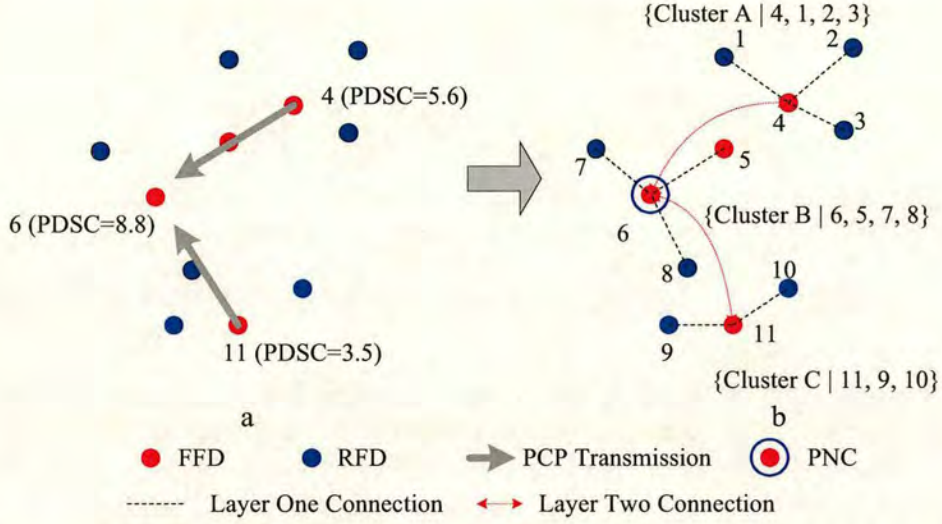


Figure 5.15: Comparing PDSC values, clusterheads choose a clusterhead as the PNC. a: After comparing PDSC values, clusterheads send PSPPs to the clusterhead with the maximum PDSC value; b: Two-layer cluster-tree topology, where the PNC is selected.

are randomly located in a $100m \times 100m$ area.

The energy consumption is estimated by the “first order radio” model discussed in [54]. This energy model can be described as follows:

$$E_{i.tx} = E_{tx} \times P_{tx} + \varepsilon_{amp} \times P_{tx} \times d_{i-j}^2 \quad (\text{Joules})$$

$$E_{i.rx} = E_{rx} \times P_{rx}$$

where $E_{i.tx}$ is the energy consumed in transmission, and $E_{i.rx}$ the energy consumed in reception for node i . E_{tx} and E_{rx} are the radio transmitter and receiver energy dissipation per bit. We assume the node has some form of power control to achieve an acceptable signal-to-noise ratio. ε_{amp} is set to obtain the desired signal strength for transmissions to j . P_{tx} and P_{rx} are the transmitted packet size and the received packet size. d_{i-j} is the distance between the source node i and the destination node j . In the simulation, $E_{tx} = E_{rx} = 50nJ/bit$, $E_{amp} = 100nJ/bit/m^2$. Each node is given an initial energy, calculated from a uniform probability distribution function (PDF) with the range [800J,1000J].

A CSMA/CA strategy is used for the IEEE802.15.4-based MAC layer. The residual energy threshold, E_{TH} , is set to 50J, the cluster refreshing period, T is 2s, and N is 3. The data rate is fixed at 40kbts/s. Each data message is 1000bits. All cluster diameters are the same, and are set to 10m.

Figure 5.18 shows the percentage of the number of devices that remain alive during simulation. The plot shows that devices die out more quickly using direct transmission than LEACH. Our proposed clustering scheme has the longest lifetime, nearly 40 minutes longer than LEACH. Through measuring the energy change in devices, the proposed clustering method can avoid fre-

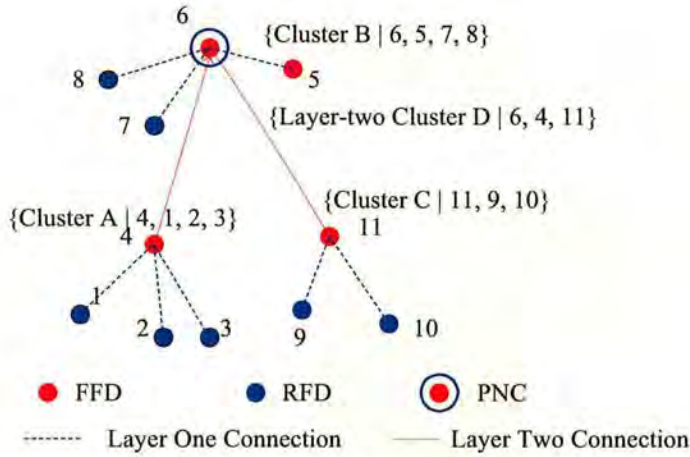


Figure 5.16: *Cluster-tree topology in the example.*

quently selecting an FFD as the clusterhead, thus averaging the energy consumption across the whole network. Moreover, use of the PDSC results in a cluster having more cluster members. In other words, more devices use a smaller transmission power for inter-cluster communication. On the other hand, in the proposed scheme, the byproduct of the clustering algorithm is power control in terms of the transmission distance, which can greatly decrease energy consumption. In contrast, direct transmissions have to cover the whole network, so it is clear the direct transmission scheme will have the worst power-saving performance.

The throughput performance of the proposed clustering method is also compared to the direct transmission and LEACH scheme (Figure 5.19). As we know, in CSMA/CA media access mechanism, collisions will strongly influence the throughput. In the proposed algorithm, the coverage is reduced by controlling transmission power. Therefore, the interference, introduced by a cluster's communication, can be greatly reduced, thus improving the throughput. While, in LEACH and direct communication schemes, each device's transmission will affect most devices trying to occupy the channel. When the simulation time increases, more and more devices will become energy exhausted. In the early stage of the simulation for the direct communication or LEACH scheme, the death of some devices improves the contention condition for channel access, thus the throughput will increase slowly. Then, the throughput will sharply decrease, since most of the devices become energy-exhausted. The initial energy configuration will also be a significant factor for those trends in the curves.

5.3 Summary and Conclusions

If the capabilities of devices are different in large scale networks, a cluster-tree topology may exploit the potential of each device better than other network topologies. Bandwidth and energy reservation is a major challenge in the IEEE802.15.4-based LR-WPAN. To prolong lifetime of the whole network, improve network throughput, and support a simple topology management method in a large scale network, a hierarchical clustering algorithm is proposed. Through

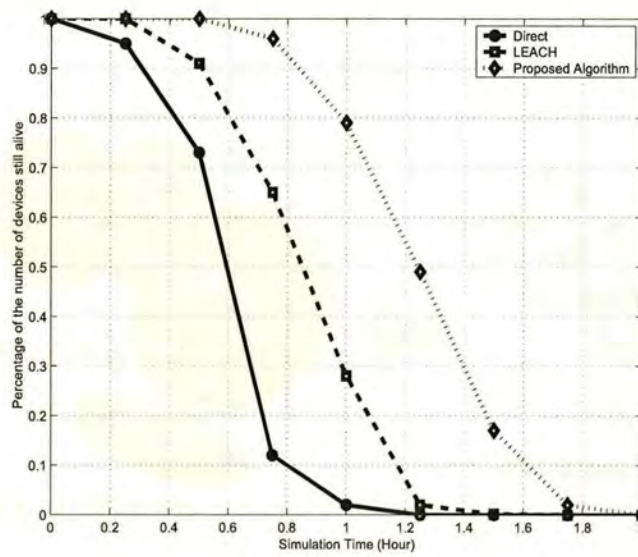


Figure 5.18: System lifetime using direct transmission, LEACH, and the proposed clustering method.

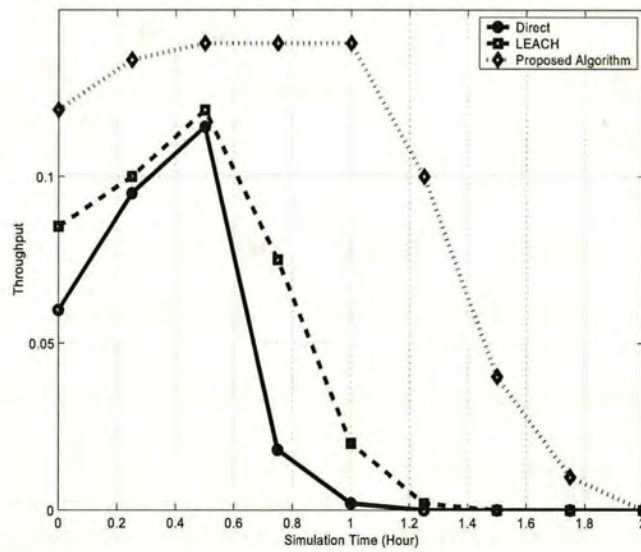


Figure 5.19: System throughput using direct transmission, LEACH, and the proposed clustering method.

Chapter 6

Power Control in Wireless Ad Hoc Networks

In wireless communication devices, energy used for transmission is a major factor in battery drain. Therefore, it is important to cut down the transmission power for energy efficiency. In addition to battery considerations, excessive transmission power will block neighbouring devices'/networks' communication, thus impairing network throughput. From the above considerations, power control relates to not only the energy efficiency, but also the interference mitigation. In MANETs, because of mobility, a dynamic radio environment, and distributed networking operations, the power control is different from those for other types of networks:

- No centralized schedulers can be utilized for power control, the transmission power should be self-disciplined, thus the power control will be performed by distributed operations;
- The transmission power should be adjusted with an appropriate frequency to adapt to the dynamically changing environment;
- A node might have many links to its neighbors, so a power control should consider the different characteristics of all the related links.

In this chapter, firstly, various power control methods for ad hoc networks are introduced in section 6.1. As a practical example, a novel power control method combined with PNC selection in WPANs is discussed in section 6.2. To prove the concepts proposed in 6.2, section 6.3 introduced the details of implementing and validating the proposed methods into real devices and networks.

6.1 Power Control Methods for Ad Hoc Networks

6.1.1 RTS/CTS-Based Power Control

The four-way handshake with RTS/CTS (Request-To-Send/Clear-To-Send) mechanism is widely used in wireless networks to avoid the so called "hidden terminals" problem. Before transmitting a data packet, a source device should send an RTS packet to the destination. Only if the source node successfully receives a CTS packet from the destination, can it transmit a data packet. The RTS/CTS transmission can be utilized to sense the quality of the radio channel before properly setting the transmission power for data packets.

In [55] [56], and [57], the authors present power control methods based on the RTS/CTS handshake mechanism. Before the source node, A , sends data packets to node B , A sends an

6.1.3 Power Control Based on Packet Size

Normally, lower transmission power results in higher bit error rate (BER), though it saves energy. A higher bit error rate leads to more retransmissions, thus the overall energy consumption could be higher. In [60] and [61], the transmission power level is varied in terms of the packet size. For instance, a large size packet will use a higher power level to make sure that this packet can be received properly without retransmissions. Obviously, the drawback is this method may increase the probability of retransmission of short packets, which could also be important. For example, in a four-way handshake media access scheme, the ACK packets are very small, but if this short ACK packet cannot be received properly, the whole handshake procedure and the data packet transmission should be re-processed, which also wastes energy (Figure 6.2).

6.1.4 Power Control and Interference Mitigation

Generally speaking, a power control scheme, which chooses an appropriate transmission power level, results in not only energy saving but also interference mitigation. Interference mitigation is another significant issue to wireless communication systems, especially now, when the spectrum resource is becoming more and more limited. For instance, in CSMA/CA-based wireless networks, such as IEEE802.11 WLANs, higher transmission power levels will lead to more stations experiencing interference. These stations will sense the channel is busy, thus the system throughput will decrease. In figure 6.3, if station *A* only needs to communicate with *B*, the transmission power level should set to P_{t1} . When *A* chooses power level, P_{t2} , *D* and *E* will sense the radio channel is occupied, thus lose opportunities for transmission during *A*'s transmission period.

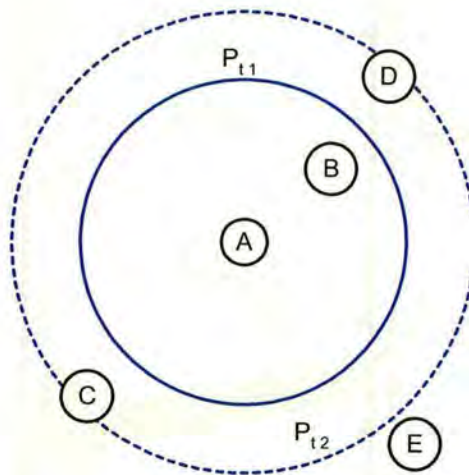


Figure 6.3: More stations will sense the channel is busy, if station *A* uses a higher transmission power level.

6.2 A Novel Power Control and Interference Mitigation Method in WPANs

In WPAN MACs, the PNC is important as it centrally controls all networking operations, such as synchronization, channel access, and power control, etc. As a result, the PNC experiences a much heavier traffic load and energy consumption than other nodes in the Piconet. If the most capable device could be dynamically selected as a PNC with efficient power control, then the stability of the whole network could be improved.

Currently, the WPAN MAC protocols use a “PNC Handover” mechanism for PNC selection. The “PNC Handover” mechanism is only triggered when a new device joins a Piconet. The existing PNC will compare its capabilities with the new device, and then decide whether or not it hands over the PNC role to the new device. No other device has the rights to participate in the PNC selection, though their capability may be better than the current PNC’s. If there is no new device joining the Piconet, the standardized “PNC Handover” mechanism can be seen as a fixed PNC scheme. No more details about the decision of the PNC Handover mechanism have been specified in the standard.

In this section, focusing on the solution in the MAC layer, a novel PNC selection method, called Least Distance Square PNC (LDS-PNC) selection is presented, to manage the critical power control, interference mitigation, and power saving in WPANs.

6.2.1 Coordinator Selection and Power Control

It is clear that reducing the transmission distance can decrease the transmission power required. As described in [62], if $P_r(d_{i,j})$ is the desired receiving power level for a correctly decoded packet between device i and j , then the relationship of the transmission power $P_t(d_{i,j})$ and received power can be described by:

$$P_r(d_{i,j}) = P_t(d_{i,j}) \cdot \left(\frac{\lambda}{4\pi d_{i,j}} \right)^n \frac{G_t G_r}{L} \quad (6.3)$$

where $d_{i,j}$ is the distance between transmitter i and receiver j , G_t and G_r are the antenna gains of the transmitter and receiver respectively, L is the system loss factor, n is the path loss exponent with a typical value between 2 and 4.

In terms of the standard, the most capable DEV may be dynamically selected as the PNC of a WPAN. Generally, the capability function, C_i , of a source limited DEV is determined by the transmission rate, memory capacity, CPU speed, residual energy or other characteristics. The mechanism for defining the capability function is not explicitly specified by the standard.

To reduce the interference introduced by PNC communication and save energy consumption within a Piconet, the distance between the PNC and other DEVs must be considered in the capability function, C_i , for the PNC selection and power control method. For example, in fig. 6.4, the red rectangle defines a WPAN area. Assume that DEV 1 is chosen for the PNC. In this case, to cover all the DEVs, the PNC has to increase transmission power to satisfy the emission radius d_1 . Compared with the PNC selection scheme which selects DEV 3 as the PNC, we

can see that the interference area is reduced and less energy is consumed in the PNC and other remote DEVs, such as DEVs 5 and 6, who also require less power to successfully exchange information with the PNC. Generally, selecting a DEV, which has the least distance square, as the PNC can decrease the interference area and the extra transmission power introduced by the PNC.

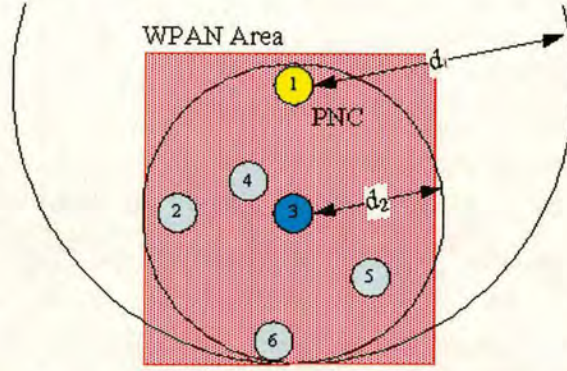


Figure 6.4: Interference area introduced by different PNC selections

However, from the point of view of improving the survivability of the whole WPAN, frequently selecting a PNC with low battery energy will easily lead to energy exhaustion in this PNC, thus resulting in network partitioning and topology instability [63] [64]. Therefore, the residual energy should also be considered in PNC selection.

A PNC Selection Counter (PSC), which controls the frequency of the PNC selection operation, is configured to an initial value, T , when a PNC is selected. A PNC decreases its PSC until it reaches zero. The PNC selection routine is started by a PNC when either:

1. The PSC meets zero;
2. The PNC's residual battery energy meets the lower bound, E_L ; or
3. The PNC needs to leave the Piconet.

To initiate the PNC selection process, the PNC attaches a PNC Selection Request (PSR) to the beacon frame and sends it to all the DEVs at the start of the superframe. When the DEVs receive the PSR, they will try to send a PSR-ACK packet back to the PNC as the acknowledgement. Each DEV attaches the value of its residual battery energy, E_i , and other characteristics, such as memory capacity, and CPU speed, to the PSR-ACK, and uses a maximum power level, P_{max} , to send this packet during the CAP. Because the PSR-ACK is a small packet, it can be successfully transmitted by most DEVs within the CAP. For simplicity, if a DEV cannot successfully transmit a PSR-ACK within the CAP, for instance, because of severe access contention, this DEV will not try to send the PSR-ACK in other CAPs, which means that this DEV will be ignored in PNC selection.

All devices within the Piconet, including the PNC and DEVs, listen for this PSR-ACK. Since our algorithm just needs a rough value of the distance between two stations, the received signal strength of the PSR-ACK is measured to estimate the value of the distance. When DEV i

receives DEV j 's PSR-ACK, it uses the equation 6.3, whose n is given by 2, to compute the distance between DEV i and j , $d_{i,j}$, as:

$$d_{i,j} = \lambda \sqrt{\frac{P_{\max} G_t G_r}{P_{r,i} L}} / 4\pi \quad (6.4)$$

where $P_{r,i}$ is the received power level measured by the station i . Assume there are $N + 1$ devices in the Piconet. The device, i , will record a set of the distances between other stations and itself, which can be depicted as:

$$D_i = \{d_{i,j}\}; \quad j = 0, 1 \cdots N - 1, N; j \neq i \quad (6.5)$$

Then the average distance square of device i , among the distance set D_i can be calculated as:

$$E(D_i^2) = \frac{1}{N} \cdot \sum_{j=0,1,2,\dots,N;j \neq i} d_{i,j}^2 \quad (6.6)$$

Generally, the PNC will consume more energy than normal DEVs, so it is necessary for a DEV to have enough battery energy to act as a PNC. Therefore, after receiving all the PSR-ACKs, the PNC tries to find a DEV set, R^* , in which the DEVs' residual battery energy is more than E_L . R^* can be defined as:

$$e(DEV_i) \geq E_L \quad (\forall DEV_i \in R^*) \quad (6.7)$$

where DEV_i is one of the DEVs in the set R^* , and $e(DEV_i)$ is its residual battery energy. This step prevents a centrally located device from being frequently chosen as a PNC without consideration of the residual energy. Without this criterion fast energy exhaustion in the PNC and network partitioning will result. In some cases, other QoS criteria, such as memory capacity, and CPU speed, may be considered in PNC selection. The capability function, $C(DEV_i)$ which includes these features, could be defined to find another set of DEVs, R^{**} , as:

$$C(DEV_i) \geq C_L \quad (\forall DEV_i \in R^{**}) \quad (6.8)$$

where C_L is the lower bound of capability.

If $R^* = \emptyset$ or $R^{**} = \emptyset$, a warning message will be sent to the application layer to make the user aware.

At the beginning of the next superframe, the PNC attaches all IDs of the DEVs in R^{**} and a Distance Report Request (DRR) in the beacon, and broadcasts it in its Piconet. To decrease energy consumed in transmission, just the DEVs, who are the member of R^{**} , and are specified in the beacon, listen for this DRR, and send DRR-ACK packets, enclosing the maximal distance square, $E(D_i^2)$, to the PNC during the following CAP. After receiving all the values of $E(D_i^2)$,

the PNC will find an optimal DEV to replace itself. If the Least Distance Square PNC (LDS-PNC) selection metric is applied, the optimal DEV, DEV_{opt} , shall satisfy the equation:

$$E(D_{opt}^2) = \min_{\forall DEV_i \in R^{**}} E(D_i^2) \quad (DEV_{opt} \in R^{**}) \quad (6.9)$$

Then the current PNC will start a procedure to hand over control of this Piconet to the selected optimal DEV. When the selected optimal DEV becomes a PNC, it will also restart a PSC for the next PNC selection timer. The new PNC will transmit beacons and other control packets with a required transmission power level calculated through equation 6.3, given $n = 2$:

$$P_t(d_{i,j}) = P_r^* \cdot \left(\frac{4\pi d_{\max}}{\lambda} \right)^2 \frac{L}{G_t G_r} \quad (6.10)$$

where P_r^* is a required receiving power level for correctly decoding, and d_{\max} is the maximal distance between the new PNC and other DEVs, which can be found in the distance set, D_i .

An example of the proposed PNC selection procedure is shown in figure 6.5. When the PSC reaches zero, the PNC broadcasts a beacon with attached PSR information. During the following CAP, all the DEVs attach their features to their PSR-ACK packets and send them to the PNC. The remaining duration of the m^{th} superframe is enough for a PNC and DEVs to calculate the set R^{**} , and the distance square. In the next beacon window, the PNC sends the DDR information to the DEVs belonging to set R^{**} through beacon transmission. Then the DEVs (DEV-#1 and DEV-#2) in set R^{**} send the DDR-ACK to the PNC. Finally the PNC uses the distance information attached in DDR-ACK packets to choose the optimal DEV as the next PNC. The message sequence chart of the LDV-PNC selection procedure is shown in fig. 6.6.

6.2.2 Simulation Results

In this section, several examples are illustrated to show the performance of the proposed PNC selection method. In the simulation, all the devices are randomly located in the same coverage area so that they can communicate directly with each other. A real-time Variable Bit Rate (rt-VBR) MPEG4 traffic generator is implemented in the simulation. Table 6.1 shows some key parameters.

The energy consumption is estimated by the “first order radio” model discussed in [54]. Each node is given an initial energy, calculated from a uniform PDF with the range[1800J,2000J].

For simulation of the PNC selection method, it is assumed that each device has same memory capability, CPU speed, and receiving/transmitting characteristics, which means $R^* = R^{**}$.

A. Interference Area Introduced by PNC Communication

Generally, a DEV, which is selected as a PNC, has smaller square distance, and will be located in the central area of the Piconet. On the other hand, the proposed method utilizes an estimated distance to control the transmission power level of the PNC, thus the area occupied by the PNC communication radiation and the battery energy consumed in the PNC could be decreased.

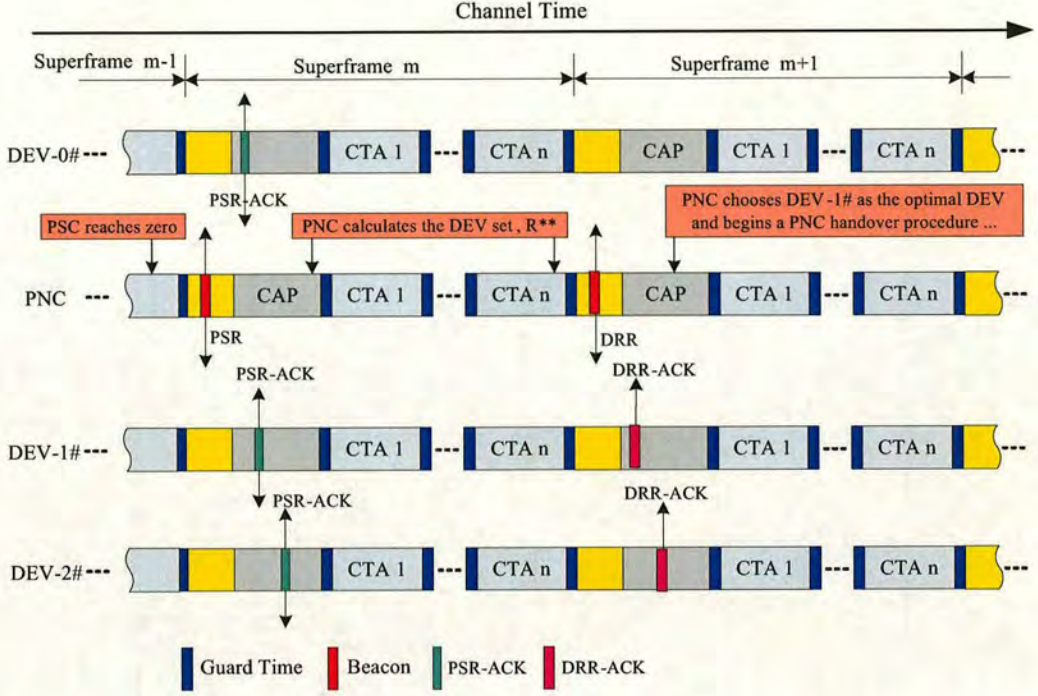


Figure 6.5: *PNC selection procedure*

Figures 6.7 and 6.8 show the coverage of PNC communication in the normal IEEE802.15.3-based WPAN and the proposed PNC selection methods. In the simulation, 10 devices (1 PNC, and 9 DEVs) are randomly located in a $10m \times 10m$ area, which is indicated by the black frame. The warm colour area means this area has been covered by the PNC's transmission for a high percentage of time. It is clear that using the proposed PNC selection method can decrease the coverage area of the PNC radiation, which means less interference to neighbouring networks and energy saving for the PNC.

B. Average Residual Energy in Each Device

To measure the power-saving features of the proposed PNC selection algorithm, the average battery energy of the 10 devices, is measured in a 4-hour simulation. The measured values are normalized by the initial battery energy in each device. Fig. 6.9 compares the results of the LDS-PNC selection method against the normal IEEE802.15.3 mechanism. Because the transmission power is decreased through avoiding long transmission paths, more energy is saved when using LDS-PNC selection. For example, the devices in the piconet employing LDS-PNC selection survive 1 hour longer than the devices in the normal IEEE802.15.3 WPAN when 50% of the initial battery energy is used.

C. PNC Survival Probability

When E_L is configured to zero, which means the PNC selection method does not consider the residual energy in the selection, the central DEVs will have a high probability of being

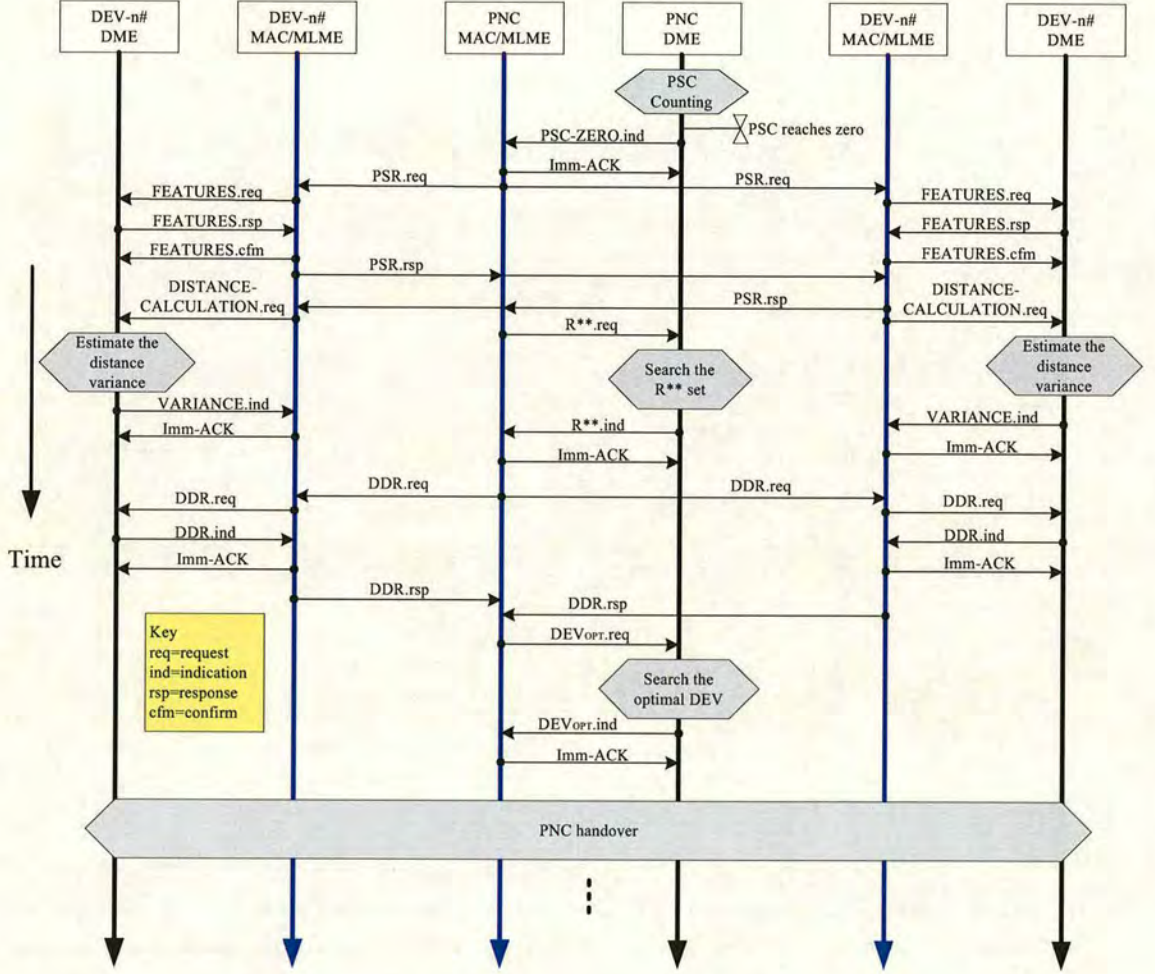


Figure 6.6: The message sequence chart of the LDV-PNC selection procedure

selected as the PNC. However, frequently selecting DEVs with small square distance will easily lead to energy exhaustion of these devices, thus resulting in network partitioning and topology instability. Figure 6.10 compares the PNC survival probability of the proposed LDS, LDS without the lower limitation of residual energy, and the normal IEEE802.15.3-based WPAN PNC selection. It is obvious that the proposed PNC selection method can prolong the lifetime of PNCs in WPANs.

From Fig. 6.9 and Fig. 6.10, we also can find that after 2.5 hours simulation time, the energy drain rate, which is the gradient of the energy decrease [64], for the network with normal IEEE802.15.3 method is much lower than that in the network with LDS, because the number of alive devices in the network with the normal IEEE802.15.3 method becomes less than that in the network with LDS. This is one reason why the average residual energy and the survival probability with the two methods have the trend to be similar at the end.

Parameters	Value
Superframe size	10ms
Mean offered load by rt-VBR	8Mbps
Simulation area	10m x 10m
Total number of devices (including PNC)	5,10,15,20,25,30
PNC selection period	150ms
Channel Bit Rate	100Mbit/s
Packet deadline	33ms
Lower limitation of the residual energy in devices	500 Joul

Table 6.1: *Simulation Parameters*

D. Percentage of Energy Consumption for PNC Selection

The drawback of the proposed PNC selection method is that it may result in more packet exchanges, produced by PSR, PSR-ACK, DRR, and DRR-ACK packets. The energy used for receiving and transmitting these packets is the majority of energy consumption for the PNC selection mechanism. As depicted in Fig. 6.11, the percentage of the energy consumption for PNC selection mechanism is strongly linked to the PNC selection period and the number of devices, N . A short PNC selection period can help the algorithm accurately obtain the change of the devices' status, but this will result in frequent transmission of the control packets, whose tradeoff should be considered carefully in real systems. However, because the control packets are very small, and the beacon frames are also used for PNC selection, the additional energy consumption for the PNC selection method is very small. For instance, when the selection period is 150ms, the average energy consumed for the PNC selection is less than 1.75% of the total energy consumption.

6.3 Validation of the Method in a Real Network

To validate the proposed power control and PNC selection mechanisms in section 6.2, the mechanism is implemented in Crossbow IEEE802.15 wireless motes by using the TinyOS embedded operating system. This project was supported by the Fujitsu Laboratories Europe. Ltd.

6.3.1 System Architecture

The MICAz MPR2400CA mote [65] (figure 6.12) is selected as the hardware processor/radio platform. This device is 802.15 compliant, and can support ad hoc networking. The MICAz mote uses Direct Sequence Spread Spectrum (DSSS) radio, and works in the ISM band, 2.4 to 2.4835 GHz. The motes also support power control. The minimal receiver sensitivity is $-90dBm@PER = 1\%$ [66]. The motes run TinyOS as their embedded operating system, on which we will implement the PNC selection algorithm. TinyOS is a small, open-source, energy-efficient, software operating system, which was developed by UC Berkeley [67] [68]. Figure 6.14 shows the system architecture. Figure 6.13 shows the implemented system. A Piconet is composed of devices $A \sim F$. The PNC is dynamically selected by our mechanism.

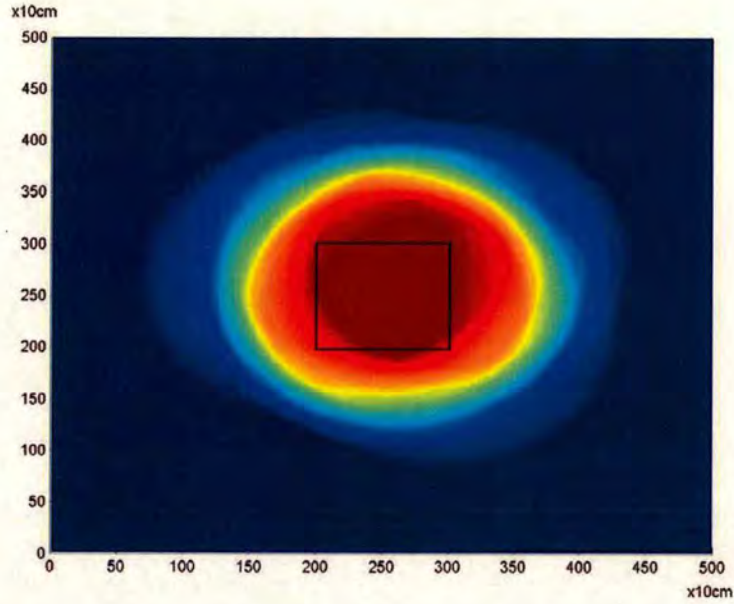


Figure 6.7: *The interference area introduced by PNC communication in normal PNC selection.*

An extra MPR2400 is used to monitor the network operations of the WPAN, and transfer the collected parameters, such as transmission power of each device, to the laptop through the serial port function module MIB510. Host software in Matlab visualizes the results on the laptop screen. This architecture is used to compare the performance of the proposed reselection method against the standardized “PNC Handover” mechanism, and a random PNC selection method. There are two selection mechanisms working in the devices. But only the decision of the new reselection mechanism presented in section 6.1 will be put into effect. The results from the standardized “PNC Handover” mechanism are just recorded for comparison purpose. The MPR2400 connected to the laptop is not a member of the WPAN, it just acts as a wireless interface for the laptop to monitor the network behaviour. The host software (including serial port communication and real-time result display functions) in the laptop is based on MATLAB.

6.3.2 Embedded Software

The embedded software in the motes is built in TinyOS. TinyOS is designed for wireless embedded sensor networks and features a component-based architecture, which enables rapid implementation while minimizing code size as required by the severe memory constraints inherent in sensor networks. In this section, the main components used in the PNC reselection method are introduced in detail.

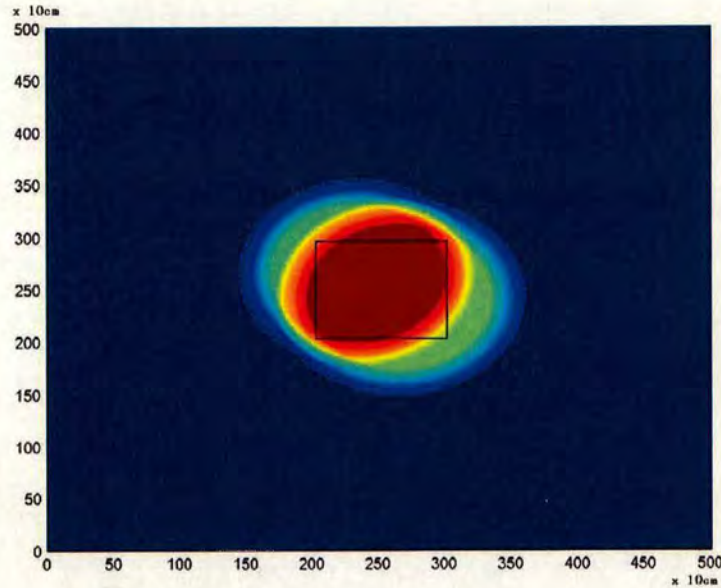


Figure 6.8: *The interference area introduced by PNC communication in LDS PNC selection.*

6.3.2.1 Transmitting Packets

Transmission is implemented through using the interface, `SendMsg`, in the designed module, `GenericComm`. This interface is wired to (provided by) the interface, `SendMsg`, in the model `AMStandard`. The module, `GenericComm`, can support not only radio communication, but also serial port (RS232) communication. Fig. 6.15 shows the wired interfaces in module, `GenericComm`. The `SendMsg` interface provides for up to 256 different instances. This could correspond to the Active Message handler ID, which could be used to distinguish between different packet types. Each communicating node within a group is given a unique address assigned at compile time. Two common reserved destination addresses are `TOS_BCAST_ADDR` (0XFFF) to broadcast to all nodes, and `TOS_UART_ADDR` (0X007E) to send packets to the serial port. The group ID and mote address can be set by “`Makelocal`” file and “`make`” command at compile time. The local address and group address are saved in two global constant, `TOS_LOCAL_ADDRESS` and `DEFAULT_LOCAL_GROUP`. The maximum payload size is `TOSH_DATA_LENGTH` and is set to 29 by default. If `send()` returns `SUCCESS`, the message is queued for transmission, and this message owns the send buffer and the requesting component should not modify the buffer until the send is complete, which is indicated by the “`sendDone()`” event. A flag is used to keep track of the status of the buffer. If the previous message is still being sent, we cannot modify the buffer, so we have to drop the sending operation and return `FAIL`.

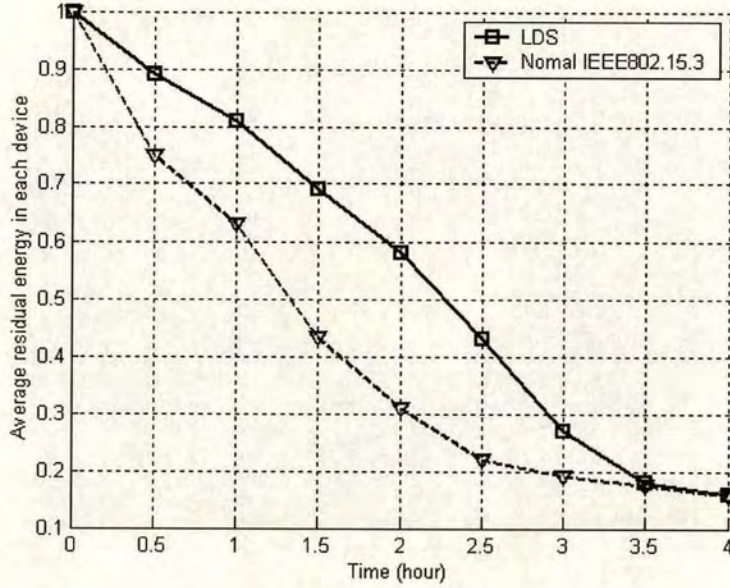


Figure 6.9: *Average residual energy in each device.*

6.3.2.2 Receiving Packets

The message receiving operation is implemented by the “receive()” event defined in the interface, `GenericComm.ReceiveMsg[AM_INTMSG]`. The value of `AM_INTMSG` is the Active Message handler ID. This means that this interface will respond to messages with the specified ID. The `ReceiveMsg` interface declares event, `receive()`, which is passed a pointer to the received message. This pointer is the address of a message structure, which contains the fields for destination address, message type (the AM handler ID), length, payload, etc.

6.3.2.3 Accessing RSSI and Link Quality Information

The MPR2400CA mote has a built-in received signal strength indicator (RSSI) and link quality indicator (LQI). A corresponding 8-bit value can be read from the register to indicate the received signal strength. The RSSI value is always averaged over 8 symbol periods (128us) and a status bit indicates when the RSSI value is valid. The real power of the received signal can be calculated as:

$$P = \text{RSSI_VALUE} + \text{RSSI_OFFSET}(\text{dBm}) \quad (6.11)$$

Where `RSSI_OFFSET` is found empirically from the front-end gain and it is approximately equal to -45dBm.

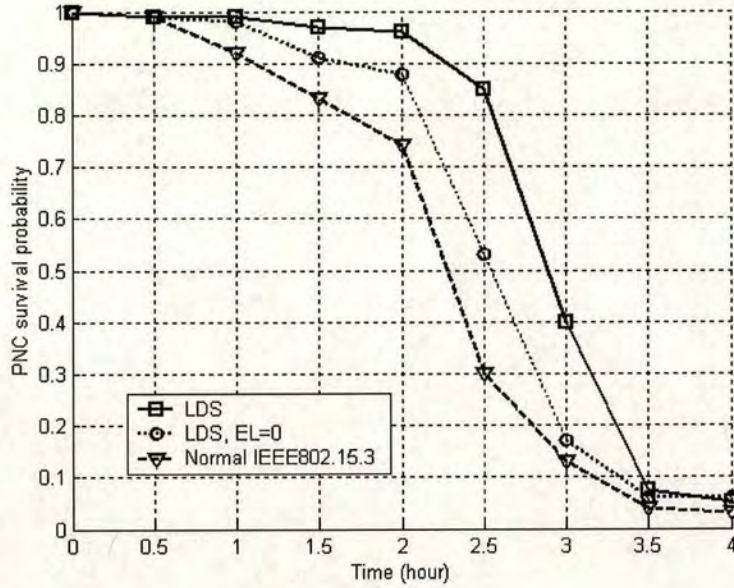


Figure 6.10: *PNC survival probability.*

6.3.2.4 Control the Transmission Power

Setting/obtaining the transmission power is implemented by the interface, CC2420Control, provided by the model, CC2420ControlM. CC2420Control.SetRFPower(uint8_t power) is used to set the transmit RF power. Valid values are 1 to 31 with a corresponding power of $-25dBm$ to maximum power $0dBm$.

6.3.2.5 Traffic Control

All devices, including the PNC, will randomly select a device within its Piconet as the destination for a data packet. The interval of the packet sending and the size of the data packets are controlled by the traffic load control component. The wired interface in TinyOS is shown in Fig. 6.16. The component, RandomLFSR, is used to generate two random numbers to assign the interval of the data packet sending and the size of the data packets. The component, TimerC, is used to control the interval for data packet

6.3.3 Host Software

The main objective of the host software is to process and visualize the information of networking. The GUI (Graphic User Interface) of the host software is shown in fig. 6.17.

The boxes on right hand side show the transmission power used for each device and the ID of current selected PNC. The ID number of the PNC is coloured red. Comparing the transmission

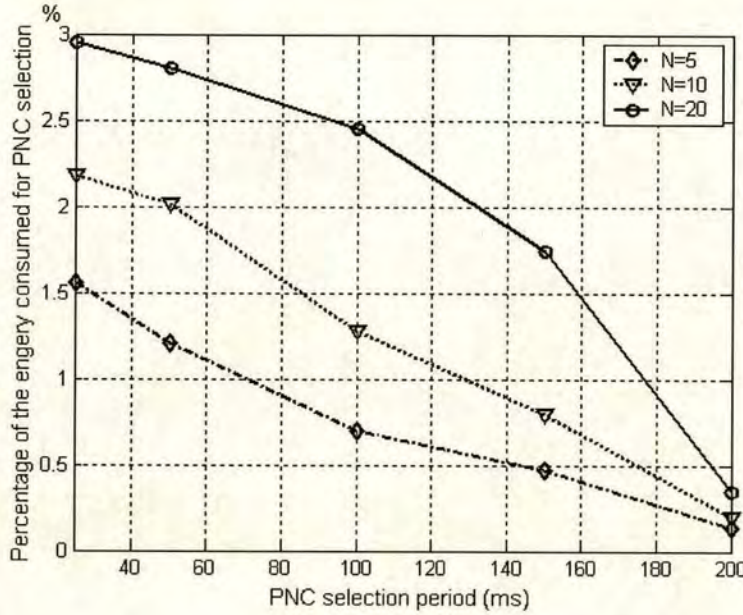


Figure 6.11: *Percentage of the energy consumed by PNC selection mechanism vs. different PNC selection period.*

power used in our mechanism and the random PNC selection mechanism, the percentage of the saved transmission power is also given by the host software. There are two figures in the window, the upper one is the transmission power for three different PNC selection mechanisms. The lower one illustrates the battery power saved in PNCs. The figures can be zoomed out/in by the “+/-” buttons. An edit box on right side also shows how many beacon packets have been monitored.

6.4 Summary and Conclusions

Power control is an essential MAC component in wireless networks to constrain the transmission power, thus for energy saving and interference mitigation. Due to the mobility, dynamic radio environment and distributed networking operations, a power control scheme in wireless ad hoc network has its own characteristics. For example, there is no central controller in wireless ad hoc networks. The RTS/CTS-based power control and multiple channel access power control can appropriately adjust the transmission power before sending data packets. However, because of the existence of a threshold on the RTS/CTS mechanism, neither power control method could be implemented when the size of the data packets are small. Moreover, the multiple channel access scheme will waste bandwidth resources, since a dedicated channel is used for control packets and signalling of power control. Packet-size-based power control tries to improve the signal quality by giving a higher transmission power level to larger packets, thus reducing the retransmission time and saving energy. In this scheme, small packets use lower transmission power levels, though the failure of sending these packets will also waste substan-



Figure 6.12: *The MICAz MPR2400CA mote*



Figure 6.13: *The implemented system*

tial energy. Based on the discussion of the various power control methods in wireless ad hoc networks, a novel power control and PNC selection method for WPANs was proposed in this chapter. In this method, a universal distance estimation method is used to help the periodical PNC reselection and power control. The simulation results show this method can decrease the transmission coverage of PNC and save energy. To adapt to different radio/mobility environment, the frequency of the power control can be adjusted by changing the initial value of the PNC Selection Counter (PSC). The drawback of this scheme is that the exchange of control packets for PNC selection will consume extra energy, but the simulation shows this energy consumption is really negligible since the control packets are very small, and the beacons are reused for PNC selection and power control. To practically prove the concepts in 6.2, the presented PNC reselection and power control method has been implemented into a real WPAN. The experimentation results show that the proposed method can lessen the transmission power and diminish the interference area introduced by PNC's communication.

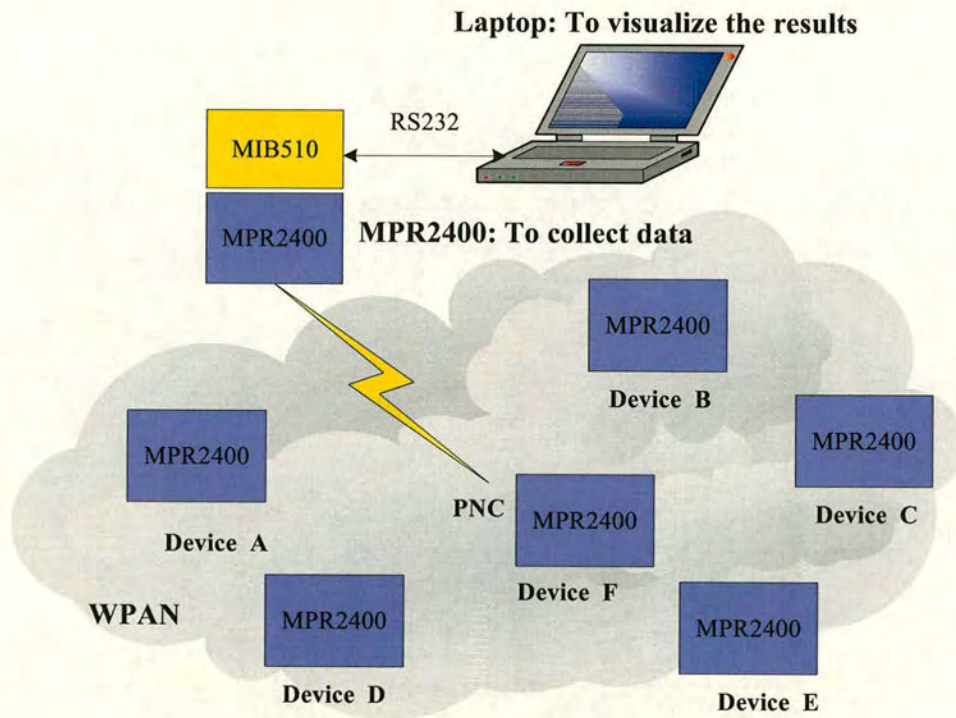


Figure 6.14: System architecture

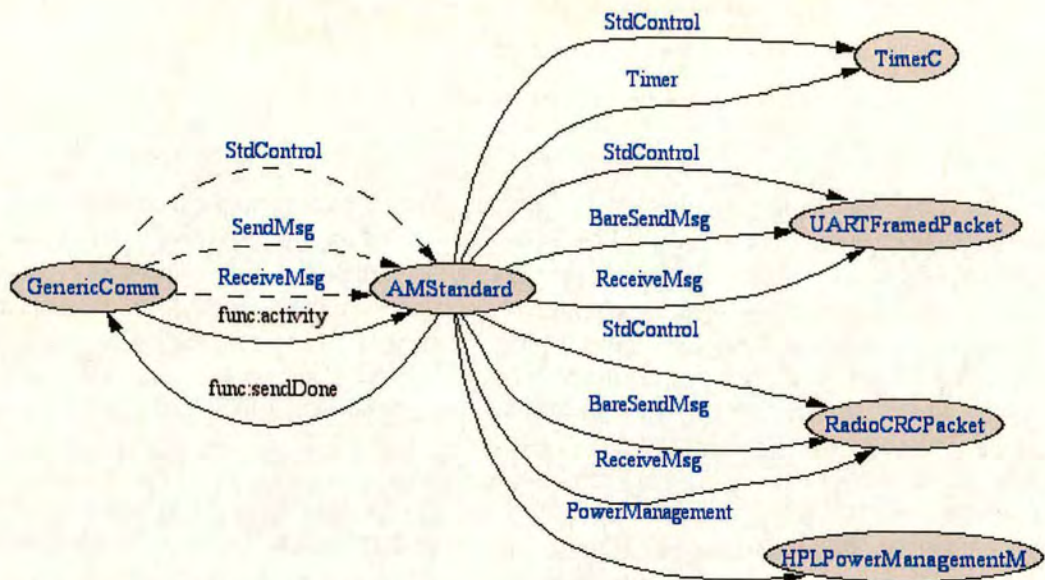


Figure 6.15: The wired interfaces in module, GenericComm

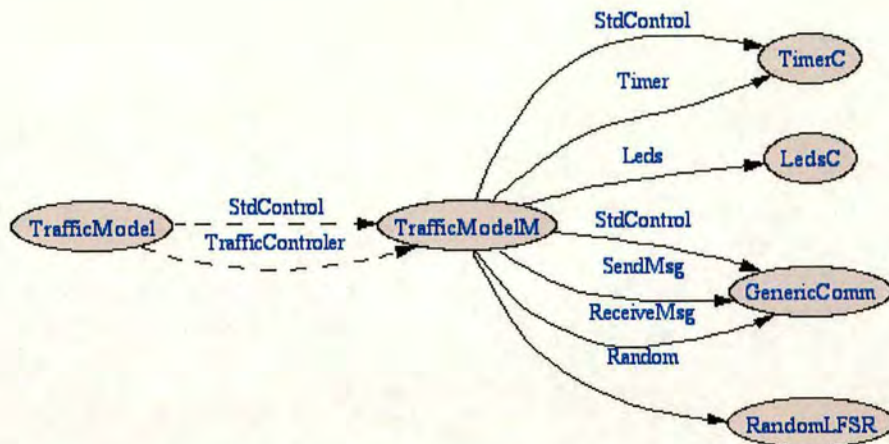


Figure 6.16: The wired interfaces in component, TrafficModel

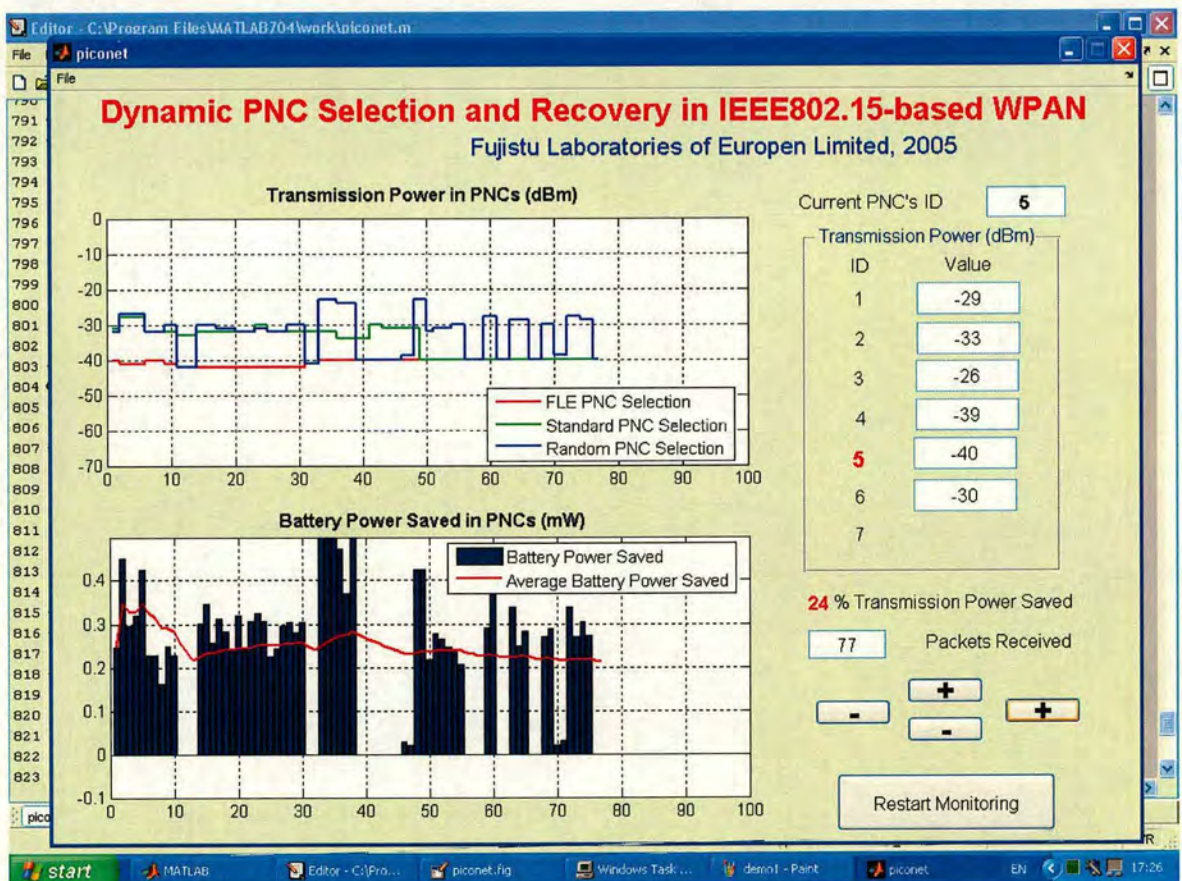


Figure 6.17: The host software

Chapter 7

Conclusions

The research carried out for this thesis examines existing standardized energy-efficient MAC protocols for wireless ad hoc networks. Then, based on the analysis of the typical energy-efficient MACs in a wireless ad hoc network, such as IEEE802.11, IEEE802.15, improved energy-efficient MAC algorithms are proposed and evaluated. The enhancements of energy-efficient MAC algorithms presented in this thesis focus on multi-hop issues, including the impact on ad hoc routing protocols, topology management, and power control.

In this chapter, the main conclusions of the work are presented, and some suggestions for further research are given.

7.1 Summary and Achievements of the Work

Though the analytical models for many typical MAC mechanisms, such as CSMA, and ALOHA, have been proposed and validated recently, few researchers have examined analytical models of the performance of power-saving MACs. A typical synchronized IEEE802.11-based power-saving mode is chosen as an example for the analytical modelling in Chapter 3. The proposed analytical model evaluates the successful control/data packet transmission rate, the throughput, and the latency in the ad hoc network power saving MAC mode with the capture effect, operating on a channel impaired by Rayleigh fading, shadowing, and the near-far effect. From the analytical model, it is concluded that the performance of the power saving MAC is sensitive to the number of stations, the size of the different portion of the superframe, and the capture effect. In the synchronized power-saving mode, such as IEEE802.11 ad hoc network power saving mode, the ATIM packet transmission rate strongly affects the data packet transmission rate, the throughput and the packet delay. The capture effect improves the performance of power saving MAC, since it allows for successful reception even if packets collide. The analytical model also shows that the four-way handshake with RTS and CTS access is better than the basic access method if there are more stations in the network.

Timing synchronization, which is essential for power management, and media access coordination in multi-hop environment, is also studied. Subsequently, a novel power-saving mechanism for multi-hop networks is presented based on the analyzed results, indicating that the timing of the window will strongly affect the performance of power saving MAC. By adapting the timing window to the dynamically changing traffic load, the proposed power-efficient mechanism can balance the bandwidth efficiency and power consumption. The simulation results show, compared with original IEEE802.11 power-saving mode, that the proposed method can support a higher average throughput with energy efficiency.

When a power-saving MAC is used for multi-hop ad hoc networks, the routing procedure and data transmission may be delayed since the end-to-end delay in the power-saving MAC mode

is much worse than that in the normal mode. Based on the proposed analytical model in chapter 3, chapter 4 investigates the impact of a power saving MAC on ad hoc network routing. Both the numerical and simulation results show that the power-saving MAC will seriously degrade the performance of the ad hoc network protocol, because a station can transmit packets only after getting synchronization and exchanging ATIM packets. Two methods are proposed to improve the performance of ad hoc network routing with a power-saving MAC by applying higher priority for transmission of routing control packets.

The topology of a network is determined by the characteristics of the communication technologies of devices, and the objectives of the network. The peer-to-peer topology is a basic network structure that is widely used in IEEE802.11-based WLANs. Devices within such topology have similar capabilities and equal roles. However, due to lack of central management, it is difficult to have global media access control for peer-to-peer topology, thus the free style competition will result in bandwidth waste. On the other hand, the network cannot easily be synchronized. A network coordinator within a star topology can centrally execute operations with relation to the global quality metrics, thus improves the network efficiency. The contention for channel access and the control overhead are linear in the number of the nodes of an ad hoc network in the star topology or peer-to-peer topology. The clustering topology is particularly useful for applications that require load balancing, efficient resource utilization, and data aggregation for hundreds or thousands of nodes. The clustering topology can reduce the number of devices contending for channel access, minimize control overhead, and simplify the routing method in large scale networks. Especially, when the capabilities of the devices are different, a cluster-tree topology may exploit the potential of each device better than other network topologies. In the IEEE802.15-based WPAN, bandwidth and energy reservation are major challenges. To prolong the lifetime of the whole network, improve the network throughput and simplify topology management in a large scale network, a novel hierarchical clustering algorithm is proposed in Chapter 5. The clusterhead is selected by computing and comparing the defined potential value of serving as the clusterhead. By comparing the simulation results among the proposed method and other clustering methods, such as LEACH, it can be shown that the proposed method has higher throughput and energy efficiency.

In wireless communication devices, energy used for transmission normally forms a major part of energy consumption. Therefore, it is important to control the transmission power, which can benefit the energy efficiency and decrease the probability of blocking neighbouring devices'/networks' communication. In MANETs, because of mobility, the dynamic radio environment and distributed networking operations, power control is different from those in other types of networks. Various power control methods for wireless ad hoc networks, such as RTS/CTS-based power control, multiple channel access power control, and packet-size-based power control, are discussed in Chapter 6. Focusing on the solution in the MAC layer, a novel power control and interference mitigation method for WPANs is described in detail. The method proposed is based on the PNC selection mechanism in the WPAN, since the PNC is important as it centrally controls all networking operations, such as synchronization, channel access, and power control. As a result, the PNC experiences a much heavier traffic load and energy consumption than other nodes in the Piconet. If the most capable device could be dynamically selected as a PNC with efficient power control, then the stability of the whole network could be improved. The simulation results show this method can decrease the transmission coverage of the PNC and save energy. To adapt to different radio/mobility environments,

the frequency of the power control can be adjusted by changing the value of the PNC selection counter. The drawback of this scheme is that the exchange of control packets for PNC selection will consume extra energy, but the simulation shows this energy consumption is really negligible since the control packets are very small, and the beacons are reused for PNC selection and power control. Supported by Fujitsu Laboratories of Europe Limited, we implemented this method into a real IEEE802.15 devices, MICAz MPR2400CA mote with an embedded operating system, TinyOS. The experimental results demonstrates that the proposed method can dramatically improve the energy efficiency and network robustness.

7.2 Limitations of the Work and Scope for Further Research

Since the network density has not been considered in the modelling of the impact of the power-saving MAC to ad hoc network routing, the experimental results of the power-saving ad hoc network in Chapter 4 differ from the analytical results, when the number of stations is small. To improve the accuracy of the analytical model, more factors, such as network density, and traffic type, may be included in the calculation.

Throughout the research presented in this thesis, the study of the energy-efficiency MAC strategies is restricted to the standards of WLANs and WPANs. Other networks, such as UMTS and WiMAX, will also support ad hoc network behaviour in the future, therefore, expanding the research of energy efficient MAC strategies to those networks is a possible direction for future work.

Furthermore, in some networks, such as WiMAX, the radio resource management/scheduler for energy efficiency becomes more complicated. For instance, in OFDMA-based WiMAX, the power control will relate to the radio channel quality, optimal subcarrier selection, and adaptive modulation and encoding scheme. To optimize the energy consumption, the MAC strategies should also consider the interference mitigation to neighbouring cells or sectors.

References

- [1] N. Abramson, "The ALOHA system - another alternative for computer communications," in *In Proceedings of the Fall Joint Computer Conference*, vol. 37, pp. 281–285, 1970.
- [2] E. M. Royer and C.-K. Toh, "A review of current routing protocols for ad-hoc mobile wireless networks," *IEEE Personal Communications*, vol. 6, pp. 46 – 55, April 1999.
- [3] D. Maltz, J. Broch, and J. Jetcheva, "The effects of on-demand behavior in routing protocols for multihop wireless ad hoc networks," *IEEE Journal on Selected Areas in Communications*, vol. 8, pp. 1439–1453, 1999.
- [4] H. S. Chaya and S. Gupta, "Performance of asynchronous data transfer methods of IEEE802.11 MAC protocol," *IEEE Personal Communications*, vol. 3, pp. 8–15, Oct. 1996.
- [5] G. Bianchi, L. Fratta, and M. Oliveri, "Performance evaluation and enhancement of the CSMA/CA mac protocol for 802.11 wireless LANs," *Proc. of PLMRC'96*, vol. 2, pp. 392–396, 1996.
- [6] Y. C. Tay and K. C. Chua, "A capacity analysis for the IEEE802.11 MAC protocol," *ACM/Baltzer Wireless Networks*, vol. 7, pp. 159–171, March 2001.
- [7] H. WU, Y. Peng, K. Long, S. Cheng, and J. Ma, "Performance of reliable transport protocol over IEEE802.11 wireless LAN analysis and enhancement," *Proc. Of INFO-COM'2002*, pp. 599–607, 2002.
- [8] J. H. Kim and J. K. Lee, "Throughput and packet delay analysis of IEEE 802.11 MAC protocol for wireless LANs," *Wireless Personal Communication*, vol. 11, pp. 161–183, Nov. 1999.
- [9] IEEE, "Wireless lan medium access control (MAC) and physical layer (PHY) spec.," *P902.11/D5 Draft Standard IEEE 802.11*, vol. 11, pp. 161–183, May 1996.
- [10] G. Bianchi, "Performance analysis of the IEEE 802.11 distributed coordination function," *IEEE Journal on Selected Area Communications*, vol. 18, pp. 535–547, March 2000.
- [11] L. Kleinrock and F. A. Tobagi, "Packet switching in radio channels: Part ii the hidden terminal problem in carrier sense multiple access and the busy tone solution," *IEEE Transactions on Communications*, vol. 12, pp. 1417–1433, 1975.
- [12] E. B. R. A. N. (BRAN), "High performance radio local area network (HIPERLAN) type 2," *TR 101 031 Requirements and Architectures for wireless broadband access*, Jan. 1999.
- [13] K. Pahlavan, A. Zahedi, and P. Krishnamurthy, "Wideband local access: Wireless LAN and wireless ATM," *IEEE Commun. Mag.*, vol. 35, pp. 34–40, Nov. 1997.
- [14] G. Anastasi, L. Lenzini, and E. Mingozzi, "Stability and performance analysis of HIPER-LAN," in *Proc. INFOCOM'98 San Francisco, CA*, pp. 134–141, Apr. 1998.

- [15] <http://www.bluetooth.com>.
- [16] <http://www.thewirelessdirectory.com/bluetooth-overview>.
- [17] B. A. Miller and C. Bisdikian, "Bluetooth revealed: The insider's guide to and open specification for globe wireless communications," in *Prentice Hall*, 2001.
- [18] S. B. G. V. Zaruba and I. Chlamtac, "Bluetrees-scatternet formation to enable bluetooth-based ad hoc networks," in *In Proceedings of IEEE International Conference on Communications*, vol. 1, pp. 273–277, 2001.
- [19] LAN MAN Standards Committee of the IEEE Computer Society, "IEEE Std 802.15.3 - 2003, wireless MAC and PHY specification for WPANs," in *IEEE*, 2003.
- [20] L. M. S. C. of the IEEE Computer Society, "IEEE Std 802.15.4 - 2003, wireless MAC and PHY specification for LR-WPANs," in *IEEE*, 2003.
- [21] K. M. Sivalingam, M. B. Srivastava, and P. Agrawal, "Low power link and access oprotocols for wireless multimedia networks," *IEEE Journal on Selected Areas in Communications*, vol. 6, pp. 1331–1335, May 1997.
- [22] T. R. Hsing, D. C. Cox, L. F. Chang, and T. V. Landegem, "Special issue on wireless ATM," *IEEE Journal on Selected Areas in Communications*, vol. 15, Jan. 1997.
- [23] J. Chen, K. M. Sivalingam, P. Agrawal, and S. Kishore, "A comparison of MAC protocols for wireless local networks based on battery power consumption," *IEEE Communication transaction*, pp. 234–257, Jan. 1998.
- [24] M. Stemm and R. H. Katz, "Measuring and reducing energy of network interfaces in hand-held devices," in *IEICE Transactions on Communications*, pp. 1125–1131, August 1997.
- [25] D. Newman and K. Tolly, "Wireless LANs: How far? how fast," in *Data Communication*, Mar. 1995.
- [26] S. Eduardo and C. Takahashi, "Application aware scheduling for power management on IEEE 802.11," in *Performance, Computing, and Communications Conference, 2000*, pp. 247 – 253, 20-22 Feb. 2000.
- [27] M. Stemm, "Measuring and reducing energy consumption of network interfaces in hand-held devices," in *MoMuC-3*, Sept. 1996.
- [28] T. Imielinsky, S. Viswanathan, and B. R. Badrinath, "Energy efficient indexing on air," in *ACM-SIGMOD*, pp. 215–36, May 1994.
- [29] I. Chlamtac, C. Petrioli, and J. Redi, "Analysis of energy-conserving protocols for wireless identi-fication networks," in *Conference on Telecommunication Systems - Modeling and Analysis*, March 1997.
- [30] J. P. Linnartz, "Narrowband land-mobile radio networks," in *Norwood, MA: AArtech*, 1993.

- [31] C. V. D. Plas and J. P. M. G. Linnartz, "Stability of mobile slotted ALOHA network with rayleigh fading , shadowing, and near-far effect," in *IEEE Trans. Veh. Technol.*, vol. 39, pp. 359–366, Nov. 1990.
- [32] Z. Hadzi-Velkov and B. Spasenovski, "Capture effect in IEEE 802.11 basic service area under in-fluence of rayleigh fading and near/far effect," in *The 13th IEEE International Symposium on Per-sonal, Indoor and Mobile Radio Communications*, vol. 1, pp. 172 – 176, 15-18 Sept 2002.
- [33] G. Bianchi, "Performance analysis of IEEE 802.11 distributed coordination function," in *IEEE Journal on Selected Areas in Communications*, vol. 18, pp. 535–547, March 2000.
- [34] "NS2." <http://www.isi.edu/nsnam/ns/>.
- [35] Y.-C. Tseng, C.-S. Hsu, and T.-Y. Hsieh, "Power-saving protocols for IEEE 802.11-based multi-hop ad hoc networks," in *INFOCOM 2002. Twenty-First Annual Joint Conference of the IEEE*, vol. 1, pp. 200 – 209, June 2002.
- [36] E.-S. Jung and N. H. Vaidya, "An energy efficient MAC protocol for wireless LANs," in *In Proceedings of the 21st Annual Joint Conference of the IEEE Computer and Communications Societies 2002*, vol. 3, pp. 1756–1764, June 2002.
- [37] D. B. Johnson, D. A. Maltz, and Y. C. Hu, "The dynamic source routing protocol for mobile ad hoc net-works," in *IETF Internet Draft (work in progress), draft-ietf-manet-dsr-09-txt*, April 2003.
- [38] D. Maltz, J. Broch, and J. Jetcheva, "The effects of on-demand behavior in routing protocols for multihop wireless ad hoc networks," in *IEEE Journal on Selected Areas in Communications*, vol. 17(8), pp. 1439–1453, April 1999.
- [39] L. Kleinrock and J. Silvester, "Optimum transmission radii for packet radio networks," in *Proc. IEEE National Telecommunication Conference (NTC)*, pp. 120–130, 1978.
- [40] O. Younis and S. Fahmy, "HEED: A hybrid, energy-efficient distributed clustering approach for ad hoc sensor networks," *IEEE Transaction on Mobile Computing*, vol. 3, pp. 366–376, Oct. to Dec. 2004.
- [41] S. Bandyopadhyay and E. Coyle, "An energy-efficient hierarchical clustering algorithm for wireless sensor networks," in *Proc. IEEE INFOCOM*, Apr. 2003.
- [42] K. Sohrabi, J. Gao, V. Ailawadhi, and G. Pottie, "Protocols for self-organization of a wireless sensor network," *IEEE Personal Communications Mag.*, vol. 7, pp. 16–27, Oct. 2000.
- [43] A. Cerpa, J. Elson, D. Estrin, L. Girod, M. Hamilton, and J. Zhao, "Habitat monitoring: Application driver for wireless communications technology," in *Proc. the 2001 ACM SIG-COMM Workshop on Data Communications in Latin America and the Caribbean*, Apr. 2001.
- [44] E. Biagioni and K. Bridges, "The application of remote sensor technology to assist the recovery of rare and endangered species," *Special Issue on Distributed Sensor Networks for the International Journal of High Performance Computing Applications*, vol. 16, Aug. 2002.

- [45] L. Schwiebert, S. K. S. Gupta, and J. Weinmann, "Research challenges in wireless networks of biomedical sensors," *Mobile Computing and Networking*, pp. 151–165, 2001.
- [46] "TinyOS." <http://tinyos.millennium.berkeley.edu>.
- [47] C. Guo, L.-C. Zhong, and J. M. Rabaey, "Low power distributed MAC for ad hoc sensor radio networks," in *Proc. Global Telecommunications Conference*, Nov. 2001.
- [48] W. Ye, J. Heidemann, and D. Estrin, "An energy-efficient MAC protocol for wireless sensor networks," in *Proc. Twenty-First Annual Joint Conference of the IEEE Computer and Communications Societies*, pp. 1567 – 1576, June 2002.
- [49] D. J. Baker and A. Ephremiders, "The architecture organization of a mobile radio network via a distributed algorithm," in *IEEE Transactions on Communications*, pp. 1694–1701, Nov. 1981.
- [50] M. Gerla and J. T.-C. Tsai, "Multicluster, mobile, multimedia radio network," in *ACM-Baltzer J. Wireless Networks*, vol. 1, pp. 155–165, 1995.
- [51] A. Michalski and J. Czajewski, "The accuracy of the global positioning systems," *IEEE Instrumentation Measurement Mag.*, vol. 7, pp. 56–60, Mar. 2004.
- [52] I. Stojmenovic and X. Lin, "Power-aware localized routing in wireless networks," *IEEE Transactions on Parallel and Distributed Systems*, vol. 12, pp. 1122–1133, Nov. 2001.
- [53] W. Heinzelman, A. Chandrakasan, and H. Balakrishnan, "Energy efficient communication protocol for wireless microsensor networks," in *The 33rd Hawaii International Conference on System Sciences*, pp. 3005–3014, 2001.
- [54] W. Heinzelmann, A. Chandrakasan, and H. Balakrishnan, "Energy-efficient communication protocol for wireless microsensor networks," in *In Proc. Hawaii International Conference on System Science*, vol. 2, p. 10, 2000.
- [55] P. Karn, "A new channel access method for packet radio," in *9th ARRL Computer Networking Conference*, 1990.
- [56] J. Gomez, A. T. Campbell, M. Naghshineh, and C. Bisdikian, "Conserving transmission power in wireless ad hoc networks," in *ICNP01*, November 2001.
- [57] P. Lettieri and M. B. Srivastava, "Adaptive frame length control for improving wireless link throughput, range, and energy efficiency," in *INFOCOM 98*, vol. 2, pp. 564–570, March 1998.
- [58] S. L. Wu, Y. P. Tseng, C. Y. Lin, and J. P. Sheu, "A multi-channel MAC protocol with power control for multi-hop mobile ad hoc networks," in *The Computer Journal (SCI)*, vol. 45, pp. 101–110, 2002.
- [59] J. P. Monks, V. Bharghavan, and W. Mei, "A power controlled multiple access protocol for wireless packet networks," in *INFOCOM 2001*, April 2001.
- [60] J. P. Ebert, B. Stremmel, E. Wiederhold, and A. Wolisz, "An energy efficient power control approach for WLANs," in *Journal of Communications and Networks (JCN)*, vol. 2, pp. 197–206, September 2000.

- [61] J. P. Ebert and A. Wolisz, "Combined tuning of RF power and medium access control for WLANs," in *IEEE International Workshop on Mobile Multimedia Communications (MoMuC'99)*, November 1999.
- [62] I. Stojmenovic and X. Lin, "Power-aware localized routing in wireless networks," in *IEEE Transactions on Parallel and Distributed Systems*, vol. 12, pp. 1122–1133, Nov. 2001 2001.
- [63] R. C. Shah and J. M. Rabaey, "Energy aware routing for low energy ad hoc sensor networks," in *Wireless Communications and Networking Conference*, vol. 1, pp. 350 – 355, March 2002.
- [64] Y. Zhou, D. I. Laurenson, and S. McLaughlin, "High survival probability routing in power-aware mobile ad hoc network," in *IEE Electronics Letters*, vol. 40, pp. 1424–1426, Oct. 2004.
- [65] CrossBow, "MOTE VIEW user manual," March 2004.
- [66] C. A. SmartRF, "2.4 GHz IEEE 802.15.4 ZigBee-ready RF transceiver," in *CC2420 Preliminary Datasheet (rev 1.2)*, June 2004.
- [67] D. Gay, P. Levis, D. Culler, and E. Brewer, "nesC 1.1 language reference manual," 2004.
- [68] J. Hui, "TinyOS network programming," in *Version 1.0*, August 2004.

High Survival Probability Routing in Power-Aware Mobile Ad Hoc Networks

Yuefeng Zhou, David I. Laurenson, Steve McLaughlin

Abstract: A novel metric and a routing mechanism are presented for high route survival probability in power-aware mobile ad hoc networks. Simulations using NS2 show it can provide energy saving with more robust connectivity.

Introduction: In mobile ad hoc networks (MANET), various communication devices with different features comprise a wireless network that has no fixed infrastructure and unpredictable connectivity. These nodes are not only the means to data interchange but also the managers for the routes to data and access to services. Many mobile devices in a MANET are likely to be battery operated, making energy exhaustion an important issue for network stability. As a consequence energy-consumption should be regarded as an essential metric in MANET routing mechanism. Many currently proposed power aware routing schemes are based on minimal total transmission power (MTTP); obvious examples being localized routing (LR) [1], or residual battery energy (RBE), or conditional max-min battery capacity routing (CMMBCR) [2]. However, it is impractical to obtain an accurate value of the transmission power for MTTP, as this is dependant on the distance between nodes. When using RBE, more traffic load will be put on the node with the highest residual battery energy, which may result in rapid energy exhaustion in parts of the network. Consequently mechanisms based on such metrics cannot guarantee that the route can survive for the duration of a transfer. A low route survival probability (RSP) means the route is likely to become invalid during transmission, which will lead to unstable network connectivity and additional route discovery operations. This would require additional energy expenditure, especially under conditions of heavy traffic load. In this letter, we propose a novel metric, relay capacity (RC), and a new routing mechanism named the conditional maximum relay capacity routing (CMRCR), which increases the RSP, and supports continuous services with longer node lifetime.

Details of the CMRCR: In a practical MANET, the capability of a resource-limited node to transmit is of great concern. This relates not only to the residual energy but also to the data rate and energy efficiency. We define a novel metric RC, which is constrained by a relay efficiency (RE) metric, to specify the node's capability to transmit.

RC_i indicates the traffic capacity that the node i can support within its lifetime, which can be defined as:

$$RC_i = L_i D_i \quad (1)$$

where D_i is the current data rate and L_i is the lifetime of the node i . The unit of RC_i is the bit. The lifetime L_i can be described as:

$$L_i = E_i(t) / \overline{R_i(t)} \quad (2)$$

where $E_i(t)$ is the node's residual energy. We also define $R_i(t) = \partial E_i(t) / \partial t$ to indicate how much energy is used per second at node i .

In order to obtain the average trend of $R_i(t)$, an α low-pass filter is applied to $R_i(t)$, to give:

$$\overline{R_i(t)} = \alpha \cdot R_i(t-T) + (1-\alpha) \cdot R_i(t) \quad (3)$$

where T is the sample period of $R_i(t)$. α and T have to be chosen carefully to accurately reflect the energy consumption of a node. $\overline{R_i(t)}$ can be used to determine whether the node i will be available under a specified traffic load or not. Using the same amount of energy, different nodes can transmit different amounts of data. This energy feature can be denoted by another metric, RE_i , which is defined as:

$$RE_i = D_i / \overline{R_i(t)} \quad (4)$$

Clearly, the unit of RE_i is bits/joule.

The new conditional maximum relay capacity routing (CMRCR) mechanism is based on $\overline{R_i(t)}$ and RE_i . In CMRCR, we define the relay capacity function of the route r_j as:

$$\phi(r_j) = \min_{\forall n_i \in r_j} \overline{R_i(t)} \quad (r_j \in r^*) \quad (5)$$

where r^* is the set of all possible routes with the same source node n_0 and the destination node n_d . n_i is one of the nodes in route r_j . During the route discovery routine, the source node should attach the value of the traffic load T_{Load} of the whole transfer to the route request packet, which specifies how much data each node in the route should relay. Then r^{**} is the set of the possible routes, which satisfy the condition:

$$\phi(r_j) \geq T_{Load} \quad (\forall r_j \in r^{**} \in r^*) \quad (6)$$

We also define the relay efficiency function of the route r_j as:

$$\eta(r_j) = \frac{1}{N_j} \sum_{n_i \in r_j} RE_i \quad (\forall r_j \in r^{**} \in r^*) \quad (7)$$

where N_j is the node number of the route j .

The optimal route r_{opt} is the one, which satisfies the following condition:

$$\eta(r_{opt}) = \max_{\forall r_j \in r^{**}} \eta(r_j) \quad (8)$$

If $r^{**} = \phi$, then select the route which satisfies the condition:

$$\phi(r_{opt}) = \max_{\forall r_j \in r^{**}} \phi(r_j) \quad (9)$$

In this case, a message should feed back to the source node to inform it that there are no routes able to support the whole transmission task. The source node will either cancel this transmission or divide up the transmission to fit the route conditions.

Simulation Details: We developed a 40-node MANET simulation environment in Network Simulator 2 (NS2) [3] to compare the performance of CMRCR against dynamic source routing (DSR) [4], LR and CMMBCR. The nodes are randomly located in a $600m \times 600m$ area. The nodes' mobility follows a "Random Waypoint" model with a speed selected from a uniform probability distribution function (PDF) with a maximum speed of $10ms^{-1}$. This model, whilst describing an unrealistic node behaviour, is typically used by many researchers, and hence useful for comparison purposes [3][5]. The nodes adopt IEEE802.11 as the MAC strategy. The energy consumed in the node i in the refresh period T is calculated by the following equation:

$$E_i = I_{tx} \times V \times t_{tx} + I_{rx} \times V \times t_{rx} \quad (\text{Joules}) \quad (10)$$

where I_{tx} is the transmission current and I_{rx} is the receiving current. They are 280mA and 240mA respectively [6]. t_{tx} and t_{rx} are the transmission time and the receiving time. The voltage V is 5V in our simulation. The node's energy is initialised using an exponential PDF with an average of 9000J. We use $T=5s$ and $\alpha=0.25$. The source node selects the packet-sending interval from an exponential PDF with the average value 0.5s. The packet length is fixed at 2048bits. In each data transfer, a file, whose length is taken from an exponential PDF with the average value 5Mbits, is sent to a random destination address.

Simulation Results and discussion: In our simulation, we compare the performance based on route survival probability, the average residual energy and other measures, of CMRCR with pure DSR, LR and CMMBCR.

1. Route survival probability (RSP): If the route is invalid during a transfer, a new route discovery operation must be executed to finish the data transmission, or the transmission should be abandoned, thus energy will be wasted. The RSP simulation results are illustrated in Fig. 1. From the results, we can see that CMRCR results in the highest RSP with a service half an hour longer than provided by LR and CMMBCR, and over one hour more than DSR. This suggests more data transfers can be fulfilled without new route rediscovery. After about 4 hours, the RSP

drops sharply due to energy exhaustion of most of the nodes. Clearly, the CMRCR mechanism can improve the RSP, resulting in more robust network connectivity.

2. Node average residual energy (NARE): The NARE can be expressed as:

$$E_{NARE}(t) = \frac{1}{N} \sum_{i=0}^{N-1} E_i(t) \quad (11)$$

where N is the number of mobile nodes in the simulation scenario.

The NARE simulation result is illustrated in the Fig. 2, which shows that the CMRCR mechanism can prolong battery lifetime. The reason is that this mechanism decreases the time spent on route discovery and selects the route with lower energy consumption.

3. Other characteristics: The mean end-to-end delay and the mean hop count are listed in the table 1. All mechanisms show similar performance results.

Conclusion: Energy limitation is a critical issue in MANETs. A number of routing methods use residual energy, transmission power, or link distance as the metric by which an optimal path is selected. These routing mechanisms may cause rapid energy drain in parts of the network, thus degrade the survivability of whole network, or increase the complexity of the routing method. This letter has introduced a new metric and a novel routing method, named the CMRCR, that improves the lifetime of paths, and therefore avoids unnecessary energy wastage through frequent route re-discovery. The simulation results indicate that this method outperforms the traditional routing schemes, providing more robust network connectivity, and longer mobile lifetime.

Acknowledgment: The work reported in this paper has formed part of the Personal Distributed Environment area of the Core 3 Research Programme of the Virtual Centre of Excellence in Mobile & Personal Communications, Mobile VCE, www.mobilevce.com, whose funding support, including that of EPSRC, is gratefully acknowledged. This work is also supported by the Overseas Research Students Awards Scheme (ORS), www.universitiesuk.ac.uk, which is greatly appreciated. Fully detailed technical reports on this research are available to Industrial Members of Mobile VCE.

References

- [1] I. Stojmenovic and X. Lin, "Power-aware Localized Routing in Wireless Networks", IEEE Transactions on Parallel and Distributed Systems, Vol. 12, Issue: 11, Nov. 2001, pp. 1122-1133
- [2] C.-K. Toh, "Maximum Battery Life Routing to Support Ubiquitous Mobile Computing in Wireless Ad Hoc Networks", IEEE Communications Magazine, June, 2001, pp. 138-147
- [3] K. Fall, and K. Varadhan, "The ns Manual (Formerly ns Notes and Documentation)", <http://www.isi.edu/nsnam/ns/doc/index.html>, Dec. 2003
- [4] D. B. Johnson, D. A. Maltz, and Y. C. Hu, "The Dynamic Source Routing Protocol for Mobile Ad Hoc Networks", IETF Internet Draft (work in progress), draft-ietf-manet-dsr-09-txt,

April 2003

[5] W. Navidi, T. Camp, "Stationary Distributions for the Random Waypoint Mobility Model", IEEE Transactions on Mobile Computing, Vol. 3, Issue: 1, Jan.-March 2004, pp. 99 -108

[6] L. M. Feeney, and M. Nilsson, "Investigating the Energy Consumption of a Wireless Network Interface in an Ad Hoc Networking Environment", IEEE INFOCOM, Anchorage, AK, 2001, Vol. 3, pp. 1548-1557

Authors' affiliations:

Yuefeng Zhou, David I. Laurenson, Steve McLaughlin (School of Engineering & Electronics, University of Edinburgh, King's Buildings, Edinburgh, EH9 3JL, UK)

E-mail address: Yuefeng.zhou@ee.ed.ac.uk

Table and figure captures:

Tab. 1 Other characteristics

Fig. 1 The route survival probability

Fig. 2 The node average residual energy

Table 1

Measure	DSR	LR	CMMBCR	CMRC
Mean End-to-end Delay (s)	0.0372	0.0382	0.0384	0.0377
Mean Hop Count	2.86	2.94	2.89	2.91

Figure 1

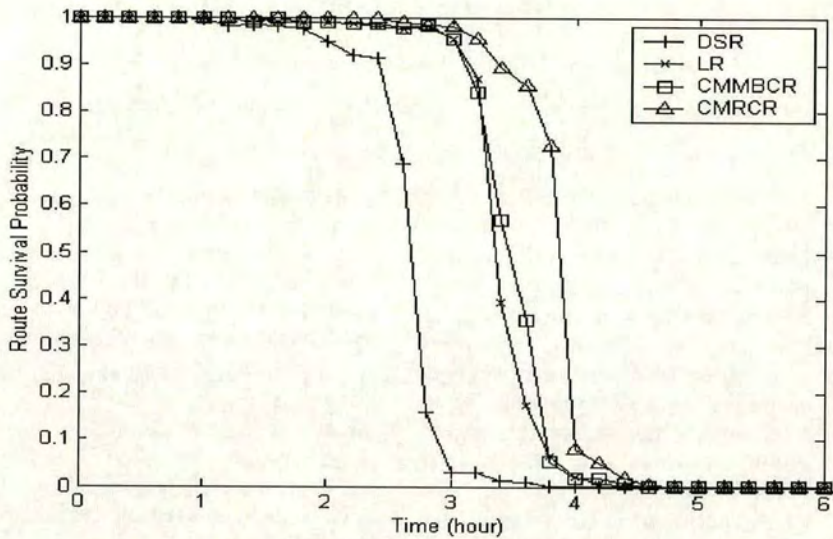
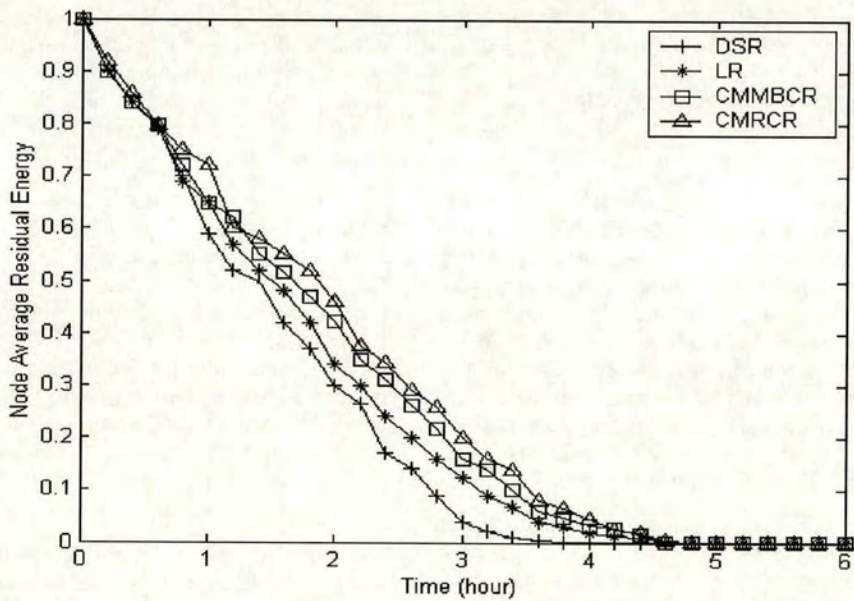


Figure 2



A High Survivability Route Selection Method in Wireless Ad Hoc Networks

Yuefeng Zhou, David I. Laurenson, Stephen McLaughlin

School of Engineering & Electronics, University of Edinburgh

Edinburgh, EH9 3JL, UK

Email: {Yuefeng.Zhou, Dave.Laurenson, Steve.McLaughlin}@ee.ed.ac.uk

Abstract—Energy limitation is a critical issue in wireless ad hoc networks. Researchers have developed some power-aware mechanisms in routing area to prolong the lifetime of connections in networks. The existed power-aware routing protocols often use residual energy, transmission power, or link distance as the metrics to select an optimal path. The investigation in this paper indicates that these route selections will cause rapid energy exhaustion in parts of the network, thus degrade the survivability of whole network. To average the energy consumption over the network with higher energy efficiency, a novel route selection mechanism, based on novel metrics, the relay capacity and the relay efficiency, is proposed. Simulation results show that this method saves energy with significantly more robust connectivity.

Keywords- ad hoc network, route selection

I. INTRODUCTION

With the rapidly increasing drive for wireless-capability of portable devices, a lot of research has been done in wireless network technologies. To provide more flexibility and convenience than traditional infrastructure networks, wireless ad hoc networks are being developed and under examination by industries and academics. In wireless ad hoc networks, various communication devices may form a temporary wireless network that has neither fixed infrastructure nor any centralized administration. These devices are not only the means of data interchanging but also the managers for the routes to data and access to services [1].

Prolonging network lifetime is one of the critical issues in wireless ad hoc networks, widely discussed in the literature, due to the limited energy stored in battery operated mobile equipments. To improve the link survivability and the stability of the topology through power saving, research has been done in each aspect of ad hoc network communications, such as routing protocols in network layer, and media access schemes in MAC layer. Current MAC designs for power saving in wireless ad hoc networks mainly concentrate on using various methods to put the communication unit of a node to sleep and minimize the time in transmission, reception and idle states [2-4], or to avoid overhearing neighbouring nodes [5]. Power-aware routing is another central means to make the connections more reliable and long lived. Generally, there will be many possible communication paths between source and destination node. Most of the proposed protocols try to find the minimum energy path to

improve the energy usage of a node. An optimal route is always determined by the relay cost, $C_{(i,j)}$, which is calculated by total transmission power [6], path distance [7-8], or residual battery energy [9]. Normally, the cost of a path is the sum of the cost of its links, $C_{Path} = \sum_{(i,j) \in Path} C_{(i,j)}$. However,

this is not a best choice from the sense of survivability of an entire network. Frequently selecting a low energy path will easily lead to energy exhaustion of the nodes along the selected path, thus resulting in network partition and topology instability [10].

In this paper, the focus is on a route selection method with novel metrics to increase path survivability of wireless ad hoc networks. The proposed novel metrics result in stable network connectivity and less additional route discovery operations. Comparing against other proposed routing metrics and selection methods, the simulation results show that the proposed metrics and route selection mechanism can support continuous services with high power efficiency.

The rest of this paper is organized as follows. Section 2 reviews the existed metrics and ad hoc route selection methods. In section 3, a novel metric, named relay capacity (RC) is formulated. Then, a new route selection method, named conditional maximum relay capacity route selection (CMRCRS), which is based on RC and the constraint metric, relay efficiency (RE), is introduced in detail. The simulation model and the results, comparing against other route selection methods, are presented and discussed in section 4. Finally, conclusions can be found in section 5.

II. BACKGROUND

According to the triggering mechanism and the style of route discovery, existing routing protocols can be divided into two categories, proactive routing, and reactive routing protocols [1, 11-12]. When using proactive routing, each node periodically exchanges route information, and maintains a routing table, which covers all paths. Each node can use a route extracted from its routing table immediately, thus minimising latency. However, proactive routing does not scale well to the highly dynamic topology, as periodic routing maintenance becomes expensive. In wireless ad hoc networks, another drawback is that a portable device may not afford storage space and extra energy to maintain a large routing table. Reactive routing protocols do not need to maintain information on the whole topology in each node. They try to discover routes when a node needs to transmit data packets. The discovered routes are only part of the

whole topology. Reactive routing protocols save resources and can adapt to sudden topology change [12]. The drawback of reactive protocols is a bigger latency than proactive routing protocols. However, as end-to-end delay performance is not primary consideration in wireless ad hoc networks, reactive routing protocols are more attractive than proactive routing protocols.

When some alternative paths with same source and destination are co-existed in a wireless ad hoc network, routing metrics are important for the route selection mechanism. Depending on the type of metric, power-aware route selection methods can be classified into three categories, maximum residual energy (MRE) [13-14], minimum transmission power (MTP) [6-7], and hybrid type [15].

A typical MRE route selection adopts the reciprocal of the residual battery energy of a node as the relay cost for routing, which can be described as:

$$f_{\text{cost}}|_i = 1/E_i(t) \quad (1)$$

where $E_i(t)$ is the residual battery energy of a node i at time t . Then the route cost, $R_{\text{cost}}(r_j)$, is defined as the maximum value $f_{\text{cost}}|_i$ along the route, r_j . The optimal route r_{opt} satisfies the following equation:

$$R_{\text{cost}}(r_{\text{opt}}) = \min_{\forall r_j \in r^*} R(r_j) \quad (2)$$

where r^* is the set of all possible routes with the same source and destination node. This route selection method avoids using paths, with a link that will become energy-exhausted. The drawback of this selection method is that the nodes with higher residual energy will have higher probability of supporting data-relay tasks, so these nodes will face high actual energy consumption, which may induce unstable connectivity. On the other hand, the so-called optimal route is not the route with better energy efficiency.

The transmission power over the hop (n_i, n_{i+1}) is proportional to $d^\lambda(i, i+1)$, where $d(i, i+1)$ is the distance between node n_i and n_{i+1} , and λ is the constant between 2 and 4 [16]. Essentially, the shortest distance routing [15, 18] protocol, in which the location information is used to select an optimal path, can be classified in the MTP category. For instance, authors in [6] proposes a typical MTP protocol, in which the relay cost of the route, r_j , is defined as following:

$$R_{\text{cost}}(r_j) = \sum_{i=0}^{d-1} T(n_i, n_{i+1}) \quad (3)$$

where $T(n_i, n_{i+1})$ is the transmission power over the hop (n_i, n_{i+1}) , n_0 is the source node, and n_d is the destination node.

The optimal route, r_{opt} , is selected based on the condition:

$$R_{\text{cost}}(r_{\text{opt}}) = \min_{\forall r_j \in r^*} R_{\text{cost}}(r_j) \quad (4)$$

Using the link distance or the transmission power as the routing metric can improve the quality of the receiving signal. However, to save energy, an accurate transmission power control mechanism should be applied, which will introduce redundant computation. Moreover, it is impractical for normal portable devices to obtain an accurate value of the distance. On the other hand, the nodes with short link distance will face more traffic load.

A hybrid scheme, which integrates the residual-energy metric and the transmission-power metric, was proposed by C.-K. Toh [15]. In this mechanism, a set of routes r^{**} was selected firstly by the MRE with the condition: $R_{\text{cost}}(r_j) \leq R_{th}$, where R_{th} is the threshold of the route cost. Then MTP is applied to the r^{**} to find an optimal route, r_{opt} . However, the performance of this mechanism depends on the uncontrollable value R_{th} and $d(i, i+1)$. Otherwise, like forenamed methods, more traffic load will put on the node with higher residual battery energy or short link distance.

III. A NEW ROUTE SELECTION METHOD IN WIRELESS AD HOC NETWORKS

In wireless ad hoc networks, the connections are easily broken due to the energy exhaustion. As discussed in the last session, some existing route selection methods will result in higher energy consumption in parts of the network, which shortens the time to network partitioning. In this session, some metrics and the corresponding route selection method are proposed to make the nodes expend energy more equitably and efficiently.

The proposed metrics has the following desirable characteristics:

- It averages the energy consumption across a whole network, thus postponing the time to network partition, and improving the survivability of the paths, therefore avoids unnecessary energy wastage through frequent route re-discovery.
- The energy efficiency is also considered into the route selection through using the constrained condition, relay efficiency.
- The nodes do not need to know their locations for routing.

A. A Novel Metric and Its Constrained Condition

In this session, a novel metric RC_i , which is constrained by relay efficiency (RE), is formulated to specify the node's capability to transmit and its energy efficiency.

Firstly, the lifetime of the node i , L_i , is defined as:

$$L_i = E_i(t) / \overline{R_i(t)} \quad (5)$$

where $E_i(t)$ is the node's residual energy.

$R_i(t) = \frac{\partial E_i(t)}{\partial t}$ is defined to indicate how much energy is used per second at node i .

To avoid rapid changes in $R_i(t)$, and obtain the average trend, an α low-pass filter is applied to $R_i(t)$, to give:

$$\overline{R_i(t)} = \alpha \cdot R_i(t - T) + (1 - \alpha) \cdot R_i(t) \quad (6)$$

where T is the sample period of $R_i(t)$. α and T have to be chosen carefully to accurately reflect the energy-consumption trend of a node.

The transmission capability of a resource-limited node relates to not only the residual energy but also the data rate. When the nodes support multi-rates, the data rate should be considered in the routing metric to exactly reflect the traffic capacity that a node can support. So the relay capacity of a node, RC_i , can be described as:

$$RC_i = L_i D_i \quad (7)$$

where D_i is the current data rate of the node i . The unit of RC_i is the bit.

Another important parameter to denote the node energy feature is RE_i , which describes the efficiency of the energy consumption in node i . RE_i is specified as:

$$RE_i = D_i / \overline{R_i(t)} \quad (8)$$

The unit of RE_i is bits/Joule. It can be used as a constraint condition to select a more energy efficient path.

B. Details of the CMRCRS

The new conditional maximum relay capacity route selection (CMRCRS) mechanism is based on RC_i and RE_i . In CMRCRS, the relay-efficiency function of the route r_j is defined by the equation:

$$\eta(r_j) = \min_{\forall n_i \in r_j} RE_i \quad (r_j \in r^*) \quad (9)$$

where r^* is the set of all possible routes with the same source node n_0 and the destination node n_d . n_i is one of the nodes in route r_j .

The allowable worst-case value of the RE_i is defined by Th_{RE} . When the RE of a node is less than Th_{RE} , it means that this node has low energy efficiency, and will expend more energy on a packet exchange. For example, when a node increases its transmission power to overcome interference, or is bearing more relay tasks, this node will suffer poor energy efficiency. In this case, the route selection method should avoid loading more relay tasks onto such nodes. So the route set, r^{**} is selected by the condition:

$$\eta(r_j) \geq Th_{RE} \quad (\forall r_j \in r^{**} \in r^*) \quad (10)$$

Moreover, the relay-capacity function of the route r_j is:

$$\phi(r_j) = \min_{\forall n_i \in r_j} RC_i \quad (\forall r_j \in r^{**} \in r^*) \quad (11)$$

The optimal route r_{opt} is the one, which satisfies the following condition:

$$\phi(r_{opt}) = \max_{\forall r_j \in r^{**}} \phi(r_j) \quad (12)$$

If $r^{**} = \emptyset$, then select the route, which satisfies the condition:

$$\phi(r_{opt}) = \max_{\forall r_j \in r^*} \phi(r_j) \quad (13)$$

IV. SIMULATION

A. Simulation Configuration

An 40-node wireless ad hoc network simulation environment in Network Simulator 2 (NS2) [18] was developed to compare the performance of CMRCRS against MRE and MTP. The nodes are randomly located in a $600m \times 600m$ area.

The energy consumption is estimated by the "first order radio" model discussed in [16]. This energy model can be described as follows:

$$E_{i_tx} = E_{tx} \times P_{tx} + \varepsilon_{amp} \times P_{tx} \times d_{i-j}^2 \quad (\text{Joules}) \quad (14)$$

$$E_{i_rx} = E_{rx} \times P_{rx}$$

where E_{i_tx} is the energy consumed in transmission, and E_{i_rx} is the energy consumed in reception for node i . E_{tx} and E_{rx} are the radio transmitter and receiver operation energy dissipation per bit. We assume the node has some form of power control to achieve an acceptable signal-to-noise ratio. ε_{amp} is set to obtain the desired signal strength for transmissions to j . P_{tx}

and P_{rx} is the transmitted packet size and the received packet size. $d_{i,j}$ is the distance between the source node i and the destination node j . In the simulation, $E_{tx}=E_{rx}=50nJ/bit$, $E_{amp}=100nJ/bit/m^2$. Each node is given an initial energy, calculated from a uniform probability distribution function (PDF) with the range $[1500J, 2000J]$.

Since the goal of our simulation is to compare the performance of route selection methods, not whole routing protocols, we simply modify dynamic source routing (DSR) [11], a typical reactive routing method, to act as the underlying route discovery and maintenance protocol. Figure 1 shows the modified procedure of the route discovery. The source node broadcasts the route request packets (RRP) to find all the possible routes. The neighbour nodes, B and F, receive RRP, and record their own node information, including the node relay capacity, node relay efficiency and other features, into the RRP and relay this to their neighbours. The destination node E will receive two distinct RRP, in which the whole routing information is recorded. Finally, node E uses the route selection method to choose the optimal route and replies with a route ACK packet (RACKP), in which the selected route information is enclosed, following the reverse direction of the selected route to the source node A. Then the source node uses this route, indicated in the RACKP, to send the data packets to E.

The CSMA/CA strategy is used for MAC layer. The relay-efficiency threshold, Th_{RE} , is set to $2kbits/Joule$, T is $2s$, and α is 0.25 . The data rate is fixed at $2Mbps/s$.

B. Simulation Results

1) Energy consumption distribution over the network:

Fig. 2 shows the total energy consumption during one-hour period of the network with MRE route selection method. This result is compared against the energy cost with MPT route selection mechanism (fig. 3) and CMCRS (fig. 4). The energy cost is normalized by the maximum value of the consumption. The warm colour area means much more energy was consumed. Using MRE or MPT, the energy consumption is concentrated in small parts of the network. The reason for this phenomenon is that more traffic was put

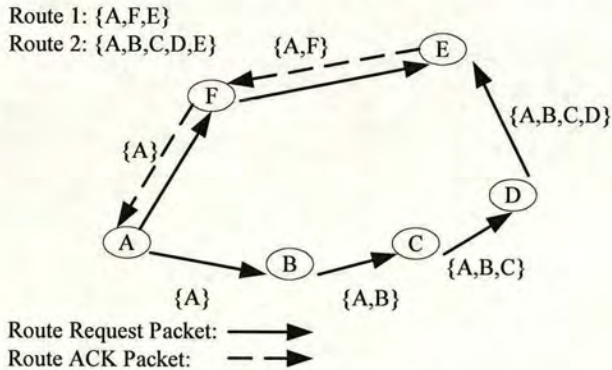


Figure 1. The procedure of the route discovery

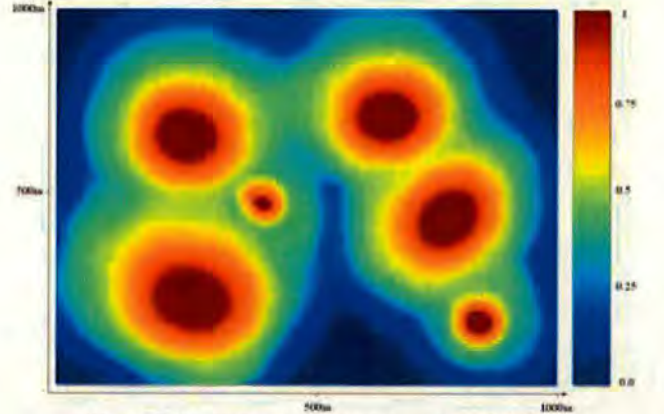


Figure 2. Normalized energy consumption in MRE

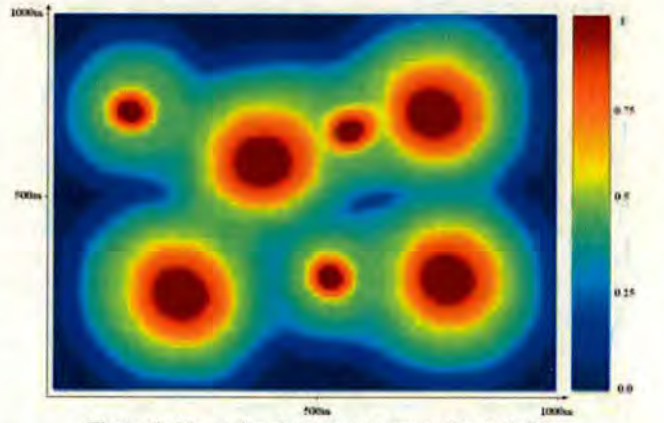


Figure 3. Normalized energy consumption in MPT

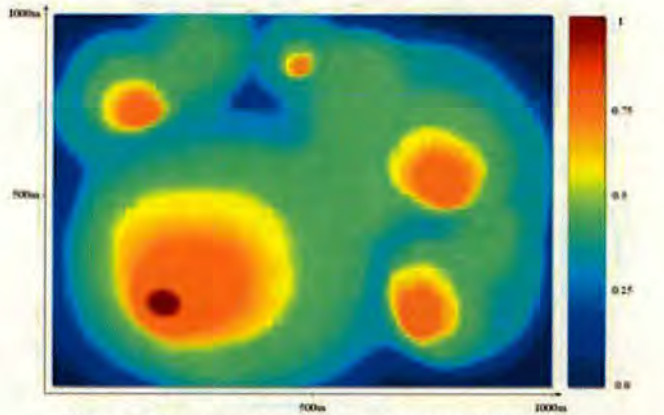


Figure 4. Normalized energy consumption in CMCRS

into the nodes with higher residual energy or shorter link distances. These nodes will face higher energy consumption, thus become readily exhausted, which will induce the network partitioning. After a period, many nodes will lost intermediate nodes for relaying their packets. So the survivability of a whole network will be degraded. In fig. 4, though most of the network area faces a 50% normalized

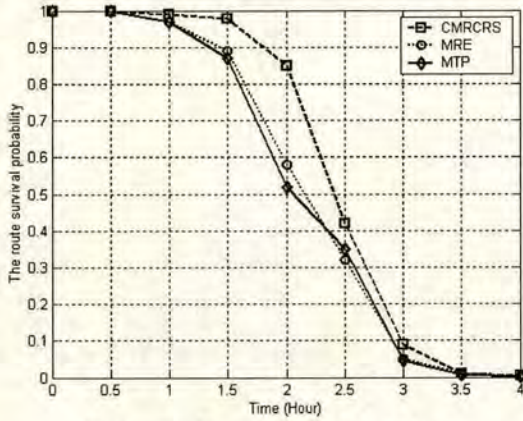


Figure 5. The route survival probability

energy consumption, the CMRCRS equalizes the energy use over the entire network. That means most of the nodes will maintain residual energy at an average level. So the lifetime of paths can be extended.

2) Route survival probability:

To describe the characteristic of the network survivability under different route selection methods, a statistical value, named the route survival probability (RSP), was calculated in the simulation. After each half-hour period, the sum of survival paths, N_{surv} , is computed. Then the RSP can be expressed by N_{surv}/N_{total} . If the route is broken, a new route discovery operation must be executed to finish the data exchange, or the transmission should be abandoned, thus energy will be wasted. So the RSP means not only robustness of connection, but also energy efficiency. This is plot for each routing selection method in fig. 5. The CMRCRS evidently increases the RSP, since it prolongs the time to network partitioning.

3) Average residual energy:

The average residual energy, E_{ARE} , can be expressed as:

$$E_{NARE}(t) = \frac{1}{N} \sum_{i=0}^{N-1} E_i(t) \quad (14)$$

where N is the number of nodes in the simulation scenario.

The E_{ARE} of the simulation is plot in fig. 6, which shows that the CMRCRS can prolong the nodes' lifetime. For instance, the nodes employing CMRCRS maintain energy above a 30% level for 1 hour longer than other nodes. The reason is that this mechanism decreases the time spent on route discovery and selects the path with lower energy consumption.

V. CONCLUSIONS

Since energy limitation is one of the critical problems in wireless ad hoc networks, many researchers are developing methods to improve the lifetime of the paths. Routing is a

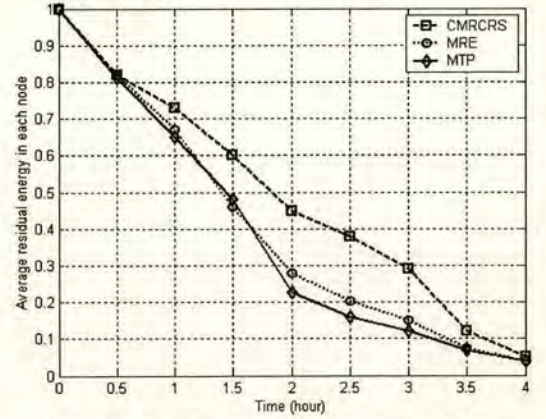


Figure 6. The average residual energy in each node

primary way to tackle the network survivability issue. A number of routing protocols use residual energy, transmission power, or link distance to decide the optimal route among the multiple paths between the source node and the destination node. The simulations in this paper show that using these metrics may result in network partitioning, and unnecessary energy wastage by frequent route discovery operations. To improve the survivability of an entire network, some new metrics are formulated in this paper. Based on these metrics, a novel route selection method, named CMRCRS, is described in detail. The simulation results show that this method can equalize the energy consumption across the whole network, decrease the probability of network partitioning, and improve the lifetime of the routes with higher energy efficiency.

ACKNOWLEDGMENT

The work reported in this paper has formed part of the Personal Distributed Environment area of the Core 3 Research Programme of the Virtual Centre of Excellence in Mobile & Personal Communications, Mobile VCE, www.mobilevce.com, whose funding support, including that of EPSRC, is gratefully acknowledged. This work is also supported by the Overseas Research Students Awards Scheme (ORS), www.universitiesuk.ac.uk, which is greatly appreciated. Full detailed technical reports on this research are available to Industrial Members of Mobile VCE.

REFERENCES

- [1] E. M. Royer, C.-K. Toh, "A Review of Current Routing Protocols for Ad Hoc Mobile Wireless Networks," IEEE Personal Communications, April 1999, pp. 46-55
- [2] Y. Zhou, D. I. Laurenson, S. McLaughlin, "An Effective Power-Saving Scheme For IEEE 802.11-based Multi-hop Ad Hoc Network", 2004 VTC Fall, Los Angeles, Sep. 26-29, 2004
- [3] C. Guo, L. C. Zhong, J. M. Rabaey, "Low Power Distributed MAC for Ad Hoc Sensor Radio Networks",

- Global Telecommunications Conference, 2001. GLOBECOM '01. IEEE, Vol. 5, 25-29, Nov. 2001, pp.2944 - 2948
- [4] W. Ye, J. Heidemann, D. Estrin, "An Energy-Efficient MAC Protocol for Wireless Sensor Networks", INFOCOM 2002, Twenty-First Annual Joint Conference of the IEEE Computer and Communications Societies Proceedings, IEEE, Vol.3, 23-27, June 2002, pp.1567 - 1576
- [5] S.Singh, C.S. Raghavendra, "PAMAS: Power Aware Multi-Access Protocol with Signalling for Ad Hoc Networks", ACM computer Communication Review, July 1998, Vol. 28, No. 3, pp. 5-26
- [6] K. Scott, N. Bambos, "Routing and channel assignment for low power transmission in PCS," Universal Personal Communications, 1996, Record., 1996 5th IEEE International Conference on Personal Communications, vol. 2, 29, Sept.-2 Oct. 1996, pp.498 - 502
- [7] Stojmenovic and X. Lin, "Power-aware Localized Routing in Wireless Networks." IEEE Transactions on Parallel and Distributed Systems, Volume: 12, Issue: 11, Nov 2001
- [8] Y. C. Tseng, T. Y. Hsieh, "Fully Power-Aware And Location-Aware Protocols for Wireless Multi-Hop Ad Hoc Networks", Computer Communications and Networks Eleventh International Conference, Oct. 2002, pp.608 - 613
- [9] C.-K. Toh, "Maximum Battery Life Routing to Support Ubiquitous Mobile Computing in Wireless Ad Hoc Networks," IEEE Communications Magazine, June, 2001
- [10] R. C. Shah, J. M. Rabaey, "Energy Aware Routing for Low Energy Ad Hoc Sensor Networks," Wireless Communications and Networking Conference, 2002, WCNC2002, IEEE, vol.1, 17-21 March 2002, pp.350 - 355
- [11] D.B. Johnson, D.A. Maltz, Y.C. Hu, "The dynamic source routing protocol for mobile ad hoc networks", IETF Internet Draft (work in progress), draft-ietf-manet-dsr-09-txt, April 2003
- [12] D. Maltz, J. Broch, J. Jetcheva, "The Effects of On-demand Behavior in Routing Protocols for Multihop Wireless Ad Hoc Networks", IEEE Journal on Selected Areas in Communications, 1999, 17(8):1439-1453
- [13] S. Singh and M. Woo, C. S. Raghavendra, "Power-aware with Routing in Mobile Ad Hoc Networks," Mobicom 1998, Dallas, TX, 1998
- [14] F. J. Block, and C. W. Baum, "An Energy-Efficient Routing Protocol For Wireless Sensor Networks," MILCOM 2002, Proceedings, vol. 1, 7-10, Oct. 2002, pp.489 - 494
- [15] C.-K Toh, "Maximum Battery Life Routing to Support Ubiquitous Mobile Computing in Wireless Ad Hoc Networks," IEEE Communications Magazine, June 2001
- [16] W. Heinzelman, A. Chandrakasan, and H. Balakrishnan, "Energy-Efficient Communication Protocol for Wireless Microsensor Networks," In Proc. Hawaii International Conference on System Science, 2000, vol. 2, pp.10
- [17] J. Zhang, H. Shi, "Energy-Efficient Routing for 2D Grid Wireless Sensor Network," Information Technology: Research and Education, 2003, ITRE2003, Aug. 11-13, 2003, pp.311 - 315
- [18] K. Fall, and K. Varadhan, "The ns Manual", <http://www.isi.edu/nsnam/ns/doc/index.html>, December 2003

A Novel Piconet Coordinator Selection Method for IEEE802.15.3-Based WPAN

Yuefeng Zhou, David I. Laurenson, Stephen McLaughlin

School of Engineering & Electronics, University of Edinburgh

Edinburgh, EH9 3JL, UK

Email: {Yuefeng.Zhou, Dave.Laurenson, Steve.McLaughlin}@ee.ed.ac.uk

Abstract- Power awareness is an essential component of wireless personal area networks (WPANs), due to the limited energy stored in battery-operated equipment. Moreover, a WPAN has to deal with coexistence problems, since it may simultaneously operate over many types of network. Especially, when UWB, which is a candidate PHY technology for IEEE802.15.3-based WPANs, is applied, decreasing the transmission power is necessary to meet the Federal Communications Commission (FCC) regulation and diminish interference to other communication systems. In a WPAN, the Piconet coordinator (PNC) acts as an important role for central controller of the whole Piconet. As specified in the standard, IEEE802.15.3, the most capable device in a Piconet could be dynamically selected as the PNC in terms of the capacity of devices. However, the standard does not explicitly define the capacity function. In this paper, a novel PNC selection method, named Least Distance Square PNC (LDS-PNC) selection for IEEE 802.15.3-based WPANs is proposed. Using the proposed selection method, the transmission power can be lessened, and the interference area introduced by PNCs can be diminished as well. The simulation results show that it has power-saving and interference mitigation characteristics.

Keywords: WPAN, Ultra-wideband (UWB), Piconet Selection

I. INTRODUCTION

The WPAN is of great importance to many industries and academics. Compared to other similar wireless networks, such as WLAN, and wireless cell network, the WPAN is operated within a smaller personal space, whose diameter is less than 10m, and higher data rate, which is more than 20Mbit/s. After establishing the strategic spectrum planning and appropriate regulation for ultra wide band (UWB) communication by FCC in 2002, UWB is regarded as a promising technology for physical layer implementation of short-range communications in WPANs. A new MAC protocol, IEEE 802.15.3 [1], was issued in September 2003, which is suitable for low power consumption and high data rate WPANs. Because of the reasonable power saving, power control management, QoS support, and security mechanisms in IEEE 802.15.3, it is also the potential MAC protocol for UWB communication [2]. Currently, most members of the IEEE 802.15.3 Working Group are supporting UWB as the technology of choice for the physical layer specification of IEEE 802.15.3.a.

An important issue for IEEE 802.15.3-based WPANs is that systems have to operate in the presence of other wireless networks, such as IEEE 802.11 WLAN, and other WPANs. The transmission power of WPAN devices should be well controlled and not exceed the limitation specified in FCC regulations. Moreover, like other portable wireless

communication systems, energy consumption is still one of the key issues. In WPAN MAC of IEEE802.15.3, the PNC plays an important role, since it controls all the networking operations. As specified in the standard, the PNC device can be changed dynamically, so a good PNC selection method could improve the performance of a WPAN.

A lot of research effort has been expended in the area related to the physical layer technology of WPAN communication, such as UWB PHY technologies, which is a striking contrast to that in WPAN MAC layer. In this paper, focusing on the solution in MAC layer, a novel PNC selection method, called Least Distance Square PNC (LDS-PNC) selection is presented, to manage the critical interference mitigation and power-saving problems with only slight modification of the IEEE 802.15.3 standard.

The rest of this paper is organized as follows. Section 2 reviews the architecture of the Piconet and the IEEE 802.15.3 MAC protocol. Section 3 explains the proposed PNC selection method in detail. The simulation results, which validate the LDS-PNC selection algorithm, are presented and discussed in section 4. Finally, section 5 concludes the paper.

II. BACKGROUND

A. Piconet in IEEE802.15.3

The Piconet in IEEE 802.15.3 is an ad hoc data communication system, which is operated within a small area around person or object. Most of the communication devices are battery operated.

In a Piconet, the PNC is a "master" device, which centrally controls the whole Piconet. All other devices in a Piconet are called DEV. The PNC uses a beacon frame to manage QoS requirements, power-saving mode, and media access of whole Piconet. The PNC also classifies various packet transmissions, which are requested by the DEVs. Different packets have different priority levels for transmission. For instance, some command-data packets have higher priority to access the media.

If a PNC finds other devices are more capable than itself, it hands over the control of this Piconet to a more appropriate DEV. That means the Piconet in IEEE 802.15.3 has a dynamic membership, thus adapting to the dynamically changing environment and topology. Though the standard specifies the PNC handover mechanism, it does not detail PNC selection policies.

The authors of this paper are among the core members of the Mobile VCE working group.

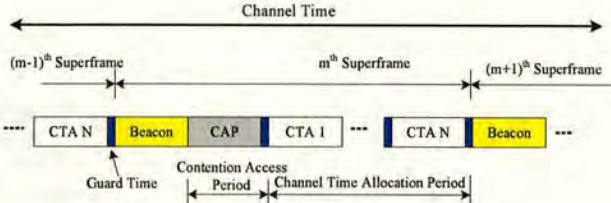


Fig. 1. The channel time and the superframe

B. Channel Access

In IEEE 802.15.3, the PNC globally controls channel access for each DEV. The channel time is divided into superframes. As illustrated in fig. 1, a superframe has three parts, Beacon, Contention Access Period (CAP), and Channel Time Allocation Period (CTAP). The CAP and the CTAP are optional periods. The allocation information about the CAP and the CTAP is indicated in the beacon.

The CAP is used for commands or non-stream data, which ensures a light traffic load. In a CAP, DEVs access the channel based on CSMA/CA. In order to minimize the collision, a DEV should wait for a random length of time at first, and then begin to transmit. When a DEV cannot receive an ACK after its sending a packet, it retransmits the packet, for up to 3 times [1].

The channel access in a CTAP is based on TDMA. The CTAP is divided into many Channel Time Allocations (CTAs) with fixed duration and start time. Each CTA is assigned to an individual DEV or a group DEVs. The location of each CTA and its duration is specified in the beacon by the PNC. The CTAP is designed for all kinds of data. A DEV makes a request of the PNC for a CTA in which to exchange data. Because the full duration of the CTA can be utilized by a DEV or a group of DEVs, successful transmission will result. The CTA can support bulk data (such as multi-Megabyte sized image files), and isochronous data (such as video stream) very well.

III. PICONET COORDINATOR SELECTION METHOD

A. Motivation

In practice, a WPAN may experience spectrum overlapping and coexistence with other wireless networks, particularly, when UWB physical layer technology is applied. Minimizing the interference to other networks is one of the key problems in a WPAN. To meet the FCC regulations and afford a good quality signal, the transmission power of a device in a WPAN should be well controlled. On the other hand, it is well known that reducing the transmission power is also an important aspect for power saving in battery-operated wireless networks [3]. It is clear that reducing the transmission distance can decrease the transmission power required, due to the transmission power is strongly linked to the transmission

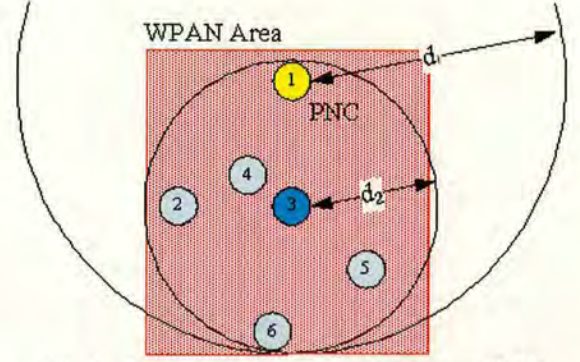


Fig. 2. Interference area introduced by different PNCs

distance. As described in [3], if $P_r(d_{i,j})$ is the desired receiving power level for a correctly decoded packet between device i and j , then the relationship of the transmission power $P_t(d_{i,j})$ and received power can be described by:

$$P_r(d_{i,j}) = P_t(d_{i,j}) \cdot \left(\frac{\lambda}{4\pi d_{i,j}} \right)^n \frac{G_t G_r}{L} \quad (1)$$

where $d_{i,j}$ is the distance between transmitter i and receiver j , G_t and G_r are the antenna gains of the transmitter and receiver respectively, L is the system loss factor, n is the path loss exponent with a typical value between 2 and 4.

In terms of the standard, the most capable DEV may be dynamically selected as the PNC of a WPAN. Generally, the capability function, C_i , of a source limited DEV is determined by the transmission rate, memory capacity, CPU speed, residual energy, or other characteristics. The mechanism for defining the capability function has not explicitly specified by the standard.

To reduce the interference introduced by PNC communication and save energy consumption within a Piconet, the distance between the PNC and other DEVs must be considered into the capability function, C_i , for the PNC selection method. For example, in fig. 2, the red rectangle defines a WPAN area. Assume that DEV 1 is chosen for the PNC. In this case, to cover all the DEVs, the PNC has to increase transmission power to satisfy the emission radius d_1 . Compared with the PNC selection scheme which selects DEV 3 as the PNC, we can see that the interference area is reduced and less energy is consumed in the PNC and other remote DEVs, such as DEVs 5 and 6, who also require less power to successfully exchange information with the PNC. Generally, selecting a DEV, which has the least distance square, as the PNC can decrease the interference area and the extra transmission power introduced by the PNC.

However, from the point of view of improving the survivability of the whole WPAN, frequently selecting a PNC with low battery energy will easily lead to energy exhaustion in this PNC, thus resulting in network partitioning and topology instability [4-5]. Therefore, the residual energy should also be considered in PNC selection.

B. Details of LDS-PNC Selection

A PNC Selection Counter (PSC), which controls the frequency of the PNC selection operation, is configured to an initial value, T , when a PNC is selected. A PNC decreases its PSC until it reaches zero. The PNC selection routine is started by a PNC when either:

1. The PSC meets zero;
2. The PNC's residual battery energy meets the lower bound, E_L ; or
3. The PNC needs to leave the Piconet.

To initiate the PNC selection process, the PNC attaches a PNC Selection Request (PSR) to the beacon frame and sends it to all the DEVs at the start of the superframe. When the DEVs receive the PSR, they will try to send a PSR-ACK packet back to the PNC as the acknowledgement. Each DEV attaches the value of its residual battery energy, E_i , and other characteristics, such as memory capacity, and CPU speed, to the PSR-ACK, and uses a maximum power level, P_{\max} , to send this packet during the CAP. Because the PSR-ACK is a small packet, it can be successfully transmitted by most DEVs within the CAP. For simplicity, if a DEV cannot successfully transmit a PSR-ACK within the CAP, for instance, because of severe access contention, this DEV will not try to send the PSR-ACK in other CAPs, which means that this DEV will be ignored in PNC selection.

All devices within the Piconet, including the PNC and DEVs, listen for this PSR-ACK. Since our algorithm just needs a rough value of the distance between two stations, the received signal strength of the PSR-ACK is measured to estimate the value of the distance. When DEV i receives DEV j 's PSR-ACK, it uses the equation (1), whose n is given by 2, to compute the distance between DEV i and j , $d_{i,j}$, as:

$$d_{i,j} = \lambda \sqrt{\frac{P_{\max} G_t G_r}{P_{r,i} L}} / 4\pi \quad (2)$$

where $P_{r,i}$ is the received power lever measured by the station i . Assume there are $N+1$ devices in the Piconet. The device, i , will record a set of the distances between other stations and itself, which can be depicted as:

$$D_i = \{d_{i,j}\}; \quad j = 0, 1 \dots N-1, N; \quad j \neq i \quad (3)$$

Then the average distance square of device i , among the distance set D_i can be calculated as:

$$E(D_i^2) = \frac{1}{N} \cdot \sum_{j=0,1,2,\dots,N-1,j \neq i} d_{i,j}^2 \quad (4)$$

Generally, the PNC will consume more energy than normal DEVs, so it is necessary for a DEV to have enough battery energy to act as a PNC. Therefore, after receiving all the PSR-ACKs, the PNC tries to find a DEV set, R^* , in which the DEVs' residual battery energy is more than E_L . R^* can be defined as:

$$e(DEV_i) \geq E_L \quad (\forall DEV_i \in R^*) \quad (5)$$

where DEV_i is one of the DEVs in the set R^* , and $e(DEV_i)$ is its residual battery energy. This step prevents a centrally located device from being frequently chosen as a PNC without consideration of the residual energy. Without this criterion fast energy exhaustion in the PNC and network partitioning will result. In some cases, other QoS criteria, such as memory capacity, and CPU speed, may be considered in PNC selection. The capability function, $C(DEV_i)$ which includes these features, could be defined to find another set of DEVs, R^{**} , as:

$$C(DEV_i) \geq C_L \quad (\forall DEV_i \in R^{**} \in R^*) \quad (6)$$

where C_L is the lower bound of capability.

If $R^* = \emptyset$ or $R^{**} = \emptyset$, a warning message will be sent to the application layer to make the user aware.

At the beginning of the next superframe, the PNC attaches all IDs of the DEVs in R^{**} and a Distance Report Request (DRR) in the beacon, and broadcasts it in its Piconet. To decrease energy consumed in transmission, just the DEVs, who are the member of R^{**} , and are specified in the beacon, listen for this DRR, and send DRR-ACK packets, enclosing the maximal distance square, $E(D_i^2)$, to the PNC during the following CAP. After receiving all the values of $E(D_i^2)$, the PNC will find an optimal DEV to replace itself. If the Least Distance Square PNC (LDS-PNC) selection metric is applied, the optimal DEV, DEV_{opt} , can be specified by:

$$E(D_{opt}^2) = \min_{\forall DEV_i \in R^{**}} E(D_i^2) \quad (DEV_{opt} \in R^{**} \in R^*) \quad (7)$$

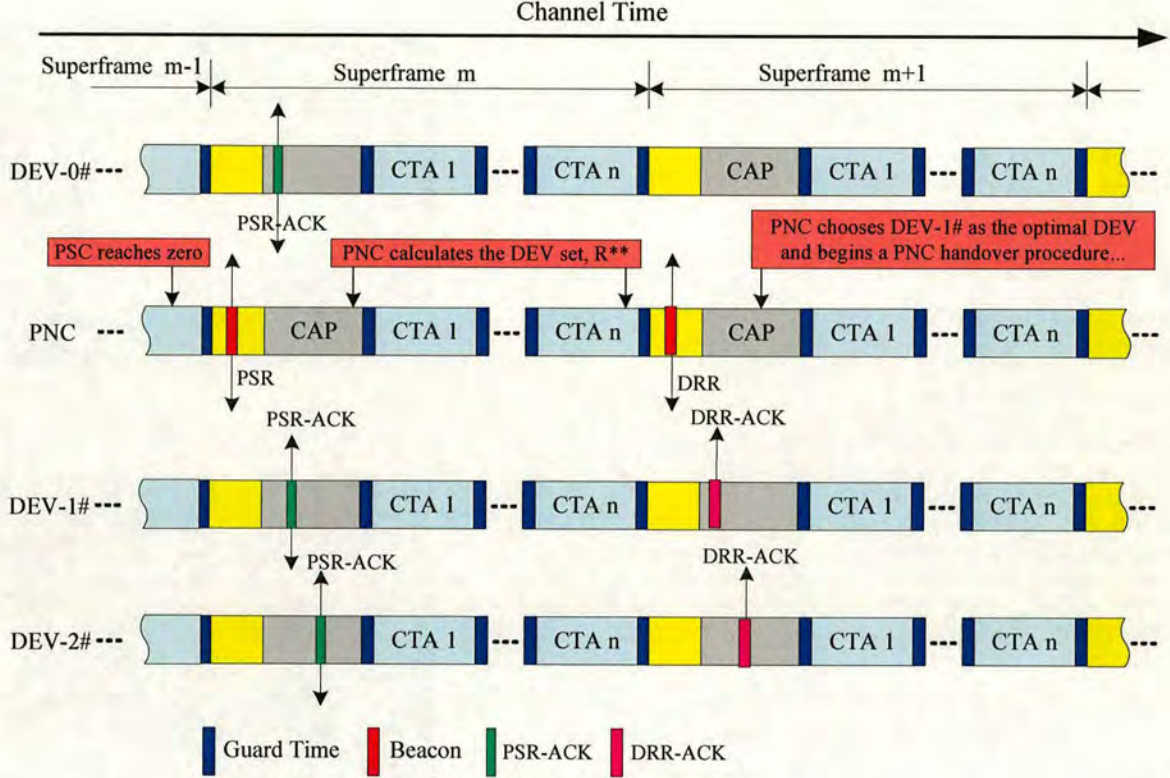


Fig. 3. PNC selection procedure

Then the current PNC will start a procedure to hand over control of this Piconet to the selected optimal DEV. When the selected optimal DEV becomes a PNC, it will also restart a PSC for the next PNC selection timer. The new PNC will transmit beacons and other control packets with a required transmission power level calculated through equation (1), given $n=2$:

$$P_i(d_{i,j}) = P_r^* \cdot \left(\frac{4\pi d_{\max}}{\lambda} \right)^2 \frac{L}{G_t G_r} \quad (8)$$

where P_r^* is a required receiving power level for correctly decoding, and d_{\max} is the maximal distance between the new PNC and other DEVs, which can be found in the distance set, D_i .

An example of the proposed PNC selection procedure is shown in fig. 3. When the PSC reaches zero, the PNC broadcasts a beacon with attached PSR information. During the following CAP, all the DEVs attach their features to their PSR-ACK packets and send them to the PNC. The remaining duration of the m^{th} superframe is enough for a PNC and DEVs to calculate the set R^{**} , and the distance square. In the next beacon window, the PNC sends the DRR information to the

DEVs belonging to set R^{**} through beacon transmission. Then the DEVs (DEV-#1 and DEV-#2) in set R^{**} send the DRR-ACK to the PNC. Finally the PNC uses the distance information attached in DRR-ACK packets to choose the optimal DEV as the next PNC.

IV. NUMERICAL RESULTS

In this section, several examples are illustrated to show the performance of the proposed PNC selection method. In the simulation, all the devices are randomly located in the same coverage area so that they can communicate directly with each other. A real-time Variable Bit Rate (rt-VBR) MPEG4 traffic generator, introduced in [6] is implemented in the simulation. Table 1 shows some key parameters.

The energy consumption is estimated by the “first order radio” model discussed in [7]. This energy model can be described as follows:

$$E_{i_tx} = E_{tx} \times S_{tx} + \varepsilon_{amp} \times S_{tx} \times d_{i-j}^2 \quad (\text{Joules}) \quad (9)$$

$$E_{i_rx} = E_{rx} \times S_{rx}$$

where E_{i_tx} is the energy consumed in transmission, and E_{i_rx} the energy consumed in reception for node i . E_{tx} and E_{rx} are the

TABLE I
Simulation Parameters

Parameters	Value
Superframe size	10ms
Mean offered load by rt-VBR	8Mbps
Simulation area	10m×10m
Total number of devices (including PNC)	5,10,15,20,25,30
PNC selection period	150ms
Channel Bit Rate	100Mbit/s
Packet deadline	33ms
Lower limitation of the residual energy in devices E_L	500Joul

radio transmitter and receiver operation energy dissipation per bit. We assume the node has some form of power control to achieve an acceptable signal-to-noise ratio. ϵ_{amp} is set to obtain the desired signal strength for transmissions to j . S_{tx} and S_{rx} are the transmitted packet size and the received packet size. d_{ij} is the distance between the source node i and the destination node j . In the simulation, $E_{tx}=E_{rx}=50nJ/bit$, $E_{amp}=100nJ/bit/m^2$. Each node is given an initial energy, calculated from a uniform PDF with the range [1800J,2000J].

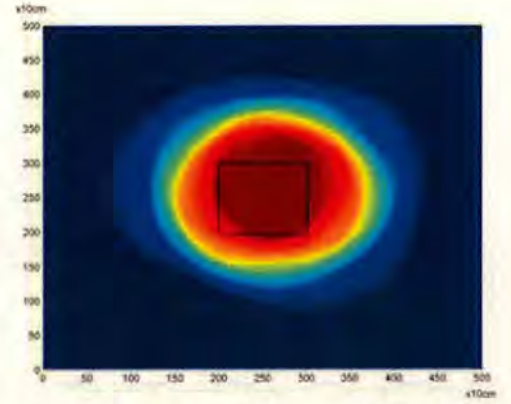
For validation of the PNC selection method, it is assumed that each device has same memory capability, CPU speed, and receiving/transmitting characteristics, which means $R^* = R^{**}$.

A. Interference area introduced by PNC communication:

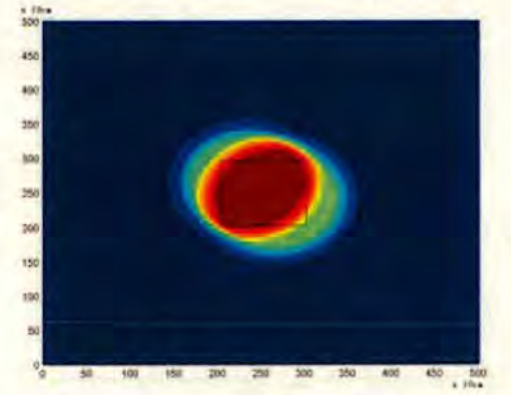
Generally, a DEV, which is selected as a PNC, has smaller distance square, and will be located in the central area of the Piconet. On the other hand, the proposed method utilizes an estimated distance to control the transmission power level of the PNC, thus the area occupied by the PNC communication radiation and the battery energy consumed in the PNC could be diminished. Fig. 4 shows the coverage of PNC communication in the normal IEEE802.15.3-based WPAN and the proposed PNC selection methods. In the simulation, 10 devices (1 PNC, 9 DEVs) are randomly located in a 10m×10m area, which is indicated by the black frame in fig. 4. The warm colour area means this area has been covered by the PNC's transmission for a high percentage of time. It is clear that using the proposed PNC selection method can decrease the coverage area of the PNC radiation, which means less interference to neighbouring networks and energy saving for the PNC.

B. Average residual energy in each device:

To measure the power-saving features of the proposed PNC selection algorithm, the average battery energy of 10 devices, including 1 PNC and 9 DEVs, is measured in a 4-hour simulation. The measured values are normalized by the initial battery energy in each device. Fig. 5 compares the results of the LDS-PNC selection method against the normal IEEE802.15.3 mechanism. Because the transmission power is decreased through avoiding long transmission paths, more energy is saved when using LDS-PNC selection. For example, the devices in



(a) Normal selection method



(b) LDS

Fig. 4. Interference area introduced by PNC communication

the piconet employing LDS-PNC selection survive 1 hour longer than the devices in the normal IEEE802.15.3 WPAN when 50% of the initial battery energy is used.

C. PNC survival probability:

When E_L is configured to zero, which means the PNC selection method does not consider the residual energy in the selection, the central DEVs will have a high probability of being selected as the PNC. However, frequently selecting DEVs with small distance square will easily lead to energy exhaustion of these devices, thus resulting in network partitioning and topology instability. Fig. 6 compares the PNC survival probability of the proposed LDS, LDS without the lower limitation of residual energy, and the normal IEEE802.15.3-based WPAN PNC selection. It is obvious that the proposed PNC selection method can prolong the lifetime of PNCs in WPANs.

D. Percentage of energy consumption for PNC selection:

The drawback of the proposed PNC selection method is that it may result in more packet exchange, which is produced by PSR, PSR-ACK, DRR, and DRR-ACK packets. The energy used for receiving and transmitting these packets is the majority

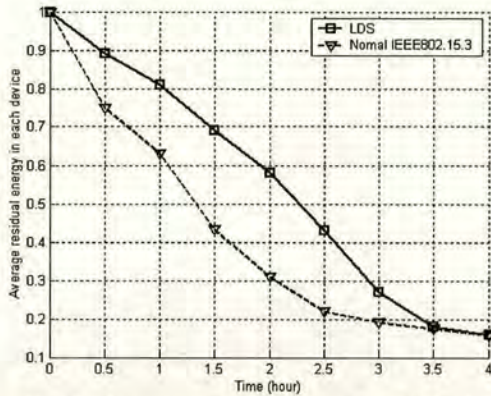


Fig. 5. Average residual energy in each device

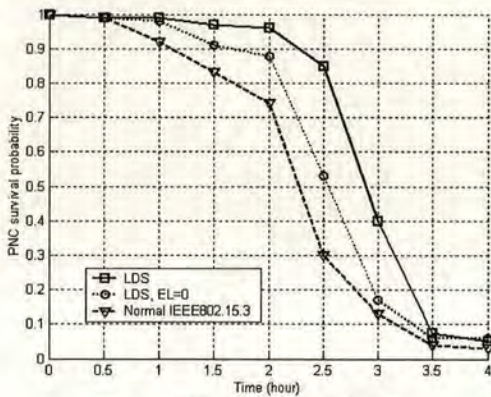


Fig. 6. PNC survival probability

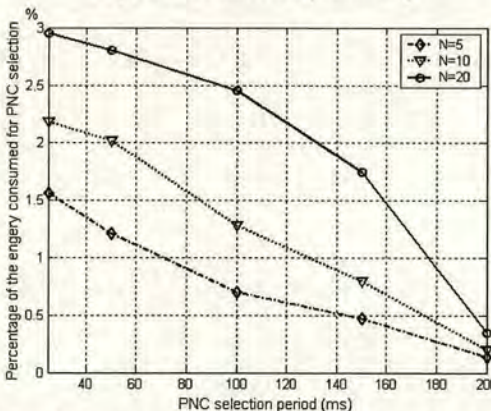


Fig. 7. Percentage of the energy consumed by PNC selection mechanism vs. different PNC selection period

of energy consumption for the PNC selection mechanism. Depicted in fig. 7, the percentage of the energy consumption for PNC selection mechanism is strongly linked to the PNC selection period and the number of devices, N . A short PNC selection period can help the algorithm accurately obtain the change of the devices' status, but this will result in frequent

transmission of the control packets, whose tradeoff should be considered carefully in real systems. However, because the control packets are very small, and the beacon frames are also used for PNC selection, the additional energy consumption for the PNC selection method is very small. For instance, when the selection period is 150ms, the average energy consumed for the PNC selection is less than 1.75% of the total energy consumption.

V. CONCLUSION

Power awareness is an essential component of WPANs, due to limited energy stored in battery-operated devices. Moreover, a WPAN has to deal with coexistence problems, since it may be simultaneously operating with other types of networks. Especially, when UWB, which is a candidate PHY technology for IEEE802.15.3-based WPANs, is applied, decreasing the transmission power is necessary to meet the FCC regulations and diminish interference to other communication systems. In this paper, a novel PNC selection method for IEEE 802.15.3-based WPANs is proposed. In this method, a universal distance estimation method is used to help the PNC selection. Using the proposed PNC selection method, the transmission power can be lessened, and the interference area introduced by PNCs can be diminished as well. The simulation results validate that this method has power-saving and interference mitigation characteristics.

ACKNOWLEDGMENT

The work reported in this paper has formed part of the Personal Distributed Environment area of the Core 3 Research Programme of the Virtual Centre of Excellence in Mobile & Personal Communications, Mobile VCE, www.mobilevce.com, whose funding support, including that of EPSRC, is gratefully acknowledged. This work is also supported by the Overseas Research Students Awards Scheme (ORS), www.universitiesuk.ac.uk, which is greatly appreciated.

REFERENCES

- [1] LAN MAN Standards Committee of the IEEE Computer Society, "IEEE Std 802.15.3 - 2003, Wireless LAN medium Access Control (MAC) specifications," IEEE, 2003.
- [2] M. Z. Win, and R. A. Scholtz, "Impulse Radio: How It Works," IEEE Communications Letters, Vol. 2, No. 2, Feb. 1998.
- [3] I. Stojmenovic and X. Lin, "Power-aware Localized Routing in Wireless Networks," IEEE Transactions on Parallel and Distributed Systems, Vol. 12, Issue: 11, Nov. 2001, pp. 1122-1133.
- [4] R. C. Shah, and J. M. Rabaey, "Energy Aware Routing for Low Energy Ad Hoc Sensor Networks," Wireless Communications and Networking Conference, 2002, WCNC2002, IEEE, vol.1, 17-21 March 2002, pp.350 - 355.
- [5] Y. Zhou, D. I. Laurenson, S. McLaughlin, "High Survival Probability Routing in Power-Aware Mobile Ad Hoc Network," IEE Electronics Letters, Vol. 40, No. 22, 28th Oct. 2004, pp.1424-1426.
- [6] <http://www.sce.carleton.ca/~amatrawy/mpeg4/>
- [7] W. Heinzelman, A. Chandrakasan, and H. Balakrishnan, "Energy-Efficient Communication Protocol for Wireless Microsensor Networks," In Proc. Hawaii International Conference on System Science, 2000, vol. 2, pp.10.

Impact of Power Saving MAC Scheme on Ad Hoc Network Routing Protocol

Yuefeng Zhou, Yow-Yiong Edwin Tan, David I. Laurenson, Stephen McLaughlin

School of Engineering & Electronics, University of Edinburgh

Edinburgh, EH9 3JL, UK

Email: {Yuefeng.Zhou, Yow.Tan, Dave.Laurenson, Steve.McLaughlin}@ee.ed.ac.uk

Abstract—To manage energy limitation problems in Mobile Ad Hoc Networks (MANETs), current power saving (PS) MAC designs mainly concentrate on using various methods to minimize the time in transmission, reception and idle states. This may degrade the latency performance and impacts the route discovery procedure of MANET routing protocols. However, the impact of the PS MAC scheme on routing and the analytical model of PS MAC have not presented before. In this paper, an analytical framework that addresses a gap in the theoretical performance, which includes the latency of the PS MAC and route discovery, is proposed. The investigation verifies that the power saving MAC scheme leads to serious latency and will significantly degrade the route discovery performance of an on-demand routing protocol.

Keywords—ad hoc network, power saving, route discovery

I. INTRODUCTION

Power saving is one of the critical issues in MANETs since many portable devices are battery operated, concerning not only the quality of service but also topology stability. Energy consumption in the wireless LAN interface is the primary part of the total energy usage in mobile devices. Generally, the energy consumption in different operating states of a WLAN interface, which are transmission, reception, idle, sleep, and power off are dramatically different. The energy consumed in an idle state is less than transmission and reception states, but significantly greater than in the sleep state. So current PS MAC designs for wireless LANs concentrate on various methods to put the mobile devices to sleep and minimize the time in transmission, reception and idle states.

The IEEE 802.11 MAC addresses an ad hoc network power saving (AHNPS) mode. Driven by the timing synchronization function (TSF), which is based on beacon transmissions, all PS stations wake up at the same time for an ad hoc traffic indication map (ATIM) duration, whose size is fixed, to listen for the traffic indication map (TIM), which indicates the list of those stations with buffered packets for exchange. If a station has packets to exchange, it will remain awake during the data window following the ATIM window; otherwise it will return to sleep, thus saving energy. A lot of research effort has been expended on the IEEE 802.11 PS mode. This includes the analysis and improvement of the TSF to avoid stations being out of synchronization and isolated [1-2]. Another important aspect is to upgrade the PS scheme to fit for multi-hop MANETs [3-5], since the original AHNPS mode is designed for a single-hop Ad Hoc Network. Though much research has focused on performance simulation and improvement of the PS

mode, very little or nothing has been done about analytical models of the IEEE 802.11 PS mode in MANETs. The impact of the PS mode to the MANET routing has not been discussed either, though routing is essential in MANETs, and may be affected by the PS MAC. In this paper, the latency performance of the IEEE 802.11 AHNPS mode is analyzed by using statistical methods. The causes of the lower successful rate of route discovery are discussed. The analytical and simulation results, for both Request-to-Send/Clear-to-Send (RTS/CTS) and basic media access mechanisms of the PS mode, simultaneously with on-demand routing, are illustrated and compared.

The rest of this paper is organized as follows. Section 2 reviews the IEEE 802.11 AHNPS mode and discusses the impact of the PS mode on the MANET routing protocol. Section 3 explains the analytical model of the PS mode and the successful route discovery rate in detail. The numerical and simulation results are presented and discussed in section 4. Finally, section 5 concludes the paper.

II. BACKGROUND

A. The Ad Hoc Network IEEE 802.11 PS Mode

In the IEEE 802.11 standard, there are two PS modes, infrastructure network PS (INPS), and ad hoc network PS (AHNPS). The main difference between these two modes is the synchronization method. In INPS, the access point (AP) centrally controls the synchronization by sending periodic beacon frames. In AHNPS, all stations have the chance to send synchronization beacons in a distributed manner. Following the beacon frame, there is an ATIM window, during which each station keeps awake to listen to the packet exchange information. In this paper, we concentrate on AHNPS.

When the ATIM window starts, all PS stations contend to send beacon frames. The successfully sent beacon is the synchronization clock signal for all stations. This beacon stops other stations trying to send a beacon frame in the current ATIM window. Then the stations with buffered unicast packets contend to send ATIM frames to each of their intended receivers in PS mode. After transmitting an ATIM frame, the station waits for an ACK from the corresponding station. If the sender does not receive an ACK, it will re-send the ATIM frame in the next ATIM window. After the ATIM window, stations with buffered packets should keep awake during the remaining time of the beacon period, which includes data window, to fulfil packet exchange tasks, other stations go into sleep mode. The buffered unicast packets are sent within the

The authors of this paper are among the core members of the Mobile VCE working group.

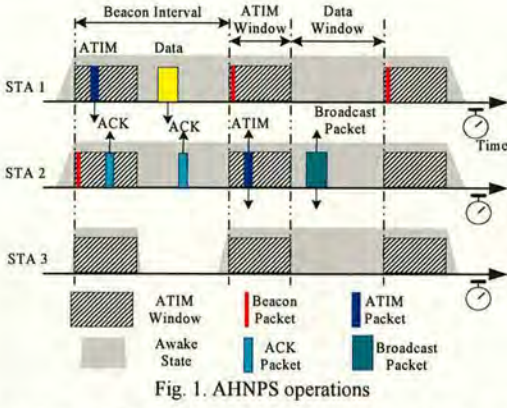


Fig. 1. AHNPS operations

data window. If a station has buffered broadcast packets, it sends an ATIM frame and transmits the broadcast packets without waiting for ACK frames. Figure 1 illustrates the AHNPS operations. Station 1 wants to transmit a data frame to station 2. Firstly, Station 1 transmits an ATIM frame during the ATIM window. Station 2 will send an ACK to station 1 after receiving the ATIM frame. If station 1 receives the ACK frame, it transmits the buffered data frame to station 2 after the ATIM window. When station 2 has a broadcast frame, it transmits the ATIM frame within the ATIM window, and then send that broadcast frame after the ATIM window. No ACK frames are needed in this case.

B. Route Discovery Timeout In MANET Routing

There are two classes of MANET routing, on-table routing and on-demand routing. Using on-table routing, each station periodically exchanges route information, and maintains routing tables, which cover the whole network. However, on-table routing does not scale well to the highly dynamic topology, as periodic route maintenance becomes expensive. On-demand routing does not need to maintain complete topology information in each station. It tries to discover the routes when this Station needs to transmit data packets. This route, which is sufficient for sending its data, is just one part of the whole topology, thus any intermediate stations do not need to maintain complete topology information, covering the total network. On-demand routing saves resources by avoiding the periodic routing table maintenance, and can adapt to sudden topology changes, so it is widely used for MANETs. In this paper, we discuss only on-demand routing.

Generally, on-demand routing can be divided into two stages, route discovery and route maintenance. When a source station cannot find any routes to the destination station, a route-discovery routine will be triggered. The Dynamical Source Routing (DSR) is a typical on-demand routing method. In the process of route discovery in DSR, the source station broadcasts route request packets (RRPs) to find all the possible routes. The neighbouring stations record their own station information into the received RRP and relay it to their neighbours. Then, the destination station replies with a route ACK packet (RACKP), in which the selected route is enclosed, following the reverse direction of the selected route to the source station. Finally, the source station uses the path, indicated in the RACKP, to send the data packets to the destination.

Assume that some method [3-5] can be implemented so that all stations can achieve synchronization in a multi-hop network. The time spent on discovering an N -hop route, D , can be specified as:

$$D = \bar{h} \cdot (E[\tau_{RRP}] + E[\tau_{RACKP}]) \quad (1)$$

where $E[\tau_{RRP}]$ and $E[\tau_{RACKP}]$ is the average end-to-end delay for RRP and RACKP respectively, and \bar{h} is the mean number of hops for each route. According to [6], the average hop count, \bar{h} , is proportional to the square root of the node count:

$$\bar{h} = \Theta(\sqrt{N}) \quad (2)$$

Because packets can only be transmitted after obtaining synchronization and receiving the packet-exchange information in AHNPS mode, it is clear that $E[\tau]$ is larger than that in active MAC mode. This means the route discovery time will be very long, especially when the hop number N is large. Moreover, when the PS network scale is large, due to the severe contention in the narrow ATIM window, the successful possibility of ATIM packet transmission will be lower so that the RRP and RACKPs will span several beacon intervals (BIs) for transmission, then the route discovery time will easily exceed the timeout limitation, maximal route request period, which is an important parameter in any on-demand routing protocol. (If the source station cannot receive a RACKP from the destination station within the maximal route request period, this route discovery operation is deemed to have failed. A new route discovery routine will then be re-triggered by the source station.) In this case, it is impossible to achieve fast route discovery. Simultaneously, the successful route discovery probability will decrease, and extra energy will be used due to the frequent re-triggering of the route discovery routine.

III. NUMERICAL ANALYSIS

A. Delay Analysis Of The IEEE 802.11 PS Mode

To study packet transmission delay under the AHNPS mode, we use some results from [7], where the packet transmission probability, τ , of a station in a random slot is derived.

Define $p_a(W_s)$ as the probability that a station successfully transmits an ATIM packet in the ATIM window, W_A , under the N -station condition. Firstly, we investigate the probability $p_{as}(W_s, k)$, which denotes that a station successfully transmits an ATIM packet, and this is the k^{th} ATIM packet transmission within the ATIM window. At the beginning of the ATIM window, N stations start to contend to transmit an ATIM packet. Assume the 1st successful transmission occurs in the slot m_1 , which means there are no successful transmissions

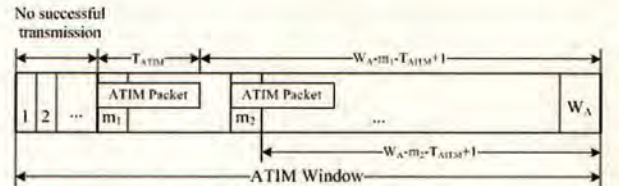


Fig. 2. ATIM packet transmission

before m_1 (fig. 2), and all other stations are scheduled to send packets within the window $[m_1+1, W_A]$. Then the probability $p_{as}(W_A, 1)$ can be written as:

$$p_{as}(W_A, 1) = \sum_{m_1=0}^{W_A-T_{ATIM}+1} N \left(\frac{W_A-m_1}{W_A} \tau(N) \right)^{N-1} \left(\frac{1}{W_A} \tau(N) \right) \quad (3)$$

$$= \sum_{m_1=0}^{W_A-T_{ATIM}+1} \psi_s(N, W_A, m_1)$$

where $\psi_s(N, W_A, m_1)$ is the probability that only one station transmits in m_1 , and all other stations transmit in the window $[m_1+1, W_A]$. The values of T_{ATIM} in the basic access mechanism and in the RTS/CTS access mechanism are specified by (4).

$$T_{ATIM_Basic} = H + S_A + SIFS + ACK + DIFS + \delta \quad (4)$$

$$T_{ATIM_RTS} = RTS + 3 \times SIFS + CTS + H + S_A + ACK + DIFS + \delta$$

In (4), S_A is the size of the ATIM packet, H is the size of the packet header, including PHY_{hdr} and MAC_{hdr}, and δ is a slot time. It is clear that the four-way handshake CSMA/CA, which uses RTS and CTS, will prolong the transmission time, though this mechanism can save bandwidth resource when collisions occur. Equation (3) depicts the probability that the first successful ATIM packet transmission occurred in slot m_1 . Conversely, when x ($x > 1$) stations transmit simultaneously in slot m_1 , a collision will occur. This collision will affect the subsequent transmission in a size-limited window. Let $p_{ac}(W_A, 1)$ be the collision probability, which can be defined as:

$$p_{ac}(W_A, 1) = \sum_{m_1=0}^{W_A-T_{ATIM}+1} \sum_{x=2}^N \binom{N}{x} \left(\frac{W_A-m_1}{W_A} \tau(N) \right)^{N-x} \left(\frac{1}{W_A} \tau(N) \right)^x \quad (5)$$

$$= \sum_{m_1=0}^{W_A-T_{ATIM}+1} \psi_c(N, W_A, m_1)$$

The RTS/CTS mechanism can reduce the average time the channel is busy during a collision. The average busy time of the channel for the two different access mechanisms is given in (6). The collision duration in the four-way handshake access mechanism is shorter than that in basic access scheme, which means the former saves bandwidth under severe channel access competition.

$$T_{c_Basic} = H + S_A + DIFS + \delta \quad (6)$$

$$T_{c_RTS} = RTS + DIFS + \delta$$

After the 1st successful ATIM packet transmission, the remaining $(N-1)$ stations continue to try to send their ATIM packets within a narrower ATIM window, whose size is $W_{A-S}^{(1)} = W_A - m_1 - T_{ATIM} + 1$ (fig. 1). When a collision occurs in slot m_1 , the size of the remainder ATIM window will become

$W_{A-C}^{(1)} = W_A - m_1 - T_c + 1$. Generally, the probability $p_{as}(W_A^{(k-1)}, k)$, which is the probability that k^{th} ATIM transmission is successful, can be written as:

$$p_{as}(W_A^{(k-1)}, k) = p_{as}(W_A^{(k-2)}, k-1) \times \sum_{m_k=m_{k-1}+T_{ATIM}-1}^{m_k=W_A^{(k-1)}-T_{ATIM}+1} \psi_s(N_s^{(k-1)}-1, W_{A-S}^{(k-1)}, m_k) \quad (7)$$

$$+ p_{ac}(W_A^{(k-2)}, k-1) \sum_{m_k=m_{k-1}+T_c-1}^{m_k=W_A^{(k-1)}-T_{ATIM}+1} \psi_s(N_c^{(k-1)}, W_{A-C}^{(k-1)}, m_k)$$

where $W_{A-S}^{(k-1)} = W_A - m_{k-1} - T_{ATIM} + 1$, $W_{A-C}^{(k-1)} = W_A - m_{k-1} - T_c + 1$, $N_s^{(k-1)}$ is the number of stations in the $(k-1)^{\text{th}}$ successful transmission, and $N_c^{(k-1)}$ is the number of stations in the $(k-1)^{\text{th}}$ collision transmission. The probability $p_w(W_A^{(k-1)}, k)$, which is the probability that the k^{th} ATIM transmission is in collision, can be written as:

$$p_{ac}(W_A^{(k-1)}, k) = p_{ac}(W_A^{(k-2)}, k-1) \times \sum_{m_k=m_{k-1}+T_{ATIM}-1}^{m_k=W_A^{(k-1)}-T_{ATIM}+1} \psi_c(N_s^{(k-1)}-1, W_{A-S}^{(k-1)}, m_k) \quad (8)$$

$$+ p_{ac}(W_A^{(k-2)}, k-1) \sum_{m_k=m_{k-1}+T_c-1}^{m_k=W_A^{(k-1)}-T_{ATIM}+1} \psi_c(N_c^{(k-1)}, W_{A-C}^{(k-1)}, m_k)$$

Finally, the probability, $p_a(W_A)$, is the aggregation of all the possible successful transmissions in the ATIM window. Therefore, $p_a(W_A)$ is:

$$p_a(W_A) = \sum_{k=1}^L p_{as}(W_A^{(k-1)}, k), 1 \leq k \leq N \quad (9)$$

The value of L , which is the maximum number of ATIM transmissions, is determined by the size of remainder ATIM window. Before computing $p_{as}(W_A, k)$ and other transfer probabilities, the program has to check the value of remainder ATIM window, $W_{A-S}^{(k-1)}$. If the residual ATIM window is less than T_{ATIM} , the program will terminate the calculation. So the value of L can be limited by the following condition:

$$2T_{ATIM} \geq W_{A-S}^{(L-1)} \geq T_{ATIM} \quad (10)$$

Like the analysis for the ATIM packet transmission rate, the probability $p_{ds}(W_D^{(k-1)}, k)$, which is the probability that the k^{th} data transmission is successful, can be written as:

$$p_{ds}(W_D^{(k-1)}, k) = p_a(W_A) \cdot [p_{ds}(W_D^{(k-2)}, k-1) \times \sum_{l_k=l_{k-1}+T_{data}-1}^{l_k=W_D^{(k-1)}-T_{data}+1} \psi_s(N_s^{(k-1)}-1, W_{D-S}^{(k-1)}, l_k) \quad (11)$$

$$+ p_{dc}(W_D^{(k-2)}, k-1) \sum_{l_k=l_{k-1}+T_c-1}^{l_k=W_D^{(k-1)}-T_{data}+1} \psi_s(N_c^{(k-1)}, W_{D-C}^{(k-1)}, l_k)]$$

where $W_{a,s}^{(k-1)} = W_a - I_{a-1} - T_{data} + 1$, $W_{D,C}^{(k-1)} = W_D - I_{k-1} - T_C + 1$. The average channel busy time, T_c , in the data window is different in the two different access mechanisms, and given by:

$$\begin{aligned} T_{c,Basic} &= H + S_D + DIFS + \delta \\ T_{c,RTS} &= RTS + DIFS + \delta \end{aligned} \quad (12)$$

Similarly, the probability $p_{dc}(W_D^{(k-1)}, k)$, which is the probability that the k^{th} data transmission is collision, can be written as:

$$\begin{aligned} p_{dc}(W_D^{(k-1)}, k) &= p_a(W_A) \cdot [p_{ds}(W_D^{(k-2)}, k-1) \\ &\times \sum_{I_s=W_a-T_{data}+1}^{I_s=W_a-T_{data}+1} \psi_c(N_s^{(k-1)}-1, W_{D,S}^{(k-1)}, I_s) \\ &+ p_{dc}(W_D^{(k-2)}, k-1) \sum_{I_k=I_{k-1}+T_c-1}^{I_k=W_a-T_{data}+1} \psi_c(N_c^{(k-1)}, W_{D,C}^{(k-1)}, I_k)] \end{aligned} \quad (13)$$

The probability, $p_d(W_D)$, is the aggregation of all possible successful transmissions in the data window, and given by:

$$p_d(W_D) = \sum_k p_{ds}(W_D^{(k-1)}, k), \quad 1 \leq k \leq N \quad (14)$$

In the IEEE 802.11 PS mode, if a station is unable to transmit the ATIM frame or the buffered data packet, for example due to the severe contention, the station retains the buffered data packets and announces this data packet again by transmitting an ATIM during the next ATIM window. Assume that the data packet is successfully sent in the k^{th} BI. This means that τ is between $(k-1) \times BI$ and $k \times BI$. The probability of k can be specified as following:

$$\begin{aligned} \Pr\{K = k\} &= \Pr\{(k-1) \cdot BI < \tau < k \cdot BI\} \\ &= (1 - p_d(W_D))^{k-1} \cdot p_d(W_D), \quad 0 < k < M \end{aligned} \quad (15)$$

where M is the maximum retransmission time.

On the other hand, the average delay within a data window, $E[u]$, can be evaluated as:

$$E[u] = \sum_{k=1}^M k \cdot p_d(W_D, k) \quad (16)$$

Moreover, a new data packet, arriving from a higher layer, cannot be transmitted immediately, it will be held in the buffer until the beginning of the next new beacon interval. The probability of this delay β is a normalized distribution with the maximum, BI , and minimum, 0 . This average delay is $BI/2$. Finally, the average end-to-end delay $E[\tau]$ is composed of three parts, the average delay in the buffer before the first ATIM window to announce this packet, the beacon intervals used for failure retransmission, and the average delay within the last beacon interval, in which the packet is successfully transmitted, thus $E[\tau]$ can be obtained as:

$$E[\tau] = \frac{BI}{2} + BI \cdot \left(\sum_{k=0}^{M-1} k \cdot \Pr\{K = k\} - 1 \right) + (W_a + E[u]) \quad (17)$$

Applying (17) to (1), the average route discovery time in AHNPS mode can be evaluated. The stochastic variable for the route discovery time, D , can be expressed as:

$$\begin{aligned} D &= \bar{h} \cdot (\beta + BI \cdot (k'-1) + u' + W_A) \\ &+ \bar{h} \cdot (\beta + BI \cdot (k''-1) + u'' + W_A) \end{aligned} \quad (18)$$

where “'” and “''” denote response to the RRP and RACKP respectively.

If the maximal route request period is Φ , then the successful route discovery rate, v , is:

$$v = \Pr\{[2\beta + BI \cdot (k' + k'' - 2) + (u' + u'') + 2W_A] > \Phi / \bar{h}\} \quad (19)$$

TABLE I SIMULATION PARAMETERS

Parameters	Value
SIFS	10 μ s
DIFS	50 μ s
Slot time	20 μ s
Maximum route request period, Φ	500ms
Channel bit rate	2Mbit/s
Maximal retransmission time, M	16

IV. NUMERICAL RESULTS

The simulations in NS2 use the parameters for the Direct Spread Sequence Spectrum (DSSS) physical layer of IEEE 802.11b. The TSF of the original AHNPS mode is modified by the method proposed in [5]. DSR is selected as the routing protocol in the simulation. Table I shows some key parameters.

A. Successful route request packet transmission rate:

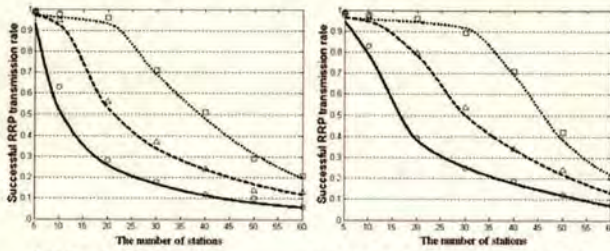
When the number of stations is big, the contention is severe and the RRP transmission rate with the RTS/CTS mechanism is higher than that with basic mechanism (fig. 3.). The reason is that the RTS/CTS mechanism can reduce the average time the channel is busy during a collision. The performance of RRP transmission is strongly linked to the ATIM packet transmission rate. Increasing the size of the ATIM window improves the RRP transmission rate.

B. Average end-to-end delay of route request packet:

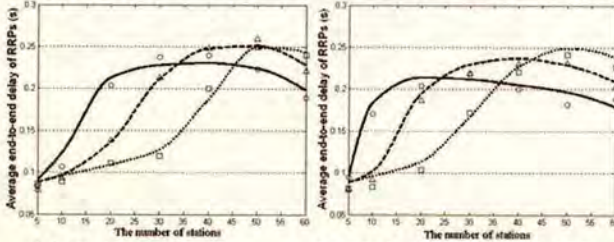
Figure 4 shows the numerical and simulation results of the average end-to-end delay of successful RRP transmission. In the IEEE 802.11 AHNPS mode, the latency is poor, being greater than 0.07s. As the number of stations in the network increases, the end-to-end delay increases up to a maximum value. After reaching the maximum value, the delay begins to decrease, as more packets are discarded due to severe channel access contention, which also means more stations begin to be blocked. The RTS/CTS mechanism can improve the performance of the end-to-end delay, since it decreases the collision duration.

C. Average successful route discovery time and rate:

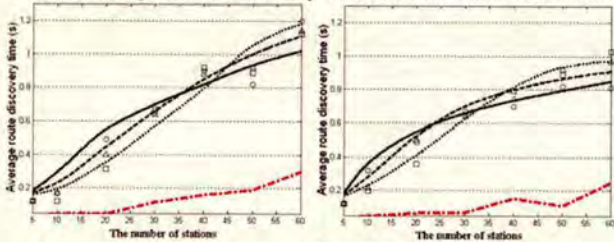
Figures 5 and 6 show the average successful route discovery time and its rate respectively. The trend of the route discovery time is the same as the end-to-end delay. In the simulation where most paths take about 2 to 3 hops, in terms of equation (1), the route discovery time is dramatically higher than in the active mode. As shown in figure 6, when the station number is small, e.g. 5, the successful route discovery rate is low in the simulation, because the network is so sparse



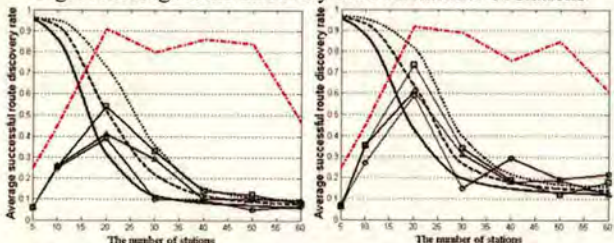
(a) Basic CSMA/CA (b) CSMA/CA with RTS/CTS
Fig. 3. Successful RRP transmission rate vs. number of stations



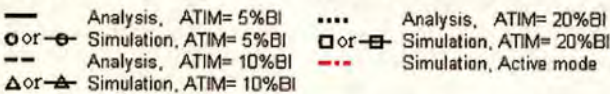
(a) Basic CSMA/CA (b) CSMA/CA with RTS/CTS
Fig. 4. Average end-to-end delay of RRP vs. number of stations



(a) Basic CSMA/CA (b) CSMA/CA with RTS/CTS
Fig. 5. Average route discovery time vs. number of stations



(a) Basic CSMA/CA (b) CSMA/CA with RTS/CTS
Fig. 6. Successful route discovery rate vs. number of stations



that a station can be out of transmission range. This is different from the analytical results, because the analytical model does not consider the density of networks.

The high latency in AHNPS mode will easily cause the route discovery time to exceed 0.5 sec. we can see the average successful route discovery rate is much lower than the active mode. As the size of ATIM window increases, the rate is improved. Another observation is that the rate is slightly higher for CSMA/CA with RTS/CTS compared to without

RTS/CTS because it can help to solve the collision problem. This illustrated example shows that the AHNPS mode significantly degrades the MANET routing protocol. To guarantee effective networking operations, one solution is to increase the timeout parameters of the routing protocol appropriately.

V. CONCLUSION

In this paper, a probabilistic model for latency performance analysis of the PS mode is defined. Using this model, the latency and successful packet transmission rate in the ATIM and data windows are found. Both the analytical and simulation results show that the successful ATIM packet transmission probability has a strong impact on the performance of IEEE 802.11 PS networks. Because packets can only be transmitted after obtaining synchronization and receiving the ATIM packets, the end-to-end delay will dramatically increase. This results in the route discovery procedure not completing within the timeout limitation, thus the route discovery operations fail, especially when the network scale is large. The successful route discovery rate also relates to the size of the ATIM window and the number of stations. When the stations are numerous, the channel access contention will be severe. In this case, the RTS/CTS mechanism can improve the performance by cutting down the collision duration.

ACKNOWLEDGMENT

The work reported in this paper has formed part of the Personal Distributed Environment area of the Core 3 Research Programme of the Virtual Centre of Excellence in Mobile & Personal Communications, Mobile VCE, www.mobilevce.com, whose funding support, including that of EPSRC, is gratefully acknowledged. This work is also supported by the Overseas Research Students Awards Scheme (ORS), www.universitiesuk.ac.uk, which is greatly appreciated.

REFERENCES

- [1] L. Huang, and T. H. Lai, "On the Scalability of IEEE 802.11 Ad Hoc Networks", MOBIHOC'02, June 9-11, 2002, Switzerland.
- [2] T. H. Lai, and D. Zhou, "Efficient and Scalable IEEE 802.11 Ad-Hoc-Mode Timing Synchronization Function", Advanced Information Networking and Applications 2003, March 2003, pp. 318 - 323
- [3] J. R. Jiang, Y. C. Tseng, C. S. Hsu, and T. H. Lai, "Quorum-Based Asynchronous Power-Saving Protocols for IEEE 802.11 Ad Hoc Networks", Parallel Processing, 2003 International Conference, Oct. 2003, pp. 257 - 264
- [4] Y. C. Tseng, C. S. Hsu, and T. Y. Hsieh, "Power-Saving Protocols For IEEE 802.11-Based Multi-Hop Ad Hoc Networks", INFOCOM 2002, Vol. 1, June 2002, pp. 200 - 209 vol.1
- [5] Y. Zhou, D. I. Laurenson, and S. McLaughlin, "An Effective Power-Saving Scheme For IEEE 802.11-based Multi-hop Ad Hoc Network", VTC Fall 2004, Sep. 2004
- [6] L. Kleinrock, and J. Silvester, "Optimum Transmission Radii for Packet Radio Networks," Proc. IEEE National Telecommunication Conference (NTC), 1978, pp.120-130
- [7] J. Bianchi, "Performance Analysis of IEEE 802.11 Distributed Coordination Function," IEEE Journal on Selected Areas in Communications, Vol. 18, No. 3, pp. 535-547, March 2000

An Effective Power-Saving Scheme for IEEE 802.11-Based Multi-hop Mobile Ad Hoc Network

Yuefeng Zhou

School of Engineering & Electronics
University of Edinburgh
Edinburgh, EH9 3JL, UK
Yuefeng.Zhou@ee.ed.ac.uk

David I. Laurenson

School of Engineering & Electronics
University of Edinburgh
Edinburgh, EH9 3JL, UK
Dave.Laurenson@ee.ed.ac.uk

Stephen McLaughlin

School of Engineering & Electronics
University of Edinburgh
Edinburgh, EH9 3JL, UK
Steve.McLaughlin@ee.ed.ac.uk

ABSTRACT—This paper investigates problems that can arise in the IEEE 802.11 power-saving mode when operating in multi-hop ad hoc networks. An enhanced power-saving scheme, which is based on reliable beacon reception and adaptive window size, is proposed. The simulation results show that this scheme is quite robust under a dynamically changing network traffic load and is more energy efficient.

Keywords— IEEE 802.11, mobile ad hoc network, power saving

I. INTRODUCTION

The growth of WLAN is accelerating due to the rapid development of portable wireless devices. To extend service and access freely, mobile ad hoc networks (MANETs), are under intensive examination by industry. In MANETs, various communication devices comprise a wireless network that has no fixed infrastructure and unpredictable connectivity. These devices are not only the means to data interchange but also the managers for the routes to data and access to services. Power saving is one of the critical issues in MANETs, widely discussed in the literature, since many portable devices are battery operated. Energy consumption in the wireless LAN interface is the primary part of the total energy usage in mobile devices. Generally, there are five operating states in a mobile device, which are transmission, reception, idle, sleep, and power off. The energy consumption in these states is dramatically different [1]. So an effective power saving technique is to put the mobile devices to sleep and minimize the time in transmission, reception and idle states.

The IEEE 802.11 MAC, as specified in the standard [2] addresses an ad hoc network power-saving (PS) mode. Driven by the timing synchronization function (TSF) based on the beacon transmission, all PS stations wake up at the same time for a fixed ad hoc traffic indication map (ATIM) duration to listen for the traffic indication map (TIM), which indicates the list of those stations with buffered packets for exchange. If a station has no packets to exchange, it will return to sleep during the data window, thus saving energy. The standard assumes all mobile stations are fully connected. Unfortunately, in multi-hop ad hoc networks, all stations cannot hear each other directly, and the unpredictable communication delays and mobility make synchronization difficult, especially in a large-scale network. In the IEEE 802.11 PS mode, the ATIM and

data windows are fixed in size, thus are not able to adapt to the dynamically changing traffic load. Some improvements for IEEE 802.11 PS mode in MANETs have been proposed over the last few years [3][4][5]. However, these do not focus on multi-hop MANETs. In [6], the authors proposed to widen the ATIM window to particular patterns in order to guarantee synchronization for multi-hop MANETs. However, this method is at the cost of the channel utility and energy, since no data packets can be exchanged in the ATIM window, and all stations remain awake during this extended window. In [7], a location-aware IEEE 802.11 PS scheme for multi-hop MANETs was proposed. In this PS scheme, to obtain location information, all of the mobile stations required a GPS receiver. Both of the above algorithms required dramatic changes to the PS mode in IEEE 802.11, which will introduce compatibility problems with existing devices.

In this paper, the focus is on the IEEE 802.11 PS mode in multi-hop MANETs. An enhanced PS scheme based on an adaptive window size is proposed through minor modification of the standard. This scheme makes the PS mode adapt to different traffic loads, decreases the amount of retransmission, and balances the bandwidth utility.

The paper is organized as follows. Section 2 reviews the ad hoc network IEEE 802.11 PS mode and describes the problems in multi-hop MANETs. Section 3 explains the enhanced PS algorithms in detail. The simulation results are presented and discussed in section 4. Finally, section 5 concludes the paper.

II. BACKGROUND

A. The Ad Hoc Network IEEE 802.11 PS Mode

In the IEEE 802.11 standard, there are two PS modes, infrastructure network PS (INPS), and ad hoc network PS (AHNPS). The main difference between these two modes is the synchronization method. In INPS, the access point (AP) centrally controls the synchronization by sending periodic beacon frames. In AHNPS, all stations have the chance to send synchronization beacons in a distributed manner. Following the beacon frame, there is an ATIM window, during which each station keeps awake to listen to the packet exchange information.

The authors of this paper are among the core members of the Mobile VCE working group.

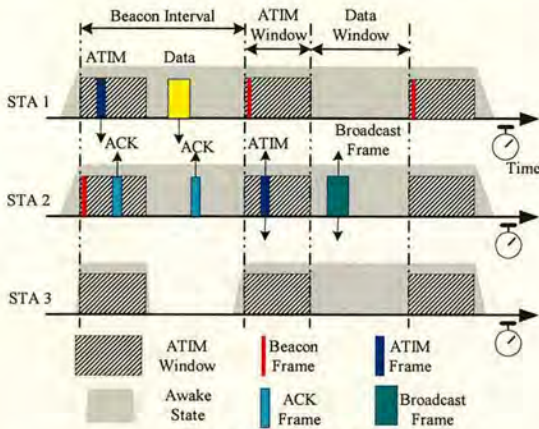


Fig. 1. AHNPS operation

In AHNPS, it is assumed that the power-saving stations can be fully connected and synchronized so that they can periodically wake up at the same time for a short ATIM window. The first thing that the stations do when their ATIM window starts is to contend to send a beacon frame. To avoid the collision, a station selects a backoff window, of up to $2 \times \text{aCWmin}$ slots, for the backoff algorithm to attempt to send a beacon frame. Here, aCWmin is the minimum contention window size defined in the standard. The successfully sent beacon is the synchronization clock signal for all stations. This beacon stops other stations trying to send a beacon frame in the current ATIM window. Stations adjust their clock only if the timestamp in the received beacon frame is beyond their own timestamps. The stations with buffered unicast packets contend to send ATIM frames to each of their intended receivers in PS mode. After transmitting an ATIM frame, the station waits for an ACK from the corresponding station. If the sender does not receive an ACK, it will re-send the ATIM frame in the next ATIM window. After the ATIM window, stations with buffered packets should keep awake during the remaining time of the beacon period, which includes data window, to fulfill packet exchange tasks, other stations go into sleep mode. The buffered unicast packets are sent within the data window. If a station has buffered broadcast packets, it sends an ATIM frame and transmits the broadcast packets without waiting for ACK frames. Figure 1 illustrates the AHNPS operations. Station 1 wants transmit a data frame to station 2. Firstly, Station 1 transmits an ATIM frame during the ATIM window. Station 2 will send an ACK to station 1 after receiving the ATIM frame. If station 1 receives the ACK frame, it transmits the buffered data frame to station 2 after ATIM window. When station 2 has a broadcast frame, it transmits the ATIM frame within the ATIM window, and then send that broadcast frame after the ATIM window. No ACK frames are needed in this case.

B. Problem Statement

In a single-hop ad hoc network, all of the power-saving stations can be fully connected so that they gain synchronization through hearing one beacon. In a multi-hop MANET, some stations may move out of the transmission

range of the beacon sending station. In addition, mobility and communication delays will make the synchronization difficult. The size-fixed window means some stations cannot transmit ATIM and data frames in time under heavy traffic load, thus increasing the end-to-end delay and degrading the channel utility. Moreover, after exchanging data packets, the station should remain awake during the remaining beacon interval, thus wasting more energy.

1) *Unstable beacon reception*: In multi-hop MANETs, it is clear that each station's transmission range may not cover all the stations. Different parts of the MANET may have their own independent beacons. The MANET may be partitioned into several groups and lose synchronization through different beacon timing. In [6], the authors let all the stations continue sending their beacons after receiving a beacon, thus keeping all stations in contact with each other. However, these flooded beacons will dramatically increase the congestion within the narrow ATIM window.

2) *Mismatch between the size-fixed window and the dynamically changing traffic load*: Under a heavy traffic load, many stations will have buffered packets waiting for transmission. In this case, a short ATIM window may not allow all the stations to successfully send ATIM frames. Some buffered packets would then be delayed by at least one beacon interval. A long ATIM window allows for more successful ATIM frames. However, this will increase the contention in the data window so that some stations will lose the opportunity to send data packets and are required to keep awake during the data window, thus wasting more energy.

III. ENHANCED SCHEME

Following on from the above discussion, several improvements to the PS mode are proposed.

1) *Reliable Synchronization*: A robust timing synchronization is essential to guarantee efficient data exchange in the IEEE 802.11 PS mode. In a multi-hop MANET, some stations may not hear the beacon. A reliable TSF should ensure that all the stations in PS mode hear each beacon and adjust clock errors.

2) *Adjustable size for ATIM and data window*: An adaptive size of ATIM and data windows can let the PS mode adapt to different traffic loads with energy efficiency.

A. Reliable Synchronization in a Multi-Hop MANET

We propose an improvement to the IEEE 802.11-based TSF as follows.

The channel time is divided into beacon intervals (BIs), with each beacon interval beginning with a beacon frame. The beacon interval is composed of three major parts: the beacon, followed by a fixed length guard time (GT), the ATIM window, followed by a fixed length size-control time (SCT), and the data window, as shown in figure 2. The differences between this enhanced scheme and the original IEEE 802.11 PS mode are the additive GT, SCT, and the adaptive size of the windows.

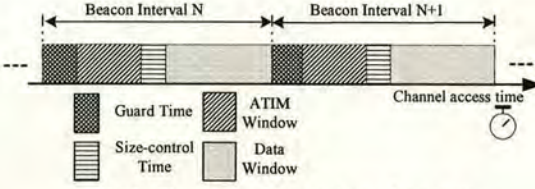


Fig. 2. The enhanced beacon interval structure

A mobile station should insist on sending beacons even if it has heard other beacons. This will allow others to be aware of its existence and exchange timing information for synchronization. To ease the pressure of the access contention in the ATIM window, a size-fixed GT duration is used for stations to send the beacon. This short GT allows most of the beacons to transmit, since the beacon is very small. In a large-scale network, the beacon transmission can extend into the ATIM window. As a result of the ATIM window size being adaptive to the traffic load, those beacons, which are extended to the ATIM window, will not affect the transmission of the ATIM frame.

A mobile station, which is initially entering the PS mode, should keep awake for 2 normal BIs to hear other station's beacon frames. Once a beacon is heard, this station can get synchronization and then enter the PS mode.

If a mobile station has not heard any beacon frames for two BIs, it means this station may have moved out of the PS network. This station should alternate between awake and idle states for a BI. When it hears a beacon, it is synchronized, and enters PS mode.

If a PS station does not receive any beacon frames with a timestamp value later than its own for N BIs, it will simply replace its own timestamp value T_{Stamp} with $T_{\text{Stamp}} + (T_{\text{Stamp}} - T_{\text{LastReceivedStamp}})$. $T_{\text{LastReceivedStamp}}$ is the last received timestamp value. This can prevent clock drift in a station with a faster clock.

B. Adaptive Window Size

Ideally, the optimised ATIM window size, W_{optATIM} , for a contention-free schedule for ATIM frame transmission should obey the following equation:

$$R_{\text{ATIM}} |_{W_{\text{ATIM}} \geq W_{\text{optATIM}}} = 1, W_{\text{ATIM}} \in [W_{\text{min}}, W_{\text{max}}] \quad (1)$$

$$W_{\text{min}} > 0, W_{\text{max}} < W_{\text{BI}} - W_{\text{GT}} - W_{\text{SCT}}$$

where R_{ATIM} is the successful rate of the ATIM frame sending, and W_{ATIM} is the ATIM window size. Each station monitors its successful rate of ATIM frame sending, R_{ATIM} , in every ATIM window. If $R_{\text{ATIM}} < 1$, the station extends its next ATIM window by Δ ($\Delta > 0$) until W_{ATIM} reaches W_{max} . If R_{ATIM} remains at 1 for two BIs, the station subtracts its ATIM window size in the next BI by Δ until it reaches W_{min} .

In this enhanced scheme, a PS station shall receive all the successful ATIM packets during the ATIM window to estimate the appropriate data window size. The transmission time

information of the data packets is easily added into the frame body of ATIM, since the ATIM frame in the standard has only MAC header, Frame Check Sequence (FCS), and an empty frame body. An estimated total data transmission time, L' , can be expressed as:

$$L' = \sum_{i=1}^N T_i + N \cdot (T_{\text{DIFS}} + T_{\text{SIFS}} + T_{\text{ACK}}) \quad (2)$$

where N is the number of received ATIM frames, and T_i is the data transmission duration, which is dependent on the data packet's length, indicated in the ATIM frame. T_{DIFS} and T_{SIFS} are the distributed coordination function interframe space and the short interframe space respectively. T_{ACK} is the ACK frame transmission time. The current data window size W_{Data} is the remaining time of the BI.

$$W_{\text{Data}} = W_{\text{BI}} - W_{\text{GT}} - W_{\text{ATIM}} - W_{\text{SCT}} \quad (3)$$

When $W_{\text{Data}} < L'$, it means that some data packets will fail to transmit. To alleviate the access contention, the station will extend the current data window by one BI.

A station, which intends to extend its ATIM window or data window, should broadcast this size-control request to its neighbours during the SCT so that they can change window size simultaneously. To avoid collisions, at the beginning of the SCT, the station should wait a random number of slots between 0 and $2 \times CW_{\text{min}} - 1$ before sending this short request frame. Once a station has received this frame, it increases the data window size in the current BI or changes the ATIM window size in the next BI. If a station receives more than one size-control request, it always responds to the request for increasing the window size.

When a station finishes the data exchange and the remainder of the data window is bigger than a threshold Th , it switches to sleep mode during the remaining data window. To prevent using extra energy for the switching between modes [8], an appropriate Th is necessary.

Fig. 3 shows an example for this enhanced scheme. At the beginning of all the BIs, stations send a beacon frame using CSMA/CA with an initial random backoff. Within the N^{th} beacon interval, station 2 hears ATIM frames, indicating that two stations have some buffered data packets for it. Station 2 calculates the transmission time of those data packets. If the transmission time is larger than its residual time in the current BI, station 2 broadcasts a SCT frame to command to widen the current data window by a normal BI length. Stations keep awake during the GT, ATIM, and SCT window. If a station does not receive ATIM frames, it goes to sleep during the data window, otherwise, it remains awake. When stations finish the data exchange, and the remaining time of the data window is larger than a threshold T , they go to sleep for the remaining data window time.

IV. SIMULATION RESULTS

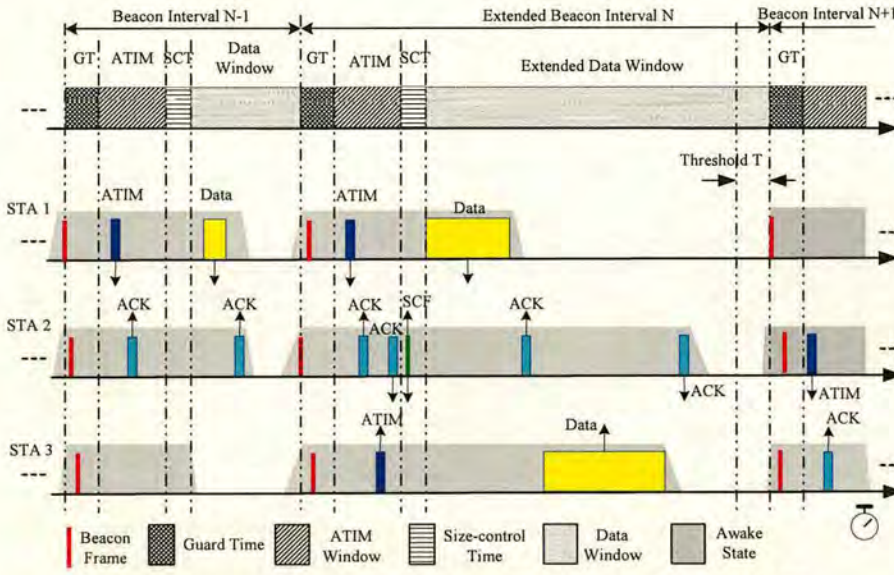


Fig. 3. An example of the enhanced scheme for IEEE 802.11-based multi-hop MANETs

In the simulation, the BI is set to the typical value of 100ms (The extended beacon interval is 200ms). In IEEE 802.11 for DSSS, the slot length is 20 μ s. We select 50 slots for the minimal ATIM window length. The size of the GT and SCT is 250 slots.

Three aspects of the enhanced scheme are compared with the original IEEE 802.11 ad hoc network PS mode, packet-sending successful rate, power efficient, and end-to-end delay. The maximal ATIM window size and the network traffic loads were adjusted in the simulation.

The network traffic load (NTL) is defined by the following equation:

$$NTL = (N \times S) / R \quad (4)$$

In this equation, N is the number of source stations, S is the traffic source's bit rate, and R is the channel bit rate. For example, if 10 stations are periodically sending packets, whose size is 512 bits, with a fixed interval of 0.1s, and the channel bit rate is 1 Mbps, then the network load traffic (NTL) is $10 \times 512 / 0.1 / (1024 \times 1024) = 4.8\%$.

In the simulation, the channel bit rate is 2Mbps, the data packet size is 1k bits, and the packet-sending interval is 0.1s. The stations are randomly located in a 600m \times 600m area with the speed selected from a uniform probability distribution function with a maximum speed of 10ms⁻¹.

A. Successful transmission rate:

Fig. 4.a and 4.b are the simulation results for the successful ATIM frame transmission rate and the successful data frame transmission rate. The successful ATIM frame transmission rate in the enhanced scheme with the maximum ATIM window size of 250 slots is a little better than that in the original IEEE 802.11 standard. This demonstrates that the synchronization problem in multi-hop MANETs may affect ATIM frame

transmission. The successful data frame transmission rate of the enhanced algorithm is higher than that of the original IEEE 802.11, since the data window size can be double the normal size under heavy traffic loads.

B. Average number of sleep slots per station:

The fig. 4.c shows that the PS station with the enhanced scheme has more sleep slots, which means that energy can be saved. The reasons are the PS stations with the enhanced scheme can be put to sleep after finishing the data exchange during the data window, and the size adapted window can help the PS stations decrease the frequency of re-transmission times, especially under heavy traffic loads. The adaptive ATIM

window can save some slots as well. The number of the sleep slots per station in original IEEE 802.11 increases, with an increasing traffic load, because the unsuccessful ATIM frame transmission results in some stations not being awake during the data window.

C. Average end-to-end delay:

Normally, in the PS mode, the end-to-end delay performance is poor, because stations simply exchange packets periodically. The adaptive window size allows the stations to adapt to dynamically changing traffic loads, and decrease the re-transmission time, so the enhanced algorithm can improve the end-to-end delay substantially (Fig. 4.d).

V. CONCLUSION

The IEEE 802.11 PS mode can support a single-hop ad hoc network, though it cannot accommodate the dynamic nature of the network traffic load. In multi-hop MANETs, the limited transmission range and the mobility make the topology complicated, thus increasing the difficulty of obtaining synchronization. Moreover, the size-fixed window in the standard is not flexible in different network traffic conditions. The enhanced PS scheme, proposed in this paper, modifies the beacon-sending behaviour in the standard to improve synchronization and use an adaptive window size for ATIM and data transmission. The simulation results show that this enhanced scheme can improve the transmission efficiency, and save energy in multi-hop MANETs.

ACKNOWLEDGMENT

The work reported in this paper has formed part of the Personal Distributed Environment area of the Core 3 Research Programme of the Virtual Centre of Excellence in Mobile & Personal Communications, Mobile VCE, www.mobilevce.com, whose funding support, including that of EPSRC, is gratefully

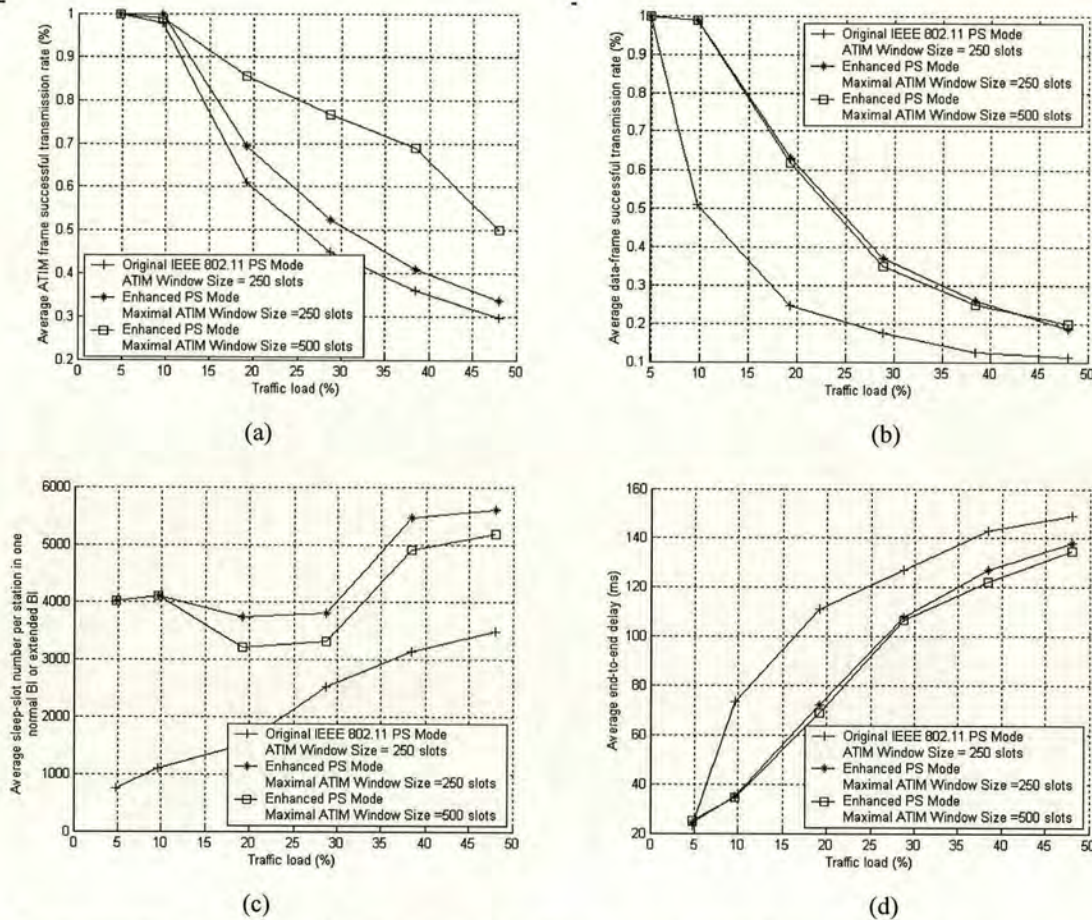


Fig. 4. Simulation results: (a) successful ATIM frame transmission rate, (b) average successful data frame transmission rate, (c) average number of sleep slots per station, (d) average end-to-end delay

acknowledged. Full detailed technical reports on this research are available to Industrial Members of Mobile VCE.

REFERENCES

- [1] Eduardo S. C. Takahashi, "Application Aware Scheduling for Power Management on IEEE 802.11," Performance, Computing, and Communications Conference, 2000, Feb. 20-22 Feb. 2000, pp. 247 - 253
- [2] LAN MAN Standards Committee of the IEEE Computer Society, "IEEE Std 802.11 - 1999, Wireless LAN medium Access Control (MAC) and Physical Layer (PHY) specifications," IEEE, 1999
- [3] Chih-Shun Hsu, Jang-Ping Sheu, and Yu-Chee Tseng, "Minimize Waiting Time And Conserve Energy By Scheduling Transmissions In IEEE 802.11-Based Ad Hoc Networks," ICT 2003, 10th International Conference, Vol. 1, March 2003, pp. 393 - 399
- [4] Liu, M., Liu, M.T., "A Power-Saving Scheduling for IEEE 802.11 Mobile Ad Hoc Network," Computer Networks and Mobile Computing, 2003, Oct. 2003, pp. 238 - 245
- [5] Jehn-Ruey Jiang, Yu-Chee Tseng, Chih-Shun Hsu, Ten-Hwang Lai, "Quorum-Based Asynchronous Power-Saving Protocols for IEEE 802.11 Ad Hoc Networks," Parallel Processing, 2003 International Conference, Oct. 2003, pp. 257 - 264
- [6] Yu-Chee Tseng, Chih-Shun Hsu, Ten-Yueng Hsieh, "Power-Saving Protocols For IEEE 802.11-Based Multi-Hop Ad Hoc Networks," INFOCOM 2002, Twenty-First Annual Joint Conference of the IEEE, Vol. 1, June 2002, pp. 200 - 209
- [7] Yu-Chee Tseng, Ten-Yueng Hsieh, "Fully Power-Aware And Location-Aware Protocols for Wireless Multi-Hop Ad Hoc Networks," Computer Communications and Networks Eleventh International Conference, Oct. 2002, pp.608 - 613
- [8] Eun-Sun Jung and Nitin H. Vaidya, "An Energy Efficient MAC Protocol for Wireless LANs," In Proceedings of the 21st Annual Joint Conference of the IEEE Computer and Communications Societies 2002, June 2002, vol. 3, pp.1756-1764